JAERI-M
90-101

NEANDC(J)-152 U
INDC(JPN)-139 L

EVALUATION OF NEUTRON NUCLEAR DATA FOR CURIUM ISOTOPES

July 1990

Tsuneo NAKAGAWA

日 本 原 子 力 研 究 所
Japan Atomic Energy Research Institute

JAERI-M レポートは，日本原子力研究所が不定期に公刊している研究報告書です。
入手の問合わせは，日本原子力研究所技術情報部情報資料課（〒319-11茨城県那珂郡東海村）あて，お申しこしください。なお，このほかに財団法人原子力弘済会資料センター（〒319-11 茨城県那珂郡東海村日本原子力研究所内）で複写による実費頒布をおこなっております。

JAERI-M reports are issued irregularly.
Inquiries about availability of the reports should be addressed to Information Division Department of Technical Information, Japan Atomic Energy Research Institute, Tokai-mura, Naka-gun, Ibaraki-ken 319-11, Japan.

編集兼発行　日本原子力研究所
印　　　刷　いばらき印刷㈱

Evaluation of Neutron Nuclear Data for Curium Isotopes

Tsuneo NAKAGAWA

Department of Physics
Tokai Research Establishment
Japan Atomic Energy Research Institute
Tokai-mura, Naka-gun, Ibaraki-ken

(Received June 1, 1990)

The evaluation of neutron nuclear data of curium isotopes was made in the energy region from 10^{-5} eV to 20 MeV. The data of ^{241}Cm were newly evaluated in the present work. The data of ^{242}Cm, ^{243}Cm, ^{244}Cm, ^{245}Cm, ^{246}Cm, ^{247}Cm, ^{248}Cm and ^{249}Cm had been evaluated previously, and those of ^{242}Cm through ^{245}Cm were stored in JENDL-2. In the present work, the recent experimental data were reviewed, and their data were reevaluated except for ^{248}Cm and ^{249}Cm. The results of the present work were compiled in ENDF-5 format and included in the latest version of Japanese Evaluated Nuclear Data Library, JENDL-3.

Keywords: Nuclear Data, Curium-241, Curium-242, Curium-243, Curium-244, Curium-245, Curium-246, Curium-247, Curium-248, Curium-249, Evaluation, JENDL-3

This work was performed under contract between Power Reactor and Nuclear Fuel Development Corporation and Japan Atomic Energy Research Institute.

Cm核種の核データ評価

日本原子力研究所東海研究所物理部
中川 庸雄

(1990年6月1日受理)

Cm核種の核データ評価を10^{-5} eVから20 MeVの中性子エネルギー範囲で行った。^{241}Cmのデータは，今回の作業で新たに評価したものである。^{242}Cm，^{243}Cm，^{244}Cm，^{245}Cm，^{246}Cm，^{247}Cm，^{248}Cmと^{249}Cmのデータについては，既に一度評価を行っており，^{242}Cmから^{245}CmのデータはJENDL-2に格納されていた。今回の作業では，最近の測定データを基にこれらのデータの見直しを行い，再評価を行った。結果を，ENDF-5フォーマットで編集し，日本の評価済み核データライブラリーの最新版JENDL-3に収録した。

本研究は，日本原子力研究所が動力炉・核燃料開発事業団の委託により行なった研究の成果である。
東海研究所：〒319-11 茨城県那珂郡東海村白方字白根2-4

Contents

目　　次

1. Introduction

The nuclear data of transuranium isotopes (TRU) are important for nuclear fuel cycle studies. For JENDL (Japanese Evaluated Nuclear Data Library), the evaluations of nuclear data for 20 nuclides from americium to californium have been completed by the group of the present author. Table 1 shows the status of our previous evaluations for curium isotopes. The evaluated data for ^{242}Cm, ^{243}Cm, ^{244}Cm and ^{245}Cm were stored in JENDL-2. For some of them, however, reevaluation is necessary, because our previous evaluations are rather old and new experimental data have been published. In this work, therefore, reevaluation of the curium isotopes was performed for JENDL-3.

The quantities evaluated are resolved and unresolved resonance parameters, total, elastic and inelastic scattering, fission, capture, (n,2n), (n,3n) and (n,4n) reaction cross sections, angular and energy distributions of emitted neutrons, and number of neutrons per fission in the incident neutron energy range from 10^{-5} eV to 20 MeV.

In Chapter 2, the present evaluation method and important parameters used are described. Review of recent experimental data and reevaluation work are given in Chapters 3 to 11. In each Chapter, our evaluation is compared with the experimental data and other evaluations in figures of the total, fission, capture, inelastic scattering, (n,2n) and (n,3n) cross sections, and in tables of thermal cross sections and resonance integrals above 0.5 eV. The experimental data of the cross sections in the figures were mainly received from the OECD/NEA Data Bank.

The data of ^{248}Cm and ^{249}Cm were not reevaluated in this work, because no new experimental data were available. The previous evaluation is, therefore, briefly described in Chapter 10 and 11.

2. Evaluation Method

2.1 Resonance parameters

The resonance parameters for the multi-level Breit-Wigner formula were given for even mass isotopes. However, the single-level Breit-Wigner formula was used for odd mass isotopes because total spin J of each resonance was unknown. The resonance parameters for low energy resonances were adjusted to well reproduce the thermal cross sections recommended by Mughabghab[7].

The unresolved resonance parameters were determined in the energy region from the upper boundary of the resolved resonance region to 30 ~ 40 keV with ASREP[8]. In general, the initial values of Γ_f, Γ_γ, D and S_0 were estimated from the resolved resonance parameters and those of S_1 and S_2 from calculation with the optical model. The parameters were adjusted to reproduce the evaluated cross sections in the unresolved resonance region.

2.2 Fission cross section

The fission cross section was determined by eye-guiding or spline fitting to the recent experimental data if available. In the high energy region where no experimental data were available, the fission cross-section shape was estimated by taking account of (n,nf) and (n,2nf) reactions.

2.3 (n,2n), (n,3n) and (n,4n) reaction cross sections

They were calculated with Pearlstein's method[9] based on the evaporation model. In this calculation, the non-elastic scattering cross section was assumed to be (compound nucleus formation cross section - fission cross section -1 mb), where the small value of 1 mb was reserved for the inelastic scattering cross section in the high energy region. This calculation was performed with an interactive nuclear data evaluation system NDES[10].

2.4 Other cross sections

The total, elastic and inelastic scattering and radiative capture cross sections were calculated with CASTHY[11] on the basis of the spherical optical and statistical models. The fission, (n,2n), (n,3n) and (n,4n) reaction cross sections were considered as the competing cross sections. If the experimental data were available for the capture cross section in the keV region, gamma-ray strength functions were determined by normalizing the cross section to the measurements.

2.5 Angular distributions of emitted neutrons

The angular distributions of elastically and inelastically scattered neutrons were calculated with CASTHY. The neutrons from the fission and (n,Xn) reactions were assumed to be isotopic in the laboratory system.

2.6 Energy distributions of emitted neutrons

Emitted neutrons from the inelastic scattering to the overlapping levels and those from the (n,Xn) reactions were assumed to have the form of evaporation spectra. Nuclear temperature was estimated from nuclear level density parameters given by Gilbert and Cameron[12] with EVAPSPEC[13].

Neutron spectra from neutron induced fission were also assumed to be in the form of evaporation spectra, and their temperature was taken from the systematics obtained by Smith et al.[14] which is given in Fig. 1. By assuming that the average energy of spontaneous fission neutrons from ^{252}Cf is 2.13 MeV, the average energy E of fission neutrons can be obtained from Fig. 1. Then the nuclear temperature θ is calculated as

$$\theta = \frac{2}{3} E \quad (\mathrm{MeV}).$$

2.7 Number of neutrons per fission

For the isotopes which have no experimental data on the number of prompt fission neutrons at the thermal energy, the semi-empirical formula of Howerton[15] was adopted.

$$\nu(Z, A_t, E_n) = 2.33 + 0.06\ [2 - (-1)^{A_t+1-Z} - (-1)^Z] + 0.15(Z-92) + 0.02\ (A_t-235) + [0.130 + 0.006\ (A_t-235)] \times [E_n - E_T(Z, A_t)],$$

where E_n stands for an incident neutron energy, A_t and Z are mass and atomic numbers of a target nucleus and E_T is a threshold energy of the fission given in the following equation.

$$E_T(Z, A_t) = 18.6 - 0.36\ Z^2/(A_t+1) + 0.2\ [2 - (-1)^{A_t+1-Z} - (-1)^Z] - B_n,$$

where B_n is a neutron separation energy from a compound nucleus.

For delayed neutrons, the following Tuttle's systematics[16] was used.

$$\nu_d = \exp\ [13.81 + 0.1754(A_c-3Z)\ (A_c/Z)],$$

where Z and A_c are the atomic and mass numbers of a compound nucleus. Below 6 MeV, the constant value of ν_d was calculated from this equation. Above 8 MeV, it was calculated for the nuclide with the mass number of A_c-1. These two ν_d values were linearly connected in the energy region from 6 to 8 MeV.

2.8 Optical potential parameters

In the present calculation, the parameters determined by Igarasi and Nakagawa[1] were adopted, which reproduced well the ^{241}Am total cross section measured by Phillips and Howe[17]. For ^{241}Cm, ^{243}Cm and ^{245}Cm, the depth of real potential was slightly modified to obtain larger neutron strength functions at low neutron energies. The parameters used in the present calculation are listed in Table 2.

2.9 Level density parameters

The level density parameters used in the previous evaluation were taken from Ref. 12. In the present work, they were newly determined on the basis of excited levels taken from ENSDF[18] and average resonance-level spacings recommended by Mughabghab[7]. The obtained level density parameters are given in Table 3. Examples of cumulative numbers of excited levels and those calculated from the level density parameters are shown in Fig. 2.

In the cases of ^{248}Cm and ^{249}Cm whose data were not re-evaluated, the previous evaluation based on the level density parameters of Ref. 12 was adopted as the final evaluation.

2.10 Q-values

The Q-values of the (n,2n), (n,3n) and (n,4n) reactions were calculated from the nuclear mass table by Wapstra and Bos[19]. They are given in Table 4.

3. Curium-241

3.1 Evaluation

No experimental data exist for ^{241}Cm. The data were evaluated as follows on the basis of the evaluation of ^{243}Cm. This is a new evaluation for JENDL-3.

3.1.1 Thermal energy region

Below 1 eV, the cross sections were determined as follows.

1) Fission cross section: $1/v$ shape and 700 barns at 0.0253 eV which was assumed to be almost the same as the ^{243}Cm fission cross section.
2) Capture cross section: $1/v$ shape and 140 barns at 0.0253 eV. The thermal cross section was determined from the ratio of the capture cross section to the fission cross section at 1 eV.
3) Elastic scattering cross section: a constant value of 11.9 barns which was the shape elastic scattering cross section calculated with the optical model.
4) Total cross section: sum of these three cross sections.

3.1.2 Above 1.0 eV

1) Fission cross section

The cross section was assumed to be the same as that for ^{243}Cm. The resonance structure below 1 keV was replaced with a smooth curve.

2) (n,2n) and (n,3n) reaction cross sections

These cross sections were calculated with the evaporation model.

3) Other cross sections

The total, elastic and inelastic scattering and capture cross sections were calculated with CASTHY on the basis of the optical and statistical models. The level scheme listed in Table 5 was taken from the evaluation by Ellis-Akovali[20]. A gamma-ray strength function was determined from Γ_γ = 40 meV and D = 6.6 eV, where the average level spacing D was obtained from the level density parameters as shown in Table 3.

3.2 Results

The present results are shown in Figs. 3 to 7, by comparing with ENDF/B-V evaluations made by Mann et al.[21] In the ENDF/B-V evaluation, the cross sections in the high energy region were extrapolated in the thermal energy region. Therefore, large discrepancies are found below 1 eV. Above 1 eV, both evaluations are in rather good agreement with each other in spite of no existence of available experimental data.

As shown in Fig. 7, however, large discrepancies are existing in the (n,2n) reaction cross section. The reason is the difference of the fission cross sections in this energy region. The present evaluation seems to be more reasonable.

In Table 6, the thermal cross sections and resonance integrals are compared with those of ENDF/B-V.

4. Curium-242

4.1 Recent experimental data

Since the previous evaluation for JENDL-2 was made in 1979, the following two experiments have been published.

1) Vorotnikov et al.[22)]

They measured the fission cross section of ^{242}Cm in the energy range from 0.1 to 1.4 MeV with the pulsed electrostatic accelerator at Kurchatov Institute of Atomic Energy. The T(p,n)^{3}He and ^{7}Li(p,n)^{7}Be reactions were used as neutron sources.

2) Alam et al.[23)]

The fission cross sections of ^{238}Pu and ^{242}Cm were measured in the energy range from 0.1 eV to 100 keV by using Rensselaer Intense Neutron Spectrometer (RINS) and fission chambers with semi-sphere shape. The cross sections were obtained from the measured ratio to the ^{235}U fission cross section and the ENDF/B-V evaluation for ^{235}U. Fission widths of 4 low-lying resonances were determined. The resonance integral of the fission cross section from 0.53 to 50.93 keV was 12.9 ± 0.7 barns.

4.2 Evaluation

The previous evaluation for the fission cross section is not in agreement with the two above-mentioned experiments. Therefore, the re-evaluation was made mainly for the fission cross section.

4.2.1 Resolved resonance parameters

In the previous evaluation, the fission widths were not given for all the resonances. In the present evaluation, the fission widths for the four resonances at low energies were given on the basis of the measurement by Alam et al., and the average width of 4 meV was adopted for the other resonances.

The neutron widths were taken from Altamonov et al.[24] The average radiative capture width was assumed to be 40 meV. In order to reproduce the thermal values of the fission and capture cross sections of 16 barns and 5 barns[7], respectively, a negative resonance was added at - 3.45 eV. However, even by assuming the large fission width of 8 meV to the negative resonance, the fission cross section was only 3 barns at 0.0253 eV. Therefore, the $1/v$ background cross section was added to obtain 5 barns at 0.0253 eV.

The effective scattering radius of 9.38 fm was adopted, which was determined from the shape elastic scattering cross section calculated with the optical model. The upper boundary of the resolved resonance region was selected to be 275 eV.

4.2.2 Unresolved resonance parameters

Unresolved resonance parameters were given in the energy range from 275 eV to 40 keV, so as to reproduce the fission cross section measured by Alam et al. Initial values of the parameters are;

$$R = 9.38 \text{ fm}, \quad \Gamma_\gamma = 40 \text{ meV}, \quad \Gamma_f = 4 \text{ meV}, \quad D = 18 \text{ eV},$$

$$S_0 = 0.92 \times 10^{-4}, \quad S_1 = 2.34 \times 10^{-4}, \quad S_2 = 0.97 \times 10^{-4}.$$

Those of R, Γ_γ, Γ_f and D were obtained from the resolved resonances and the strength functions from the optical model calculation. The s-wave neutron strength function is in very good agreement with the experimental value[7] of $(0.9 \pm 0.3) \times 10^{-4}$. In the parameter search with ASREP, Γ_f, S_1 and R were adjusted. Obtained parameters are listed in Table 7.

4.2.3 Cross sections above resonance region

As is shown in Fig. 9, the recent experimental data on the fission cross section are very different from the previous evaluation. The present evaluation was made by smoothly connecting the new experimental data below 1.2 MeV. The fission cross section of the previous evaluation was adopted above 1.2 MeV, because the previous evaluation is in rather good agreement with the experiments, and no experimental data are available above here.

The (n,2n) and (n,3n) reaction cross sections were calculated with the evaporation model as described in Section 2.3.

The other cross sections were calculated with CASTHY. The parameters used in the calculation are shown in Chapter 2. The three excited levels[18] taken into consideration are listed in Table 8. The gamma-ray strength function was calculated from Γ_γ = 40 meV and D = 18 eV.

4.3 Results

The present evaluation is compared with other evaluations and experimental data in Figs. 8 to 12.

The total cross section in Fig. 8 has no discrepancies between the previous and present evaluations except in the unresolved resonance region, where the previous evaluation has no unresolved resonance parameters.

As is shown in Fig.9, large improvement was made for the fission cross section on the basis of the new experiments. However, the experimental data in the thermal and MeV regions were not enough to determine the cross sections.

The capture cross section is shown in Fig.10. The present evaluation is slightly smaller than JENDL-2 because the fission cross section is larger, and the level density parameters and the gamma-ray strength functions are different from the JENDL-2 evaluation.

The thermal cross sections and resonance integrals are listed in Table 9. The reason why the resonance integral of the fission cross section is larger than the experimental value is that the value of Alam et al. was obtained below 50.93 keV. The contribution from 50.93 keV to 20 MeV is 8.9 barns. Therefore the present result is rather smaller than Alam et al.

5. Curium-243

5.1 Recent experimental data

1) Zhuravlev and Kroshkin[25)]

They measured the fission cross section of ^{243}Cm at the thermal neutron energy and resonance integral by using the SM-2 reactor, and obtained σ_f = 672 ± 6 barns and I_f = 1480 ± 150 barns.

2) Anufriev et al.[26)]

Transmission data were measured with the SM-2 reactor, and the total and neutron widths of 52 resonances from 0.671 eV to 66 eV were obtained for the single-level Breit-Wigner formula. The average values of resonance parameters were as follows,

$$D = 0.809 \text{ eV}, \qquad g\Gamma_n^{\,0} = 0.278 \text{ meV},$$

$$S = (1.714 \pm 0.408) \times 10^{-4}.$$

These values are very discrepant from those by Berreth et al.[27)] which were used for our previous evaluation[2)]. The absorption resonance integral calculated from the resonance parameters of Anufriev et al. was 1700 ± 300 barns.

3) Fomushkin et al.[28)]

The fission cross section of ^{243}Cm was measured in the energy range from 0.04 to 3.5 MeV by means of the TOF method and neutrons from nuclear explosion. Tracks of fission fragments were recorded on a film, and counted in 11 energy intervals.

5.2 Evaluation

5.2.1 Resolved resonance parameters

In the previous evaluation, the evaluation was made on the basis of data measured by Berreth et al.[27)] In the present work, the parameters obtained by Anufriev et al.[26)] were adopted.

The radiative width was assumed to be 40 meV, and the fission width of each resonance was calculated as,

$$\Gamma_f = \Gamma - (\Gamma_n + 40 \text{ meV}).$$

The total spin of the resonances was set to be the same as the spin of ^{243}Cm. The single-level Breit-Wigner formula was adopted.

In order to reproduce the thermal cross sections, a negative level was added by taking parameters recommended by Mughabghab[7]. The scattering radius of 10 fm was assumed. The upper boundary of the resolved resonance region was set at 70 eV. The capture cross section might be a little bit too small at energies from 50 eV to 70 eV because of level missing.

Figure 13 is a comparison of the fission cross sections calculated from the presently adopted parameters and from those of the previous evaluation. They are not in agreement with each other.

5.2.2 Unresolved resonance parameters

In the energy region form 70 eV to 40 keV, the unresolved resonance parameters were determined so as to reproduce the fission cross section described in the next section. The initial values of the parameters are as follows,

$$R = 10 \text{ fm}, \quad S_0 = 1.5 \times 10^{-4}, \quad S_1 = 1.2 \times 10^{-4},$$

$$S_2 = 1.7 \times 10^{-4}, \quad \Gamma_\gamma = 40 \text{ meV}, \quad \Gamma_f = 0.3 \text{ eV}, \quad D = 0.8 \text{ eV}.$$

The strength functions of p and d-wave neutrons were taken from the optical model calculation, and the others were based on the resolved resonance parameters. Those parameters were adjusted by the following procedure:

1) An average fission width was obtained by fitting the fission cross section in the energy region from 100 eV to 40 keV. The result was Γ_f = 1.48 eV.

2) Strength functions of S_0 and S_1 were adjusted so as to reproduce the fission cross section.

3) The effective scattering radius was adjusted to 9.81 fm so that the total cross section at 40 keV might be reproduced well.

The parameters thus obtained are given in Table 10.

5.2.3 Cross sections above resonance region

1) Fission cross section

The fission cross section recently measured by Fomushkin et al.[28] is smaller than that of Silbert[29] which was adopted in the previous evaluation. In the present evaluation, the previous evaluation was modified to smaller values in the energy region above 10 keV on the basis of the data of Fomushkin et al. However, compared with the calculated compound nucleus formation cross section of 3.0 barns, the cross section of 2.98 barns at 14.8 MeV measured by Fomushkin et al. is too large. The adopted value is 2.55 barns at 15 MeV.

2) Optical potential parameters

The neutron strength function of ^{243}Cm is larger than other curium isotopes. Anufriev et al.[26] obtained $S_0 = (1.714 \pm 0.408) \times 10^{-4}$, and Mughabghab[7] recommended $S_0 = (1.30 \pm 0.26) \times 10^{-4}$. The strength function calculated from the optical potential parameters for ^{241}Am is 0.9×10^{-4}. In order to get a larger calculated strength function, the constant term of the real potential V_0 was decreased from 43.4 MeV to 41 MeV. Then, one could get $S_0 = 1.5 \times 10^{-4}$ which is an average value of Anufriev et al. and Mughabghab. If V_0 is changed to 40.6 MeV, the calculated strength function is 1.71×10^{-4}. However, this potential was abandoned because the capture cross section calculated from this potential was too large at the low energies.

3) Other cross sections

The total, elastic scattering, inelastic scattering and capture cross sections were calculated with the optical and statistical models. The gamma-ray strength function was obtained from Γ_γ = 40 meV and D_0 = 0.809 eV deduced by Anufriev et al. which was much smaller than D_0 = 2.2 eV adopted in the previous evaluation.

The level scheme of ^{243}Cm was taken from that of Ellis-Akovali[20], which is given in Table 11.

5.3 Results

The present results are given in Figs. 14 to 18. Large discrepancies are found in the resonance region, because the present evaluation adopted the parameters of Anufriev et al. which were largely different from the previous evaluation.

The fission cross section is in good agreement with the experimental data below 3 MeV. Above this energy, new experiments are required to get more accurate cross section.

The present capture cross section is larger than the other evaluations, because the small level spacing of 0.809 eV obtained by Anufriev et al. was adopted and the optical potential was modified so as to get the large strength function.

The thermal cross sections and resonance integrals are listed in Table 12. The capture resonance integral which was too large in the previous evaluation was improved to be in good agreement with the experimental data. Other quantities are also in good agreement with the recent experiments within quoted errors.

6. Curium-244

6.1 Recent experimental data

1) Gavrilov and Goncharov[33]

They measured the capture cross sections and resonance integrals of ^{244}Cm, ^{245}Cm, ^{246}Cm, ^{247}Cm and ^{248}Cm with the cadmium difference method in the SM-2 reactor.

2) Fomushkin et al.[34]

The fission cross section of ^{244}Cm was measured in the neutron energy region from 0.3 to 4.0 MeV with the TOF method and neutrons from an underground nuclear explosion. The tracks of fission yields were recorded on a film, and counted with an optical microscope in 27 energy intervals. Those counts were transformed to the cross section by using the ^{235}U fission cross section measured with the same method.

3) Vorotnikov et al.[35]

The fission cross section was measured in the energy range from 0.39 to 1.3 MeV by using neutrons generated with a pulsed electrostatic accelerator (ESA) and a TiT target.

4) Maguire et al.[36]

By using the Rensselaer Intense Neutron Spectrometer (RINS), they measured the fission cross section of ^{244}Cm, ^{246}Cm and ^{248}Cm in the neutron energy range from 0.1 eV to 80 keV. Semi-sphere fission chambers of ^{235}U, ^{252}Cf and the curium samples were used. The fission cross section was determined by adopting the ^{235}U fission cross section of ENDF/B-V. For ^{244}Cm, the fission cross section was obtained in 155 energy bins and fission areas of 4 resonances were determined in the low energy.

6.2 Evaluation

6.2.1 Resolved resonance parameters

Maguire et al.[36] reported the fission areas of the 4 low-lying resonances. In the present reevaluation, the fission widths of the 4 resonances were modified with these new data. In addition to this modification, the parameters of the negative resonance at -1.48 eV were adjusted so as to reproduce the thermal cross sections; σ_f = 1.04 ± 0.20 barns and σ_{cap} = 15.2 ± 1.2 barns recommended by Mughabghab[7]. The effective scattering radius was determined so that the elastic scattering cross section might be 11.6 ± 0.7 barns at 0.0253 eV[7]. The other parameters were the same as the previous evaluation based on the data by Moore and Keyworth[37] and Benjamine et al.[42]

The multilevel Breit-Wigner formula was adopted and the upper boundary of the resolved resonance region was set at 1 keV.

6.2.2 Unresolved resonance parameters

The unresolved resonance parameters were evaluated in the energy region from 1 keV to 40 keV. In this energy region, the smooth fission cross section was determined on the basis of data measured by Maguire et al. The total and the capture cross sections were calculated with optical and statistical models as described in the next section.

The unresolved resonance parameters were determined with ASREP so as to reproduce the smooth cross sections thus determined. The initial values of the parameters were;

$$S_0 = 0.90 \times 10^{-4}, \quad S_1 = 2.54 \times 10^{-4}, \quad S_2 = 0.92 \times 10^{-4},$$

$$D = 12 \text{ eV}, \quad \Gamma_\gamma = 0.037 \text{ eV}, \quad \Gamma_f = 0.001 \text{ eV}, \quad R = 9.4 \text{ fm}.$$

The neutron strength functions were calculated with the optical model. The s-wave strength function is in very good agreement with the measured value[7] of $(0.92 \pm 0.17) \times 10^{-4}$. The values of S_1, R, Γ_f were adjusted. The results are given in Table 13.

6.2.3 Cross sections above resonance region

1) Fission cross section

After the completion of the previous evaluation, the fission cross section was measured by Fomushkin et al.[34], Vorotnikov et al.[35] and Maguire et al.[36].

The new experiment of Maguire et al. is in agreement with that of Moore and Keyworth[37] which was adopted to the previous evaluation. In the present work, the fission cross section was based on the data of Maguire et al. below 100 keV.

Between 100 keV and several MeV, the above-mentioned three experiments are available. The data of Fomushkin et al. are smaller than others, and neutron energies of their experiment seem to be shifted up about 20 %. After the correction of the energies, the three experiments and the previous evaluation are in very good agreement with each other. Therefore, the previous evaluation was adopted in the energy range from 100 keV to 800 keV. Between 800 keV and 8 MeV, new evaluation was made from the three experiments, and smoothly connected to the previous evaluation above 8 MeV.

There are two experiments at 14 MeV. The cross section of 3 barns by Fumushkin et al.[38] is not consistent with the compound nucleus formation cross section obtained from the optical model calculation. Therefore, the value of Koontz and Barton[39] of 2.6 barns adopted in the previous evaluation seems to be more reasonable.

2) Other cross sections

By considering the fission, (n,2n) and (n,3n) reactions as competing processes, the other cross sections were calculated with CASTHY. The optical potential parameters are given in Table 2. The s-wave strength fuction of 0.91×10^{-4} calculated from the optical potential parameters is in very good agreement with $(0.92 \pm 0.17) \times 10^{-4}$ recommended by Mughabghab[7]. The level scheme of ^{244}Cm listed in Table 14 was taken from Shurshikov[40]. The gamma-ray strength function was estimated from $\Gamma_\gamma = 0.037$ eV and D = 12 eV which were consistent with the resolved resonance parameters.

6.3 Results

The cross sections are shown in Figs. 19 to 23 together with the experimental data and the other evaluations.

The present total cross section in the resolved resonance region is larger than the others because the large scattering radius was adopted so as to reproduce the thermal cross section recommended by Mughabghab[7]. Above the resonance region, the evaluated data are in good agreement with each other.

Background cross section in the 1/v form for the fission cross section given in the previous evaluation was abandoned in the present evaluation. Therefore, the fission cross section between resonances is smaller than the previous evaluation.

The thermal cross sections and resonance integrals are listed in Table 15. The present results are in good agreement with the recommendation by Mughabghab[7].

7. Curium-245

7.1 Recent experimental data

1) White and Browne[43]

The ^{242m}Am and ^{245}Cm fission cross section measurements done with Livermore 100-MeV Linac in 1977 to 1980 were reviewed by White and Browne. The detail of ^{242m}Am was reported by Browne et al.[44] However, for ^{245}Cm, only this short review is available.

7.2 Evaluation

7.2.1 Resolved resonance parameters

No experiments on the resonance parameters were published after the previous evaluation, in which the parameters were evaluated on the basis of the data measured by Browne et al.[45] and Moore and Keyworth[37]. Therefore the previous evaluation was adopted in the present evaluation together with background cross sections. The upper boundary of the resolved resonance region is 60 eV.

7.2.2 Unresolved resonance parameters

The energy range from 60 eV to 40 keV was considered as the unresolved resonance region. The parameters were determined so as to reproduce the fission cross section evaluated on the basis of Moore and Keyworth[37] and the total and capture cross sections calculated with CASTHY. The following are initial values of the unresolved resonance parameters:

$$S_0 = 1.18 \times 10^{-4}, \quad S_1 = 2.60 \times 10^{-4}, \quad S_2 = 0.90 \times 10^{-4},$$

$$D = 1.4 \text{ eV}, \quad \Gamma_\gamma = 0.04 \text{ eV}, \quad \Gamma_f = 0.5 \text{ eV}, \quad R = 9.4 \text{ fm}.$$

The s-wave strength function, level spacing and radiative width are consistent with the resolved resonance parameters. The p-wave and d-wave strength functions were calculated with the optical model.

The final set of the parameters was determined by adjusting S_0, S_1, Γ_f and R. The results are listed in Table 16.

7.2.3 Cross sections above resonance region

1) Fission cross section

The measurement after the previous evaluation was made by White and Browne[43]. Their results are in good agreement with those of Moore and Keyworth below 100 keV, which was adopted in the previous evaluation. Therefore, the previous evaluation was adopted below 100 keV.

Above 100 keV, as shown in Fig. 24, White and Browne reported smaller values than Moore and Keyworth. Finally the present evaluation adopted a smooth curve determined with eye-guiding the data of White and Browne.

Above 10 MeV where no experimental data were available, the shape was estimated by considering the (n,3nf) reaction and normalized to 2.54 barns at 14 MeV.

2) Optical potential parameters

The optical potential parameters of ^{241}Am give too small capture cross section of ^{245}Cm below 60 keV. The strength function of 0.9×10^{-4} calculated with these parameters is much smaller than the value of 1.18×10^{-4} recommended by Mughabghab[7]. In the present work, the constant term of real potential was slightly modified as follows,

initial value : $V_0 = 43.4$ MeV, $S_0 = 0.90 \times 10^{-4}$, $\sigma_R = 37.1$ barns,
after modification: $V_0 = 42.7$ MeV, $S_0 = 1.02 \times 10^{-4}$, $\sigma_R = 41.9$ barns.

where σ_R is the reaction cross section calculated at 100 eV.

3) Other cross sections

The CASTHY calculation was made to obtain the other cross sections by considering the fission, (n,2n), (n,3n) and (n,4n) reactions as the competing processes. The level scheme listed in Table 17 was taken from Ref. 46. The gamma-ray strength function was determined from Γ_γ = 0.04 eV and D = 1.4 eV.

7.3 Results

The evaluated cross sections are shown in Figs. 25 to 29. The fission cross section of the present evaluation is the same as JENDL-2 below 10 keV, and smaller than JENDL-2 above this energy. The capture cross section are largely different from JENDL-2 because the different optical potential parameters and different gamma-ray strength function were used in the present evaluation. In Table 18 the thermal cross sections and resonance integrals are given. The present results in Table 18 are almost the same as JENDL-2 because the same resonance parameters were adopted in the both evaluations.

8. Curium-246

The previous evaluation was made by Kikuchi[5] in 1983. After his evaluation, Maguire et al.[36] reported their results of the fission cross section measurement. However, the data were the same as the paper by Stopa et al.[51] which were taken into account in the previous evaluation. Therefore, in the present evaluation, only the resonance parameters of the 1-st level and scattering radius were modified so as to reproduce well the thermal cross sections and resonance integrals recommended by Mughabghab[7]. The data for other quantities were taken from the evaluation by Kikuchi. The unresolved resonance parameters and the level scheme of ^{246}Cm are given in Tables 19 and 20, respectively.

The cross sections are shown in Figs. 30 to 34, by comparing with the experimental data and other evaluations. Table 21 lists the thermal cross sections and resonance integrals. The present evaluation is in better agreement with the values recommended by Mughabghab than the evaluation by Kikuchi.

9. Curium-247

9.1 Recent experimental data

1) Fomushkin et al.[52]

By using neutrons from an underground nuclear explosion and the TOF method, the fission cross section of ^{247}Cm was measured in the energy range from 0.02 to 3 MeV. Fission fragments (FF) were recorded on a polycarbonate film on a rotating drum. After the experiment, the film was divided into 24 energy intervals and the number of FF tracks were counted with a microscope. The ^{235}U fission cross section measured with the same method was used to obtain the absolute values of the ^{247}Cm fission cross section.

9.2 Evaluation

9.2.1 Resolved resonance parameters

In the energy range below 60 eV, which is the resolved resonance region, no new experimental data were available after the previous evaluation[5] which were based on the parameters obtained by Belanova et al.[53] and Moore and Keyworth.[37] Therefore, no reevaluation was needed except for the first resonance whose parameters were modified to agree well with the thermal cross sections and resonance integrals recommended by Mughabghab[7].

The single-level Breit-Wigner formula was chosen because the total spin J was unknown for all the levels.

9.2.2 Unresolved resonance parameters

The previous evaluation is in good agreement with the fission cross section measured by Moore and Keyworth[37] in the unresolved resonance region up to 30 keV. However, the s-wave strength function S_0 is quite large compared with Mughabghab's recommendation[7] of $(0.75 \pm 0.18) \times 10^{-4}$. As a result, the other cross sections of the previous evaluation seem to be too large in this energy range.

In the present evaluation, a new set of the unresolved resonance parameters was determined so as to have smaller S_0 values and to reproduce well the fission cross section of Moore et al. The initial values are as follows:

$$S_0 = 0.75 \times 10^{-4}, \quad S_1 = 2.80 \times 10^{-4}, \quad S_2 = 0.86 \times 10^{-4},$$

$$D = 1.4 \text{ eV}, \quad R = 9.23 \text{ fm}.$$

The s-wave strength function S_0 and level spacing D are the recommended values by Mughabghab[7]. The p-wave and d-wave strength functions are the values calculated with CASTHY. The fission widths were taken from the previous evaluation. The results of parameter fitting are listed in Table 22.

9.2.3 Cross sections above resonance region

1) Fission cross section

The above-mentioned new experiment by Fomushkin et al.[52] is available from 20 keV to 3 MeV. Their data are in good agreement with those by Moore and Keyworth[37] in the energy range from 100 to 300 keV, but in less agreement at the other energies. In other nuclides, the data measured by Moore and Keyworth are systematically higher than recent experiments in the MeV region. Therefore, the new experiment by Fomushkin et al. which is smaller than that of Moore and Keyworth was adopted in the high energy region. Below 200 keV, the fission cross section was determined on the basis of the data of Moore and Keyworth.

2) Other cross sections

The (n,2n), (n,3n) and (n,4n) cross sections were calculated with the evaporation model. The other cross sections were calculated with CASTHY.

The level scheme of ^{247}Cm was taken from the evaluation by Ellis-Akovali.[54] Fifteen levels up to 520 keV were taken into consideration. The levels above 550 keV were assumed to be overlapping. The level scheme is given in Table 23.

The optical potential parameters are listed in Table 2. The s-wave strength function calculated from them is 0.86×10^{-4} at 1 keV which is in agreement with $(0.75 \pm 0.18) \times 10^{-4}$ recommended by Mughabghab[7)] within the quoted error. The *gamma*-ray strength function was determined from Γ_γ = 40 meV and D = 1.4 eV.

9.3 Results

The evaluated cross sections are shown in Figs. 35 to 39. The present results are a little different from the previous evaluation in the low energy region because the parameters of the 1.25-eV resonance were modified. The evaluation of ENDF/B-V has different resonance structure below 20 eV because hypothetical levels were adopted in it. Above 20 eV, ENDF/B-V was based on the data of Moore and Keyworth and almost the same as the present evaluation.

In the unresolved resonance region, since the small strength functions were adopted, the present evaluation is smaller than the previous one except the fission cross section.

In the MeV region, the fission cross section is largely different from the previous values. Above 2 MeV, the evaluated values are not accurate because of no experimental data. The reason why there are large discrepancies between the present evaluation and the previous one for the inelastic, (n,2n) and (n,3n) cross sections is that the fission cross section was modified in the MeV region.

The thermal cross sections and resonance integrals are listed in Table 24. The present result of the resonance integral of the fission cross section seems to be too small. However, if the resonance parameters are modified so as to reproduce well the resonance integral, then the fission cross section at the thermal energy becomes too large.

10. Curium-248

The previous evaluation was made by Kikuchi and Nakagawa[6)] in 1984. Since no new experiments have made after 1984, reevaluation was not made in the present work.

In the previous evaluation, the resolved resonance parameters were evaluated on the basis of the measurements by Benjamin et al.[55] and by Moore and Keyworth.[37] The unresolved resonance parameters listed in Table 25 were determined so as to reproduce well the fission cross section measured by Stopa et al.[51] The fission cross section above the resonance region was based on the data by Fomushkin et al.[52] and by Stopa et al. up to 5.5 MeV. The gamma-ray strength function was determined from Γ_γ = 26 meV and D = 40 eV. The excited levels[56] given in Table 26 were adopted in the statistical model calculation.

The comparison between the evaluated and measured cross sections are made in Figs 40 to 44. The thermal cross sections and resonance integrals are listed in Table 27.

On the fission cross section, there are large discrepancies among the evaluated data in the resonance region. The evaluation made by Maino et al.[58], which is stored in INDL/V-85, adopted the fission width of 0.06 meV measured by Stopa et al. for the first level at 7.25 eV, and added a negative resonance at - 9 eV. On the other hand, our previous evaluation abandoned the small fission width by Stopa et al. and adopted the average value of 1.3 meV for the first level. However, the fission resonance integral of the previous evaluation seems to be too large. If this is really too large, it comes from the large fission width of the first resonance. There are also the large discrepancies in the capture cross section at the thermal energy. Further experimental study is needed for these quantities.

11. Curium-249

In the previous evaluation[6], the thermal cross sections were assumed as follows;

σ_{cap} = 1.6 barns[59],

σ_{fiss} = 0.82 barns, which was estimated from the ratio of cross sections in the unresolved resonance region,

σ_{el} = 10.8 barns, which was the shape elastic scattering cross section calculated with the optical model,

σ_{tot} = 13.22 barns.

The thermal energy region was assumed below 4.15 eV which was the energy of a half of the level spacing estimated from level density parameters.

The cross sections between 4.15 eV and 30 keV were represented with the unresolved resonance parameters listed in Table 28.

The fission cross section was assumed to be

$$\sigma_f(^{249}\mathrm{Cm}) = 0.95 \times \sigma_f(^{247}\mathrm{Cm}),$$

where the factor of 0.95 was determined from the systematics by Behrens and Howerton[60]. The level scheme[56] used in the previous evaluation is given in Table 29. The gamma-ray strength function was calculated from Γ_γ = 40 meV and D = 8.3 eV.

The cross sections are shown in Figs. 45 to 48. The thermal cross sections and resonance integrals are given in Table 30. In the present work, the previous evaluation was adopted without any modification.

12. Number of Neutrons per Fission

The evaluation method of ν is mentioned in Section 2.7. The results are given below;

1) ^{241}Cm

$\nu_p = 3.39 + 0.166\ E_n$

$\nu_d = 0.00146\ (E_n < 6\ \mathrm{MeV}),\ 0.00102\ (E_n > 8\ \mathrm{MeV})$

2) ^{242}Cm

$\nu_p = 3.25 + 0.172\ E_n$

$\nu_d = 0.00209\ (E_n < 6\ \mathrm{MeV}),\ 0.00146\ (E_n > 8\ \mathrm{MeV})$

3) ^{243}Cm

$\nu_p = 3.43 + 0.178\ E_n$

(The constant term was based on the measurements by Jaffy and Lerner[61] and Zhuravlev et al.[62])

$\nu_d = 0.00301\ (E_n < 6\ \mathrm{MeV}),\ 0.00209\ (E_n > 8\ \mathrm{MeV})$

4) ^{244}Cm

$$\nu_p = 3.24 + 0.184\ E_n$$
$$\nu_d = 0.00435\ (E_n < 6\ \text{MeV}),\ 0.00301\ (E_n > 8\ \text{MeV})$$

5) ^{245}Cm

$$\nu_p = 3.60 + 0.08\ E_n$$
(taken from the recent measurement by Howe et al.[63])
$$\nu_d = 0.00630\ (E_n < 6\ \text{MeV}),\ 0.00435\ (E_n > 8\ \text{MeV})$$

The constant term of ν_p is smaller than the measured values by Jaffy and Lerner[61], Kroshkin and Zamyatnin[64] and Zhuravlev et al.[62] The coefficient of the energy dependent term is also much smaller than 0.190 obtained from Howerton's systematics.

6) ^{246}Cm

$$\nu_p = 3.19 + 0.196\ E_n$$
$$\nu_d = 0.00916\ (E_n < 6\ \text{MeV}),\ 0.00630\ (E_n > 8\ \text{MeV})$$

7) ^{247}Cm

$$\nu_p = 3.79 + 0.202\ E_n$$
(The constant term was taken from Zhuravlev et al.[62])
$$\nu_d = 0.0134\ (E_n < 6\ \text{MeV}),\ 0.00916\ (E_n > 8\ \text{MeV})$$

8) ^{248}Cm

$$\nu_p = 3.11 + 0.208\ E_n$$
$$\nu_d = 0.0196\ (E_n < 6\ \text{MeV}),\ 0.0134\ (E_n > 8\ \text{MeV})$$

9) ^{249}Cm

$$\nu_p = 3.32 + 0.214\ E_n$$
$$\nu_d = 0.0288\ (E_n < 6\ \text{MeV}),\ 0.0196\ (E_n > 8\ \text{MeV})$$

13. Concluding Remarks

The neutron nuclear data of curium isotopes were reevaluated in the present work. In particular, the recently published experiments on the fission and capture cross sections were reviewed, and our previous evaluations were modified on the basis of them. The quantities evaluated or modified are summarized in Table 31. The fission cross section of ^{242}Cm was largely improved. The other data, except ^{248}Cm and ^{249}Cm, were modified more or less. The data of ^{241}Cm were newly evaluated in the present work. The results were compiled in ENDF-5 format and stored in the latest version of Japanese Evaluated Nuclear Data Library, JENDL-3.

Acknowledgements

The author thanks to Dr. Y. Kikuchi and Dr. Y. Nakajima of the Nuclear Data Center, JAERI, for their advice on the present work and for valuable comments on the manuscript of the present report, and to Dr. K. Shirakata of PNC for his support of this work.

He also appreciates Miss S. Ishibashi's careful typewriting the manuscript.

References

1) S. Igarasi and T. Nakagawa: "Evaluation of Neutron Nuclear Data for ^{242}Cm", JAERI-M 8342 (1979).
2) T. Nakagawa and S. Igarasi: "Evaluation of Neutron Nuclear Data for ^{243}Cm", JAERI-M 9601 (1981).
3) S. Igarasi and T. Nakagawa: "Evaluation of Neutron Nuclear Data for ^{244}Cm", JAERI-M 7175 (1977).
4) S. Igarasi and T. Nakagawa: "Evaluation of Neutron Nuclear Data for ^{245}Cm", JAERI-M 7733 (1978).
5) Y. Kikuchi: "Evaluation of Neutron Nuclear Data for ^{246}Cm and ^{247}Cm", JAERI-M 83-236 (1984).
6) Y. Kikuchi and T. Nakagawa: "Evaluation of Neutron Nuclear Data for ^{248}Cm and ^{249}Cm", JAERI-M 84-116 (1984).
7) S.F. Mughabghab: "Neutron Cross Sections, vol.1, Neutron Resonance Parameters and thermal Cross Sections, part B", Academic Press, (1984).
8) Y. Kikuchi: private communication.
9) S. Pearlstein: Nucl. Sci. Eng. 23, 238 (1965).
10) T. Nakagawa: J. Atomic Energy Soc. of Japan, 22, 559 (1980) [in Japanese].
11) S. Igarasi: J. Nucl. Sci. Technol. 12, 67 (1975).
12) A. Gilbert and A.G.W. Cameron: Canadian J. Phys. 43, 1446 (1965).
13) Y. Kikuchi: private communication.
14) A. Smith, P. Guenther, G. Winkler and R. Mcknight: "Prompt-Fission-Neutron Spectra of ^{233}U, ^{235}U, ^{239}Pu and ^{240}Pu Relative to that of ^{252}Cf", ANL/NDM-50 (1979).
15) R.J. Howerton: Nucl. Sci. Eng. 62, 438 (1977).
16) R.J. Tuttle: Proc. Consultant's Meeting on Delayed Neutron Properties, 1979 Vienna, INDC(NDS)-107/G+Special, p.29 (1979).
17) T.W. Phillips and R.E. Howe: Nucl. Sci. Eng., 69, 375 (1979).
18) ENSDF: Evaluated Nuclear Structure Data File, as is Jan. 1989.
19) A.H. Wapstra and K. Bos: Atomic Data and Nucl. Data Tables, 19, No.3 (1977).
20) Y.A. Ellis-Akovali: Nucl. Data Sheets, 44, 407 (1985).

21) T.R. England, W.B. Wilson, R.E. Schenter and F.M. Mann: "Summary of ENDF/B-V Data for Fission Products and Actinides", EPRI NP-3787 (ENDF-322) (1984).

22) P.E. Vorotnikov, S.V. Dmitriev, Yu.D. Molchanov, G.A. Otroshchenko, V.A. Pchelin, L.V. Chistyakov and A.N. Smirnov: Sov. J. Nucl. Phys. 40, 726 (1984).

23) B. Alam, R.C. Block, R.E. Slovacek and R.W. Hoff: Nucl. Sci. Eng., 99, 267 (1988).

24) V.S. Altamonov, R.N. Ivanov, S.M. Kalebin, G.V. Rukolaine, V.A. Anufriev, S.I. Babich, T.S. Belanova, N.G. Kocherygin, A.G. Kolosov, S.N. Nikolskii, V.N. Nefedov, V.A. Poruchikov, V.A. Safonov and V.V. Tihomirov: Proc. of 4th All Union Conf. on Neutron Physics, Kiev 1977, vol.2, 257 (1977).

25) K.D. Zhuravlev and N.I. Kroshkin: Sov. Atomic Energy, 47, 565 (1980).

26) V.A. Anufriev, S.I. Babich, N.G. Kocherygin, V.M. Lebedev, S.N. Nikl'skii, V.N. Nefedov, V.M. Nikolaev, V.A. Poruchikov and A.A. Elesin: Sov. Atomic Energy, 51, 736 (1982).

27) J.R. Berreth, F.B. Simpson and B.C. Rusche: Nucl. Sci. Eng., 49, 145 (1972).

28) É.F. Fomushkin, G.F. Novoselov, Yu.I. Vinogradov, V.N. Vyachin, V.V. Gavrilov, A.S. Koshelev, V.N. Polynov, V.M. Surin and A.M. Shvetsov: Sov. Atomic Energy, 62, 337 (1987).

29) M.G. Silbert: "Fission Cross Section of ^{243}Cm from the Underground Nuclear Explosion, Physics-8", LA-6239 (1976).

30) H. Ihle, H. Michael, A. Neubert, A.J.F. Blair, P. Damle and M.V. Bodnarescu: J. Inorg. Nucl. Chem. 34, 2427 (1972).

31) C.E. Bemis Jr., J.H. Oliver, R. Eby and J. Halperin: Nucl. Sci. Eng., 63, 413 (1977).

32) M.C. Thompson, M.L. Hyder and R.J. Reuland: J. Inorg. Nucl. Chem., 33, 1553 (1971).

33) V.D. Gavrilov and V.A. Goncharov: Sov. Atomic Energy, 44, 274 (1978).

34) É.F. Fomushkin, G.F. Novoselov, Yu.I. Vinogradov, V.V. Gavrilov and V.A. Zherebtsov: Sov. J. Nucl. Phys. 31, 19 (1980).

35) P.E. Vorotnikov, L.D. Kozlov and Yu.D. Molchanov: Sov. Atomic Energy, 57, 504 (1985).

36) H.T. Maguire Jr., C.R.S. Stopa, R.C. Block, D.R. Harris, R.E. Slovacek, J.W.T. Dabbs, R.J. Dougan, R.W. Hoff and R.W. Lougheed: Nucl. Sci. Eng., 89, 293 (1985).
37) M.S. Moore and G.A. Keyworth: Phys. Rev., C3, 1656 (1971).
38) E.F. Fomushkin, E.K. Gutnikova, Yu.S. Zamyatnin, B.K. Maslennikov, V.N. Below, V.M. Surin, F. Nasyrov and N.F. Pashkin: Sov. J. Nucl. Phys., 5, 689 (1967).
39) P.G. Koontz and D.M. Barton: Proc. of Conf. on Nucl. Cross section and Technol., 1968 Washington, 597 (1968).
40) E.N. Shurshikov: Nucl. Data Seets, 49, 785 (1986).
41) B. Goel, and B. Krieg: "Status of the Nuclear Data Library KEDAK-4", KfK-3838 (1984).
42) R.W. Benjamin, K.W. MacMurdo and J.D. Spencer: Nucl. Sci. Eng., 47, 203 (1972).
43) R.M. White and J.C. Browne: Proc. of International Conf. on Nucl. Data for Science and Technol, 1983 Antwerp, 218 (1983).
44) J.C. Browne, R.M. White, R.E. Howe, J.H. Landrum, R.J. Dougan and R.J. Dupzyk: Phys. Rev., C29, 2188 (1984).
45) J.C. Browne, R.W. Benjamin and D.G. Karraker: Nucl. Sci. Eng., 65, 166 (1978).
46) Y.A. Ellis-Akovali: Nucl. Data Sheet, 33, 119 (1981).
47) J. Halperin, R.E. Drusched and R.E. Eby: "Thermal Neutron Capture Cross Section and Resonance Integral of ^{245}Cm and ^{246}Cm", ORNL-4437, p.20 (1969).
48) J. Halperin, H.H. Oliver and R.W. Stoughton: "The Fission Thermal-Neutron Cross Section and Resonance Integral of ^{245}Cm ^{247}Cm and ^{249}Cf", ORNL-4581, p.37 (1970).
49) K.D. Zhuravlev, N.I. Kroshkin and A.D. Chetverikov: Sov. Atomic Energy, 39, 907 (1976).
50) V.D. Garrilov, V.A. Goncharov, V.V. Ivanenko, V.N. Kustov and V.P. Smirnov: Sov. Atomic Energy, 41, 808 (1977).
51) C.R.S. Stopa, H.T. Maguire Jr., D.R. Harris, R.C. Block, R.E. Slovacek, J.W.T. Dabbs, R.J. Dougan, R.W. Hoff and R.W. Lougheed: ANS Topical Meeting on Advances in Reactor Physics and Core Thermal Hydraulics, 1982 Kiamesha Lake, New York, p.1090 (1982).

52) É.F. Fomushkin, G.F. Novoselov, Yu.I. Vinogradov, V.V. Gavrilov and V.A. Zherebtsov: Sov. Atomic Energy, 62, 340 (1987).

53) T.B. Belanova, A.G. Kolesov, A.V. Klinov, S.N. Nikol'skii, V.A. Poruchikov, V.N. Nefedov, V.S. Artamonov, R.N. Ivanov and S.M. Kalebin: Sov. Atomic Energy, 47, 772 (1979).

54) Y.A. Ellis-Akovali: Nucl. Data Sheets, 33, 161 (1981).

55) R.W. Benjamin, C.E. Ahlfeld, J.A. Harvey and N.W. Hill: Nucl. Sci. Eng., 55, 440 (1974).

56) C.M. Lederes and V.S. Shirley: "Table of Isotopes", 7th Ed. (1978).

57) R.E. Drushel, R.D. Baybarz and J. Halperin: "Chemistry Division Annual Progress Report for Period Ending May 20, 1973", p.23, ORNL-4891 (1973).

58) G. Maino, M. Rosetti, M.Vaccari and A. Ventura: "Evaluation of Cm-248 Neutron Cross Sections from 10^{-5} eV to 15 MeV", INDC(ITY)-10 (1983).

59) H. Diamond, C.M. Stevens, D.N. Metta, J.L. Lerner and F.R. Kelly: "Curium-250 Production in High-Flux Reactor", ANL-7330 (1967).

60) J.W. Behrens and R.J. Howerton: Nucl. Sci. Eng., 65, 464 (1978).

61) A.H. Jaffey and J.L. Lerner: Nucl. Phys. A145, 1 (1970).

62) K.D. Zhuravlev, Yu.S. Zamyatnin, N.I. Kroshkin: Proc. 2nd All Union Conf. Neutron Physics, 1973 Kiev, vol.4, p.57 (1973) [in Russian].

63) R.E. Howe, R.M. White, J.C. Browne, J.H. Landrum, R.J. Dougan, R.W. Lougheed and R.J. Dupzyk: Nucl. Phys., A407, 193 (1983).

64) N.I. Kroshkin and Yu.S. Zamyatnin: Sov. Atomic Energy, 29, 790 (1970).

Table 1 Previous evaluations of curium isotopes

Nuclide	evaluators	year	reference
^{242}Cm	S. Igarasi, T. Nakagawa	1979	1
^{243}Cm	T. Nakagawa, S. Igarasi	1981	2
^{244}Cm	S. Igarasi, T. Nakagawa	1977	3
^{245}Cm	S. Igarasi, T. Nakagawa	1977	4
^{246}Cm	Y. Kikuchi	1983	5
^{247}Cm	Y. Kikuchi	1983	5
^{248}Cm	Y. Kikuchi, T. Nakagawa	1984	6
^{249}Cm	Y. Kikuchi, T. Nakagawa	1984	6

Table 2 Optical potential parameters

$V_0 = 43.4 - 0.107\ E_n$ (MeV)

$\quad 42.0 - 0.107\ E_n$ (MeV) for ^{241}Cm,

$\quad 41.0 - 0.107\ E_n$ (MeV) for ^{243}Cm,

$\quad 42.7 - 0.107\ E_n$ (MeV) for ^{245}Cm

$W_s = 6.95 - 0.339\ E_n + 0.0531\ E_n^{\,2}$ (MeV)

$V_{so} = 7.0$ (MeV)

$r_0 = r_{so} = 1.282$ (fm)

$r_s = 1.29$ (fm)

$a = a_{so} = 0.60$ (fm)

$b = 0.5$ (fm)

Potential V(r) is given as

$$V(r) = -V_0 f_1(r) - iW_s f_2(r) - V_{so}\left(\frac{\hbar}{m_\pi c}\right)^2 \left|\frac{df_3(r)}{dr}\right| \frac{1}{r}(\vec{\sigma}\cdot\vec{\ell}),$$

where

$$f_1(r) = 1/[1 + \exp(\frac{r-R_0}{a})],$$

$$f_2(r) = 4\exp(\frac{r-R_s}{b})/[1 + \exp(\frac{r-R_s}{b})]^2,$$

$$f_3(r) = 1/[1 + \exp(\frac{r-R_{so}}{a_{so}})],$$

$$R_0 = r_0 A^{1/3},$$

$$R_s = r_s A^{1/3},$$

$$R_{so} = r_{so} A^{1/3}.$$

Table 3 Level density parameters for curium isotopes

Nuclides	a (MeV^{-1})	T (MeV)	Δ (MeV)	α_M ($MeV^{-1/2}$)	E_x (MeV)	C_0 (MeV^{-1})	D_0^{cal} (eV)	D_0^{Exp} (eV)
239	28.0	0.4	0.72	29.75	3.886	7.582		-
240	27.0	0.4	1.21	29.30	4.200	1.6206		-
241	28.57	0.378	0.72	30.22	3.560	5.287	6.6	-
242	28.0	0.4	0.15	30.00	4.3163	2.5771	1.8	-
243	28.0	0.4	0.72	30.08	3.8863	7.5405	18	25 ± 8
244	28.0	0.395	1.22	30.17	4.2893	1.8807	1.0	1.1 ± 0.2
245	30.0	0.391	0.72	31.31	4.0295	11.288	12	12.0 ± 1.0
246	27.7	0.395	1.11	30.17	4.1307	2.2560	1.4	1.4 ± 0.1
247	29.3	0.408	0.72	31.11	4.2678	13.967	34	34 ± 7
248	31.0	0.385	1.623	32.09	4.9631	1.2545	1.6	1.4 ± 0.3
249	32.0	0.370	0.72	32.69	3.8937	11.680	37	33 ± 5
250	30.0	0.4	1.585	31.74	5.0821	1.6351	20	-

D_0^{cal} : Calculated from the level density parameter a.
D_0^{exp} : Resonance level specing recommended by Mughabghab[7].

Table 4 Q-values and threshold energies of (n,2n), (n,3n) and (n,4n) reactions

Unit:MeV

Nuclide	(n,2n)	(n,3n)	(n,4n)
^{241}Cm	-6.0877	-13.5374	-19.9171
	6.1132	13.5940	20.0004
^{242}Cm	-6.9662	-13.0539	-20.5036
	6.9952	13.1083	20.5890
^{243}Cm	-5.6958	-12.6620	-18.7497
	5.7194	12.7145	18.8275
^{244}Cm	-6.7995	-12.4953	-19.4615
	6.8276	12.5469	19.5419
^{245}Cm	-5.5200	-12.3195	-18.0153
	5.5427	12.3702	18.0894
^{246}Cm	-6.4570	-11.9770	-18.7765
	6.4835	12.0261	18.8534
^{247}Cm	-5.1577	-11.6147	-17.1347
	5.1787	11.6621	17.2046
^{248}Cm	-6.2127	-11.3704	-17.8274
	6.2380	11.4166	17.8999
^{249}Cm	-4.7127	-10.9254	-16.0831
	4.7318	10.9696	16.1482

Upper: Q-value
Lower: threshold energy

Table 5 Level scheme of ^{241}Cm

No.	Energy (keV)	Spin and parity
Gr.	0.0	1/2 +
1	53.0	3/2 +
2	103.0	5/2 +
3	157.0	7/2 +
4	255.0	9/2 +

Levels above 350 keV were assumed to be overlapping.

Table 6 Thermal cross sections and resonance integrals of ^{241}Cm

Quantity	Reference	(barns)
σ_{cap}	ENDF/B-V[21]	250.3
	Present	140.0
σ_{fiss}	ENDF/B-V	2599
	Present	700.0
σ_{tot}	ENDF/B-V	2862
	Present	851.9
RI_{cap}	ENDF/B-V	112
	Present	160
RI_{fiss}	ENDF/B-V	1180
	Present	969

Table 7 Energy dependence of the unresolved resonance parameters and the calculated cross sections for ^{242}Cm

Energy independent parameters

$R = 9.093$ fm, $S_0 = 0.92 \times 10^{-4}$, $S_2 = 0.97 \times 10^{-4}$,
$\Gamma_\gamma = 40$ meV

E_n (keV)	Γ_f (meV)	S_1 ($\times 10^{-4}$)	D_{obs} (eV)	σ_{tot} (b)	σ_{cap} (b)	σ_{fiss} (b)
0.275	8.25	3.04	17.99	33.43	8.98	1.59
0.3	8.21	3.04	17.99	32.46	8.45	1.49
0.4	8.78	3.04	17.98	29.55	6.86	1.29
0.5	9.41	3.04	17.98	27.57	5.83	1.17
0.6	9.85	3.04	17.98	26.11	5.12	1.07
0.7	9.95	3.04	17.97	24.98	4.59	0.974
0.8	9.73	3.04	17.97	24.07	4.20	0.875
0.9	9.53	3.04	17.97	23.32	3.88	0.795
1.0	9.30	3.04	17.96	22.68	3.62	0.726
1.5	10.9	3.04	17.94	20.54	2.76	0.636
2.0	13.0	3.04	17.92	19.28	2.29	0.617
3.0	16.3	3.04	17.89	17.81	1.81	0.589
4.0	17.9	3.04	17.85	16.95	1.56	0.550
5.0	18.8	3.04	17.81	16.37	1.41	0.519
6.0	18.7	3.04	17.78	15.95	1.32	0.480
8.0	18.0	3.04	17.70	15.38	1.19	0.420
10.0	17.0	3.02	17.63	14.99	1.11	0.374
15.0	17.8	3.02	17.44	14.42	0.956	0.338
20.0	18.6	3.03	17.26	14.10	0.854	0.318
25.0	17.8	3.12	17.08	13.94	0.791	0.287
30.0	19.1	3.05	16.91	13.74	0.719	0.280
35.0	19.1	3.27	16.73	13.77	0.685	0.270
40.0	20.0	3.22	16.56	13.65	0.635	0.265

Table 8 Level scheme of ^{242}Cm

No.	Energy(keV)	Spin and parity	
Gr	0.0	0	+
1	42.13	2	+
2	138.0	4	+
3	284.0	6	+

Levels above 350 keV were assumed to be overlapping.

Table 9 Thermal cross section and resonance integrals of ^{242}Cm

Quantity	Reference	(barns)
σ_{cap}	Mughabghab[7]	16 ± 5
	ENDF/B-V[21]	16.87
	JENDL-2[1]	15.92
	Present	15.90
σ_{fiss}	Mughabghab	< 5
	ENDF/B-V	3.02
	JENDL-2	5.0
	Present	5.06
σ_{tot}	ENDF/B-V	30.69
	JENDL-2	32.53
	Present	32.57
RI_{cap}	Mughabghab	110 ± 20
	ENDF/B-V	111
	JENDL-2	116
	Present	106
RI_{fiss}	88 Alam[23]	12.9 ± 0.7 (< 50.93 keV)
	ENDF/B-V	6.25
	JENDL-2	11.1
	Present	19.9

Table 10 Energy dependence of unresolved resonance parameters and the calculated cross sections for ^{243}Cm

Energy independent parameters

$R = 9.8096$ fm, $S_2 = 1.70 \times 10^{-4}$, $\Gamma_\gamma = 40$ meV, $\Gamma_f = 1.481$ eV

E_n (keV)	S_0 (10^{-4})	S_1 (10^{-4})	D_{obs} (eV)	σ_{tot} (b)	σ_{cap} (b)	σ_{fiss} (b)
0.07	1.81	1.45	0.800	101.5	14.88	72.0
0.08	1.61	1.29	0.800	86.5	12.44	60.0
0.10	1.26	1.01	0.800	64.1	8.77	42.0
0.15	1.07	0.853	0.800	48.0	6.04	29.0
0.20	1.04	0.832	0.800	42.4	5.07	24.5
0.25	1.09	0.875	0.800	40.6	4.71	23.0
0.30	1.10	0.876	0.800	38.2	4.27	21.0
0.35	1.01	0.811	0.799	34.4	3.66	18.0
0.40	0.994	0.795	0.799	32.6	3.35	16.5
0.50	1.08	0.865	0.799	32.0	3.20	16.0
0.60	1.19	0.951	0.799	32.1	3.15	16.0
0.70	1.25	0.998	0.799	31.5	3.01	15.5
0.80	1.29	1.04	0.799	30.9	2.88	15.0
1.0	1.32	1.06	0.799	29.4	2.59	13.7
1.5	1.31	1.05	0.798	26.0	2.04	11.0
2.0	1.32	1.06	0.797	24.2	1.74	9.60
3.0	1.32	1.05	0.796	21.9	1.38	7.80
4.0	1.34	1.08	0.794	20.8	1.19	6.90
5.0	1.37	1.10	0.792	20.0	1.07	6.30
6.0	1.38	1.10	0.791	19.3	0.968	5.80
8.0	1.39	1.12	0.788	18.3	0.833	5.10
10.0	1.43	1.14	0.786	17.7	0.753	4.70
15.0	1.48	1.18	0.779	16.7	0.630	4.05
20.0	1.50	1.20	0.771	16.0	0.558	3.65
30.0	1.53	1.23	0.758	15.1	0.479	3.20
40.0	1.53	1.22	0.744	14.5	0.430	2.90

Table 11 Level scheme of ^{243}Cm

No.	Energy (keV)	Spin and prity	
Gr.	0.0	5/2	+
1	42.0	7/2	+
2	87.4	1/2	+
3	94.0	9/2	+
4	94.0	3/2	+
5	133.0	7/2	+
6	153.0	11/2	+
7	164.0	9/2	+
8	219.0	13/2	+
9	228.0	11/2	+
10	260.0	9/2	+
11	530.0	15/2	-
12	729.0	1/2	-
13	769.0	3/2	-

Levels above 842 keV were assumed to be overlapping.

Table 12 Thermal cross sections and resonance integrals of ^{243}Cm

Quantity	Reference	(barns)
σ_{cap}	72 Ihle[30]	200
	77 Bemis[31]	137.4 ± 9.6 [σ(0.0253 eV) = 130.7 ± 9.6]
	Mughabghab[7]	130 ± 10
	ENDF/B-V[21]	58
	JENDL-2[2]	131.3
	Present	130.2
σ_{fis}	72 Ihle	750
	77 Bemis	633.3 ± 26.9 [σ(0.0253 eV)=609.6 ± 25.9]
	80 Zhuravlev[25]	672 ± 60
	Mughabghab	617 ± 20
	ENDF/B-V	691.2
	JENDL-2	612.3
	Present	617.4
σ_{abs}	Mughabghab	747 ± 23
	Present	747.6
σ_{tot}	ENDF/B-V	755.8
	JENDL-2	753.3
	Present	757.5
RI_{cap}	77 Bemis	214.4 ± 20.3
	Mughabghab	215 ± 20
	ENDF/B-V	249
	JENDL-2	404
	Present	232
RI_{fis}	71 Thompson[32]	1860 ± 400
	77 Bemis	1575 ± 136
	80 Zhuravlev	1480 ± 150
	Mughabghab	1570 ± 100
	ENDF/B-V	1950
	JENDL-2	1750
	Present	1560
RI_{abs}	72 Berreth[27]	2345 ± 470
	82 Anufriev[26]	1770 ± 300
	ENDF/B-V	2199
	JENDL-2	2114
	Present	1792

Table 13 Energy dependence of unresolved resonance parameters and the calculated cross sections for ^{244}Cm

Energy independent parameters

$R = 9.2208$ fm, $S_0 = 0.9 \times 10^{-4}$, $S_2 = 0.92 \times 10^{-4}$

$\Gamma_\gamma = 37$ meV

E_n (keV)	Γ_f (meV)	S_1 (10^{-4})	D_{obs} (eV)	σ_{tot} (b)	σ_{cap} (b)	σ_{fiss} (b)
1.0	2.44	3.06	11.98	22.72	4.49	0.279
2.0	2.87	2.91	11.95	19.37	2.88	0.209
3.0	3.08	2.89	11.93	17.92	2.30	0.178
4.0	3.15	2.88	11.90	17.07	2.00	0.158
5.0	3.17	2.88	11.88	16.50	1.81	0.144
7.0	3.16	2.87	11.83	15.77	1.59	0.126
10.0	3.06	2.87	11.75	15.14	1.41	0.108
20.0	2.87	2.90	11.51	14.26	1.12	0.0815
30.0	2.81	2.93	11.27	13.91	0.961	0.0690
40.0	2.79	2.96	11.04	13.71	0.855	0.0613

Table 14 Level scheme of ^{244}Cm

No.	Energy (keV)	Spin and parity	
Gr	0.0	0	+
1	42.97	2	+
2	142.35	4	+
3	296.21	6	+
4	501.79	8	+
5	970.0	2	+
6	984.91	0	+
7	1020.8	2	+
8	1038.0	2	+
9	1040.2	6	+
10	1084.2	1	+
11	1105.9	1	-
12	1187.0	2	+

Levels above 1.2 MeV were assumed to be overlapping.

Table 15 Thermal cross sections and resonance integrals of ^{244}Cm

Quantity	Reference	(barns)
σ_{cap}	71 Thompson[32]	14 ± 4
	78 Gavrilov[33]	15.2 ± 1.2
	Mughabghab[7]	15.2 ± 1.2
	ENDF/B-V[21]	10.36
	KEDAK-4[41]	14.40
	JENDL-2[3]	14.41
	Present	15.10
σ_{fis}	71 Thompson	1.5 ± 1.0
	Mughabghab	1.04 ± 0.20
	ENDF/B-V	0.604
	KEDAK-4	1.03
	JENDL-2	1.18
	Present	1.037
σ_{ela}	Mughabghab	11.6 ± 0.7
	Present	11.06
σ_{tot}	72 Berreth[27]	23 ± 3
	Mughabghab	27.6 ± 1.4
	ENDF/B-V	17.95
	KEDAK-4	23.00
	JENDL-2	22.24
	Present	27.20
RI_{cap}	71 Thompson	650 ± 50
	72 Berreth	605 ± 40 (from res. params.)
	78 Gavrilov	626 ± 53
	Mughabghab	650 ± 30
	ENDF/B-V	594
	KEDAK-4	637
	JENDL-2	594
	Present	661
RI_{fis}	71 Thompson	12.5 ± 2.5
	72 Benjamin[42]	18.0 ± 1.0
	Mughabghab	12.5 ± 2.5
	ENDF/B-V	18.7
	KEDAK-4	19.1
	JENDL-2	18.4
	Present	13.2

Table 16 Energy dependence of unresolved resonance parameters and the calculated cross sections for ^{245}Cm

Energy independent parameters

$R = 9.43$ fm, $S_0 = 1.02 \times 10^{-4}$, $S_1 = 2.24 \times 10^{-4}$,
$S_2 = 0.9 \times 10^{-4}$, $\Gamma_\gamma = 40$ meV

E_n (keV)	Γ_f (meV)	D_{obs} (eV)	σ_{tot} (b)	σ_{cap} (b)	σ_{fiss} (b)
0.06	1.65	1.400	65.31	8.63	44.17
0.08	1.69	1.400	58.06	7.32	38.28
0.10	1.71	1.400	53.13	6.46	34.24
0.20	1.79	1.399	40.88	4.34	24.21
0.30	1.83	1.399	35.46	3.43	19.77
0.50	1.91	1.399	30.04	2.53	15.34
0.70	1.96	1.398	27.16	2.07	12.99
1.0	2.01	1.397	24.56	1.65	10.91
2.0	1.99	1.395	20.76	1.11	7.81
3.0	1.98	1.392	19.09	0.898	6.45
5.0	2.00	1.387	17.43	0.713	5.12
7.0	1.91	1.381	16.52	0.627	4.38
10.0	1.77	1.374	15.81	0.568	3.85
20.0	1.72	1.348	14.67	0.464	3.12
30.0	1.44	1.322	14.17	0.451	2.79
40.0	1.32	1.298	13.83	0.429	2.62

Table 17 Level scheme of ^{245}Cm

No.	Energy (keV)	Spin and parity	
Gr	0.0	7/2	+
1	54.8	9/2	+
2	121.5	11/2	+
3	197.4	13/2	+
4	252.85	5/2	+
5	295.8	7/2	+
6	350.86	9/2	+
7	355.95	1/2	+
8	361.5	3/2	+
9	388.3	9/2	-
10	416.7	11/2	+
11	418.8	5/2	+
12	431.0	5/2	+
13	442.9	11/2	-
14	498.0	13/2	+
15	509.1	13/2	-
16	532.0	9/2	+
17	555.0	11/2	+
18	633.65	3/2	-
19	643.5	7/2	-
20	661.55	5/2	-
21	701.8	9/2	-
22	722.0	7/2	+
23	741.0	1/2	+

Some levels with higher spin than 13/2 or whose spin was unknown were neglected. Levels above 770 eV were assumed to be overlapping.

Table 18 Thermal cross sections and resonance integrals of ^{245}Cm

Quantity	Reference	(barns)
σ_{cap}	69 Halperin[47]	340 ± 20
	71 Thompson[32]	360 ± 50
	78 Gavrilov[33]	350 ± 18
	Mughabghab[7]	369 ± 17
	ENDF/B-V[21]	383.0
	JENDL-2[4]	346.4
	Present	346.4
σ_{fiss}	70 Halperin[48]	1920 ± 180
	71 Thompson	2030 ± 200
	72 Benjamin[42]	2018 ± 37
	76 Zhuravlev[49]	2070 ± 150
	77 Gavrilov[50]	1900 ± 100
	78 Browne[45]	2143 ± 58
	Mughabghab	2145 ± 58
	ENDF/B-V	2161.0
	JENDL-2	2000.7
	Present	2000.7
σ_{tot}	72 Berreth[27]	2900 ± 450
	ENDF/B-V	2556.0
	JENDL-2	2358.6
	Present	2358.6
RI_{cap}	69 Halperin	101 ± 8
	71 Thompson	110 ± 20
	78 Gavrilov	108 ± 81
	Mughabghab	101 ± 8
	ENDF/B-V	118
	JENDL-2	108
	Present	110
RI_{fiss}	70 Halperin	1140 ± 100
	71 Thompson	750 ± 150
	72 Benjamin	772 ± 40
	76 Zhuravlev	805 ± 80
	77 Gavrilov	850 ± 60
	Mughabghab	840 ± 40
	ENDF/B-V	833
	JENDL-2	799
	Present	801
RI_{abs}	72 Berreth	897 ± 180
	ENDF/B-V	951
	JENDL-2	907
	Present	911

Table 19 Energy dependence of unresolved resonance parameters and the calculated cross sections for ^{246}Cm 5)

Energy independent parameters

$S_0 = 0.94 \times 10^{-4}$, $S_1 = 3.17 \times 10^{-4}$, $S_2 = 0.88 \times 10^{-4}$
$R = 9.15$ fm, $\Gamma_\gamma = 31$ meV

E_n (keV)	Γ_f (meV)	D_{obs} (eV)	σ_{tot} (b)	σ_{cap} (b)	σ_{fiss} (b)
0.33	2.02	31.7	32.0	5.40	0.336
0.35	2.25	31.7	31.4	5.15	0..356
0.4	1.87	31.7	30.1	4.68	0.271
0.45	1.47	31.7	29.0	4.30	0.198
0.5	1.30	31.7	28.1	3.99	0.163
0.55	1.30	31.7	27.3	3.72	0.152
0.6	1.48	31.7	26.6	3.49	0.161
0.7	2.00	31.7	25.4	3.11	0.192
0.8	2.56	31.7	24.5	2.82	0.220
0.9	2.49	31.7	23.7	2.60	0.198
1.0	2.20	31.7	23.1	2.44	0.165
1.5	1.86	31.7	20.9	1.91	0.110
2.0	1.87	31.6	19.6	1.63	0.0937
2.4	1.96	31.6	18.9	1.49	0.0895
2.7	2.26	31.6	18.5	1.40	0.0970
3.0	2.31	31.6	18.1	1.34	0.0940
4.0	2.33	31.5	17.2	1.18	0.0836
5.0	2.22	31.5	16.6	1.08	0.0733
6.0	2.17	31.4	16.2	1.01	0.0667
8.0	2.18	31.3	15.6	0.897	0.0600
10	2.23	31.2	15.3	0.816	0.0558
15	2.25	30.9	14.7	0.677	0.0470
20	2.33	30.6	14.4	0.585	0.0422
30	2.57	30.1	14.0	0.468	0.0373

Table 20 Level Scheme of ^{246}Cm

No.	Energy (keV)	I^{π}	No.	Energy (keV)	I^{π}
GS	0	0^+	15	1165	3^+
1	42.85	2^+	16	1175	0^+
2	141.99	4^+	17	1179	8^-
3	295.5	6^+	18	1211	2^+
4	500.0	8^+	19	1220	4^+
5	841.7	2^-	20	1250	1^-
6	876.4	3^-	21	1289	0^+
7	923.3	4^-	22	1300	3^-
8	981.0	5^-	23	1318	2^+
9	1051	6^-	24	1349	1^-
10	1079	1^-	25	1367	2^-
11	1105	2^-	26	1379	4^+
12	1124	2^+	27	1452	1^+
13	1128	3^-	28	1478	2^+
14	1129	7^-	29	1509	3^+

Levels above 1526 keV were assumed to be overlapping.

Table 21 Thermal cross sections and resonance integrals of ^{246}Cm

Quantity	Reference	(barns)
σ_{cap}	71 Thompson[32)]	1.5 ± 0.5
	78 Gavrilov[33)]	1.14 ± 0.3
	Mughabghab[7)]	1.22 ± 0.16
	ENDF/B-V[21)]	1.297
	Previous Eval.[5)]	1.334
	Present	1.291
σ_{fiss}	72 Benjamin[42)]	0.17 ± 0.10
	76 Zhuravlev[49)]	0.14 ± 0.05
	Mughabghab	0.14 ± 0.05
	ENDF/B-V	0.0632
	Previous Eval.	0.1421
	Present	0.1401
σ_{el}	Mughabghab	11.1 ± 0.2
	ENDF/B-V	9.68
	Previous Eval.	9.49
	Present	11.08
RI_{cap}	71 Thompson	135 ± 25
	78 Gavrilov	118 ± 15
	Mughabghab	121 ± 7
	ENDF/B-V	104
	Previous Eval.	103
	Present	111
RI_{fiss}	72 Benjamin	10.0 ± 0.4
	76 Zhuravlev	13.3 ± 1.5
	Mughabghab	10.2 ± 0.4
	ENDF/B-V	10.4
	Previous Eval.	15.5
	Present	9.90

Table 22 Eerngy dependence of unresolved resonance parameters and the calculated cross sections for ^{247}Cm

Energy independent parameters

$R = 9.3863$ fm, $\Gamma_\gamma = 40$ meV, $S_2 = 0.86 \times 10^{-4}$

$\Gamma_f^{(4-)} = 53.4$ meV, $\Gamma_f^{(5-)} = 500$ meV

$\Gamma_f^{(3+)} = 80$ meV, $\Gamma_f^{(4+)} = 680$ meV

$\Gamma_f^{(5+)} = 50$ meV, $\Gamma_f^{(6+)} = 470$ meV

E_n (keV)	S_0 (10^{-4})	S_1 (10^{-4})	D_{obs} (eV)	σ_{tot} (b)	σ_{cap} (b)	σ_{fiss} (b)
0.06	1.74	6.51	1.400	104.0	12.2	77.3
0.07	1.89	7.05	1.400	104.3	12.1	77.3
0.09	0.592	2.21	1.400	36.8	3.66	21.7
0.125	0.563	2.10	1.400	31.9	2.95	17.5
0.175	0.866	3.23	1.399	38.2	3.70	22.6
0.25	0.933	3.48	1.399	35.6	3.29	20.3
0.35	0.654	2.44	1.399	25.6	2.02	12.1
0.45	0.669	2.50	1.399	24.2	1.83	10.9
0.55	0.966	3.61	1.398	28.3	2.20	14.1
0.7	0.769	2.87	1.398	23.3	1.69	10.0
0.9	0.774	2.89	1.397	22.0	1.52	8.87
1.25	0.603	2.25	1.396	18.3	1.08	5.92
1.75	0.688	2.57	1.395	18.2	1.08	5.70
2.5	0.724	2.70	1.392	17.5	1.03	5.04
3.5	0.609	2.27	1.389	15.7	0.827	3.64
4.5	0.675	2.52	1.386	15.7	0.875	3.58
5.5	0.672	2.51	1.383	15.3	0.857	3.26
7.0	0.675	2.52	1.379	15.0	0.850	2.95
9.0	0.666	2.49	1.373	14.6	0.836	2.63
12.5	0.727	2.72	1.363	14.5	0.894	2.52
17.5	0.709	2.65	1.348	14.1	0.866	2.19
25.0	0.748	2.79	1.326	14.0	0.874	2.07
30.0	0.779	2.91	1.312	14.0	0.875	2.05

Table 23 Level scheme of ^{247}Cm

No.	Energy (keV)	Spin and parity	
Gr	0.0	9/2	-
1	61.5	11/2	-
2	135.0	13/2	-
3	217.0	15/2	-
4	227.0	5/2	+
5	266.0	7/2	+
6	285.0	7/2	+
7	318.0	9/2	+
8	344.0	9/2	+
9	361.0	11/2	+
10	396.0	11/2	+
11	403.6	1/2	+
12	433.0	3/2	+
13	449.0	5/2	+
14	506.0	1/2	+
15	520.0	3/2	+

Levels above 550 keV were assumed to be overlapping.

Table 24 Thermal cross sections and resonance integrals of ^{247}Cm

Quantity	Reference	(barns)
σ_{cap}	78 Gavrilov[33)]	60
	Mughabghab[7)]	57 ± 10
	ENDF/B-V[21)]	58.17
	Previous Eval.[5)]	59.91
	Present	57.20
σ_{fiss}	70 Halperin[48)]	120 ± 12
	72 Benjamin[42)]	82 ± 5
	76 Zhuravlev[49)]	80 ± 7
	Mughabghab	81.9 ± 4.4
	ENDF/B-V	83.43
	Previous Eval.	97.03
	Present	81.79
RI_{cap}	78 Gavrilov	490
	Mughabghab	530 ± 30
	ENDF/B-V	492
	Previous Eval.	496
	Present	535
RI_{fiss}	70 Halperin	1060 ± 110
	72 Benjamin	778 ± 50
	76 Zhuravlev	730 ± 70
	Mughabghab	760 ± 50
	ENDF/B-V	751
	Previous Eval.	784
	Present	612

Table 25 Energy dependence of the unresolved resonance parameters and the calculated cross sections for ^{248}Cm 6)

Energy independent parameters

$S_0 = 1.2 \times 10^{-4}$, $S_1 = 3.32 \times 10^{-4}$, $S_2 = 0.844 \times 10^{-4}$,
$R = 8.88$ fm, $\Gamma_\gamma = 26$ meV

E_n (keV)	Γ_f (meV)	D_{obs} (eV)	σ_{tot} (b)	σ_{cap} (b)	σ_{fiss} (b)
1.5	1.15	39.9	23.1	1.59	0.069
2	1.25	39.8	21.4	1.37	0.063
3	1.41	39.7	19.5	1.13	0.059
4	1.48	39.7	18.3	0.995	0.054
5	1.64	39.6	17.6	0.903	0.054
6	1.86	39.5	17.0	0.832	0.056
8	2.12	39.3	16.3	0.729	0.056
10	2.28	39.2	15.7	0.654	0.054
15	2.72	38.7	15.0	0.528	0.052
20	2.96	38.3	14.6	0.449	0.049
30	3.35	37.5	14.1	0.353	0.043

Table 26 Level Scheme of ^{248}Cm

No.	Energy (keV)	I^π	No.	Energy (keV)	I^π
GS	0	0^+	5	1048	2^+
1	43.40	2^+	6	1050	1^-
2	143.6	4^+	7	1084	0^+
3	297	6^+	8	1094	3^-
4	510	8^+			

Levels above 1126 keV are assumed to be overlapping.

Table 27 Thermal cross sections and resonance integrals of ^{248}Cm

Quantity	Reference	(barns)
σ_{cap}	71 Thompson[32]	3 ± 1
	73 Druschel[57]	2.63
	74 Benjamin[55]	2.51 ± 0.26
	78 Gavrilov[33]	10.7 ± 1.5
	Mughabghab[7]	2.63 ± 0.26
	ENDF/B-V[21]	2.444
	Maino et al.[58]	9.808
	Previous Eval.[6]	2.570
σ_{fiss}	72 Benjamin[42]	0.34 ± 0.07
	76 Zhuravlev[49]	0.39 ± 0.07
	Mughabghab	0.37 ± 0.07
	ENDF/B-V	0.0873
	Maino et al.	0.393
	Previous Eval.	0.370
σ_{scat}	Mughabghab	7.65 ± 0.40
	ENDF/B-V	6.137
	Maino et al.	10.41
	Previous Eval.	6.514
RI_{cap}	71 Thompson	275 ± 75
	73 Druschel	265
	74 Benjamin	259 ± 12
	78 Gavrilov	250 ± 24
	Mughabghab	270 ± 15
	ENDF/B-V	249
	Maino et al.	264
	Previous Eval.	260
RI_{fiss}	72 Benjamin	13.2 ± 0.8
	76 Zhuravlev	13.1 ± 1.5
	Mughabghab	15
	ENDF/B-V	15.4
	Maino et al.	9.59
	Previous Eval.	17.5

Table 28 Unresolved resonance parameters and calculated cross sections for ^{249}Cm 6)

$S_0 = 1.08 \times 10^{-4}$, $S_1 = 3.95 \times 10^{-4}$, $S_2 = 1.04 \times 10^{-4}$
$R = 8.80$ fm, $\Gamma_\gamma = 40$ meV, $D_{obs} = 8.3$ eV
$\Gamma_f^{(0+)} = 4070$ fm, $\Gamma_f^{(1+)} = 7.7$ meV
$\Gamma_f^{(2+)} = 1022$ meV, $\Gamma_f^{(3+)} = 146$ meV
$\Gamma_f^{(0-)} = 0$ meV, $\Gamma_f^{(1-)} = 2000$ meV
$\Gamma_f^{(2-)} = 4070$ meV,

E_n (eV)	σ_{tot} (barns)	σ_{cap} (barns)	σ_{fiss} (barns)
4.15	227.2	128.5	65.9
10	149.9	77.7	41.5
100	54.2	18.6	11.9
1000	24.2	3.76	3.50
10000	15.4	0.837	1.91
30000	14.1	0.436	1.95

Table 29 Level scheme of ^{249}Cm

No.	Energy (keV)	I^{π}	No.	Energy (keV)	I^{π}
GS	0	$1/2^+$	4	110	$9/2^+$
1	26.2	$3/2^+$	5	110.1	$7/2^+$
2	42.4	$5/2^+$	6	146	$9/2^+$
3	52.2	$7/2^+$	7	208	$3/2^+$

Levels above 220 keV were assumed to be overlapping.

Table 30 Thermal cross sections and resonance integrals of ^{249}Cm[6)]

Quantity	(barns)
σ_{cap}	1.6
σ_{fiss}	0.82
σ_{tot}	13.22
RI_{cap}	215
RI_{fiss}	139

Table 31 Summary of the present work

Quantities	Isotope 241	242	243	244	245	246	247	248	249
Resonance Param.									
resolved	No	o	o	o	×	o	o	×	No
upper boundary(eV)		275	70	1000	60	330	60	1500	
unresolved	No	o	o	o	o	×	o	×	×
upper boundary(keV)		40	40	40	40	30	30	30	30
Cross Section above resonance region									
total	o	o	o	o	o	×	×	×	×
elastic	o	o	o	o	o	×	o	×	×
inelastic	o	o	o	o	o	×	o	×	×
(n,Xn)	o	o	o	o	o	×	o	×	×
fission	o	o	o	o	o	×	o	×	×
capture	o	o	o	o	o	×	o	×	×
Angular dist.	o	o	o	o	o	×	o	×	×
Energy dist.	o	×	×	×	o	×	×	×	×
ν	o	×	×	×	o	×	×	×	×

No : Not given

o : newly evaluated or modified

× : taken from previous evaluation

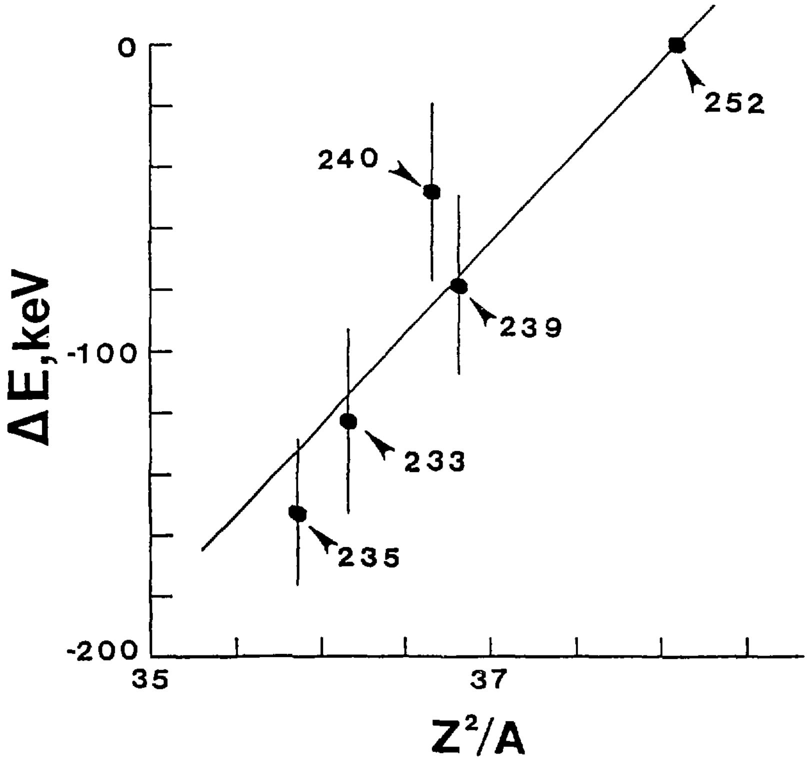

Fig. 1 Systematics of nuclear temperature of fission spectra (taken from Ref. 14).

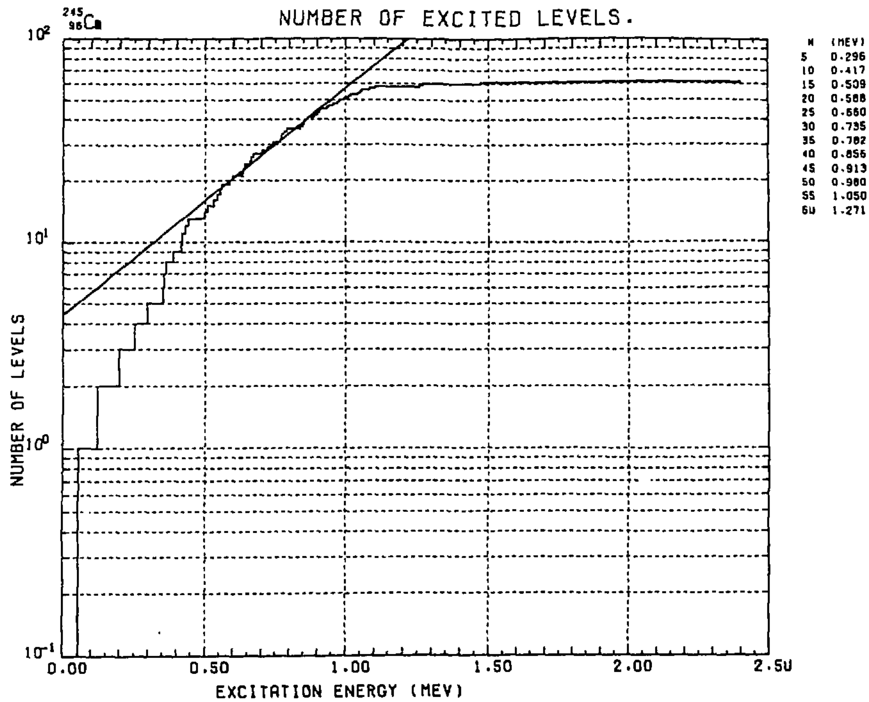

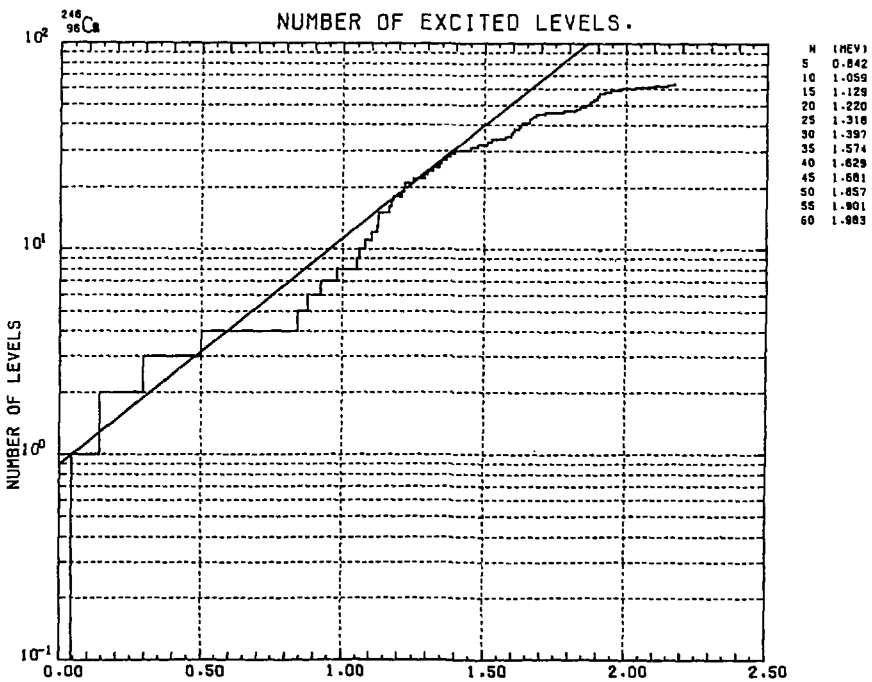

Fig. 2 Examples of staircase plots of excited levels (^{245}Cm and ^{246}Cm).

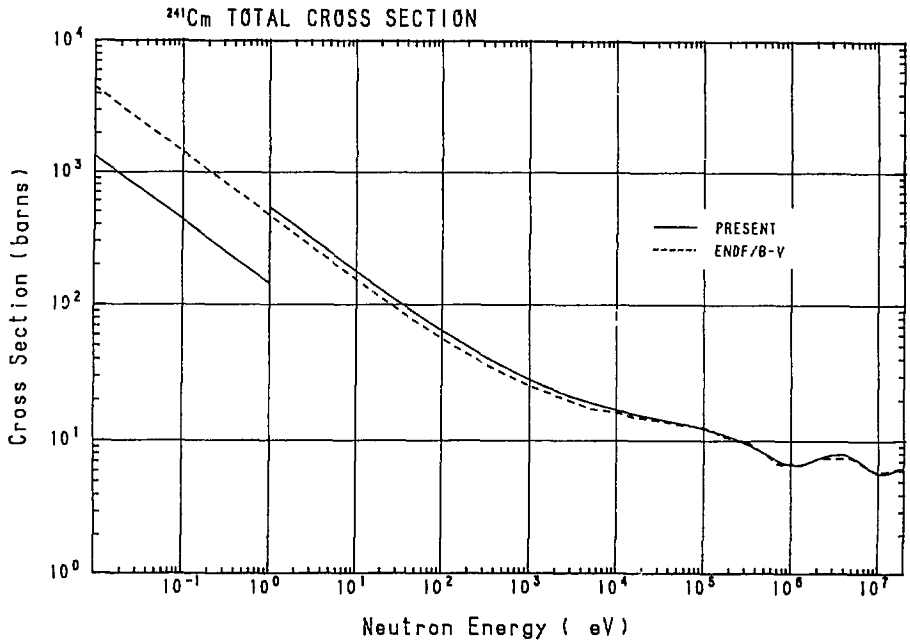

Fig. 3 Total cross section of ^{241}Cm.

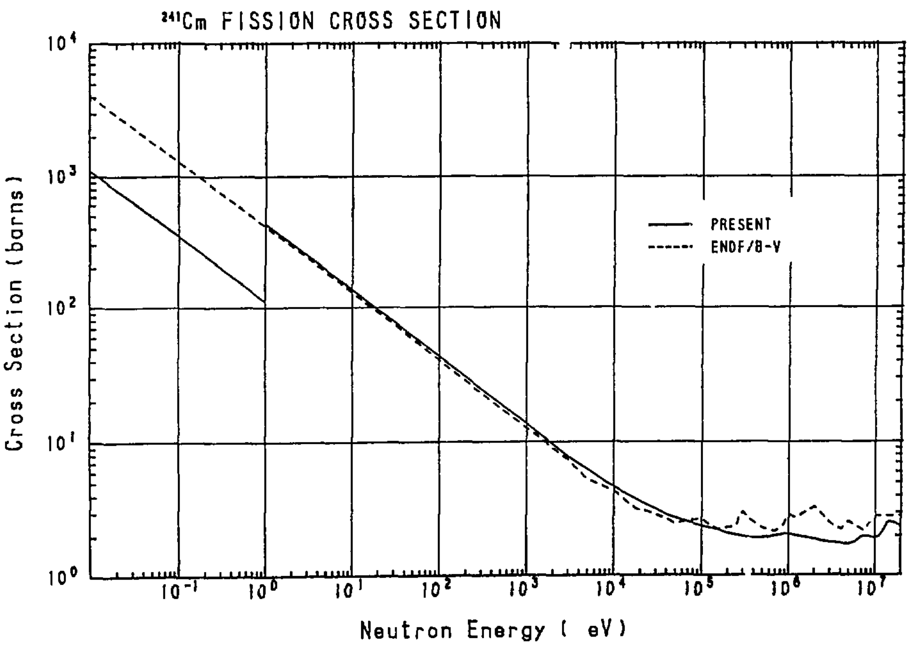

Fig. 4 Fission cross section of ^{241}Cm.

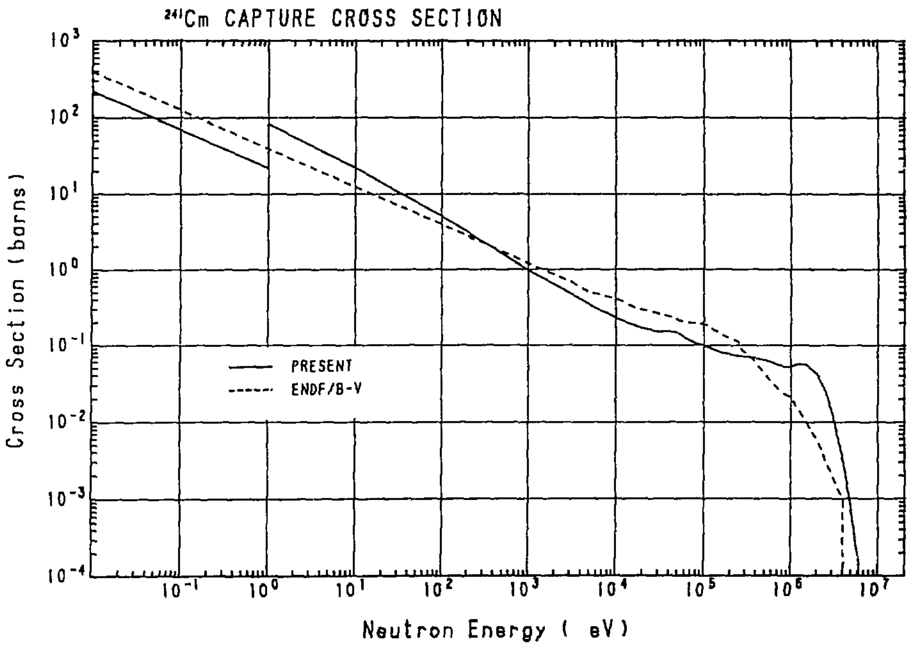

Fig. 5 Capture cross section of ^{241}Cm.

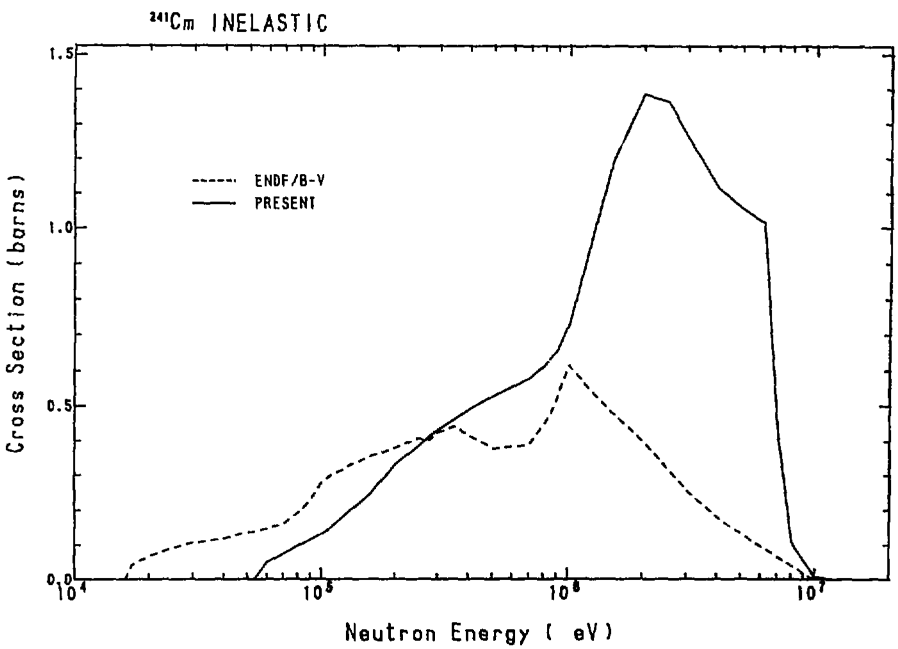

Fig. 6 Inelastic scattering cross section of ^{241}Cm.

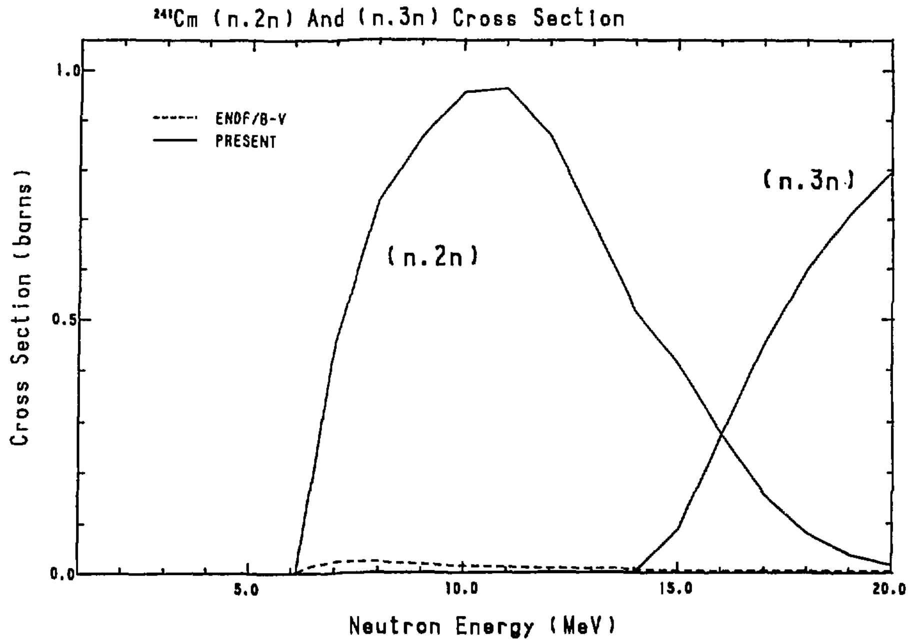

Fig. 7 (n,2n) and (n,3n) reaction cross sections of ^{241}Cm.

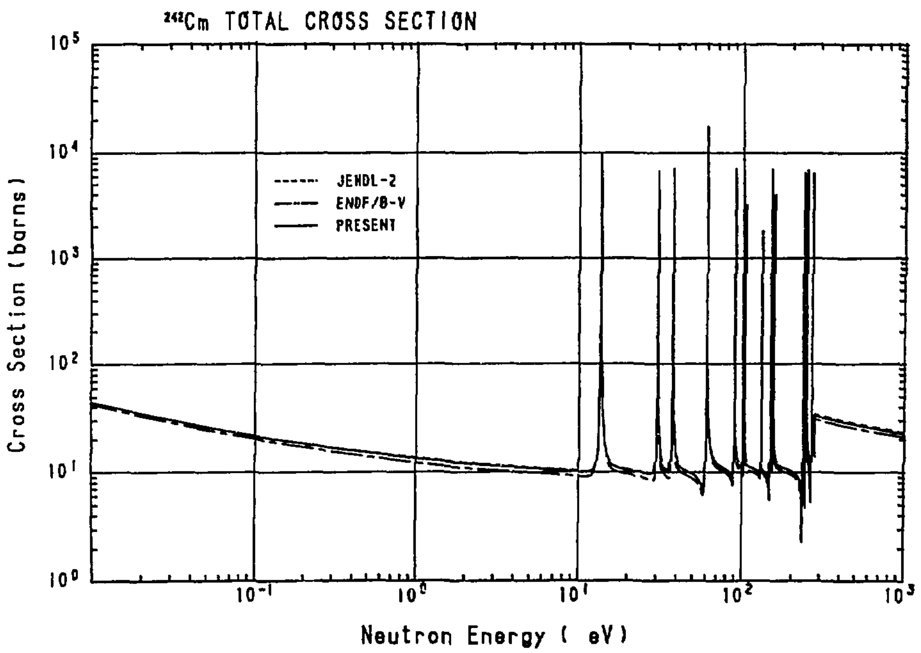

Fig. 8(a) Total cross section of ^{242}Cm (0.01 eV ~ 1 keV).

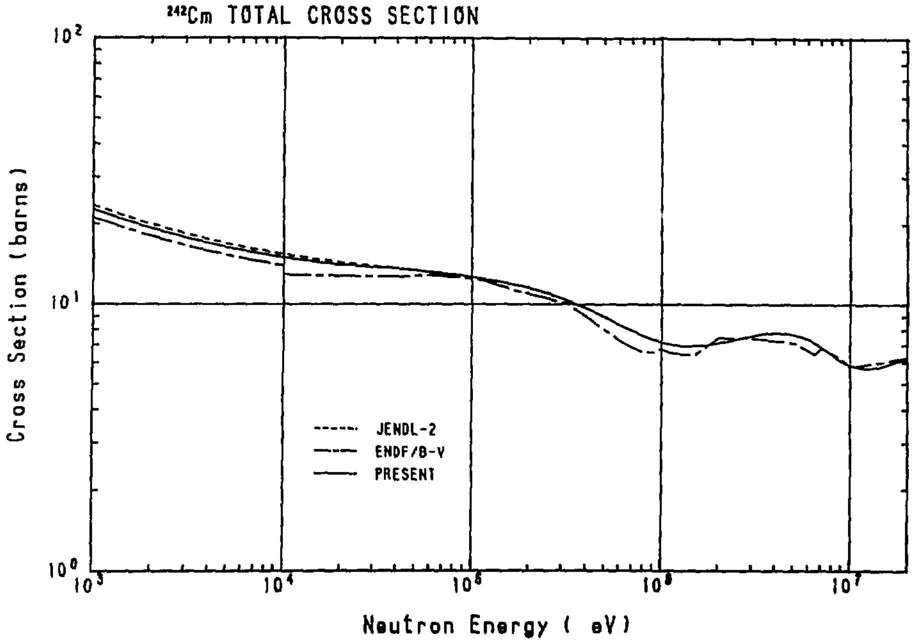

Fig. 8(b) Total cross section of ^{242}Cm (1 keV ~ 20 MeV).

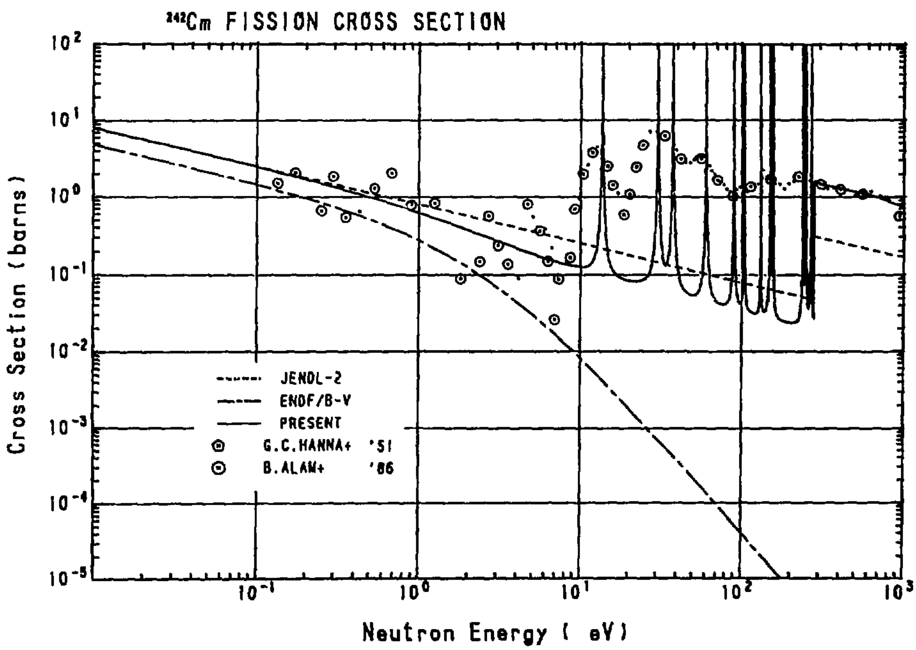

Fig. 9(a) Fission cross section of ^{242}Cm (0.01 eV ~ 1 keV).

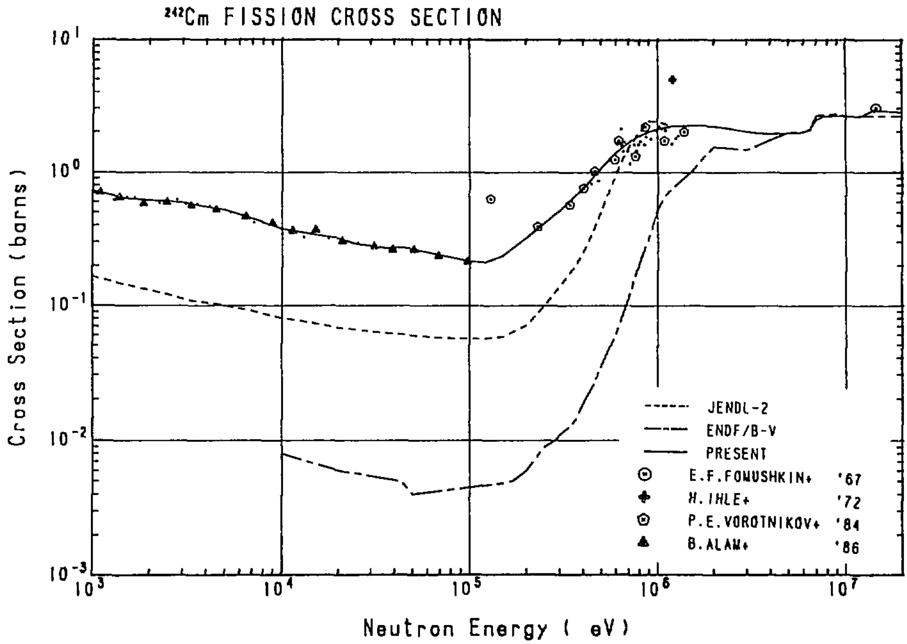

Fig. 9(b) Fission cross section of ^{242}Cm (1 keV ~ 20 MeV).

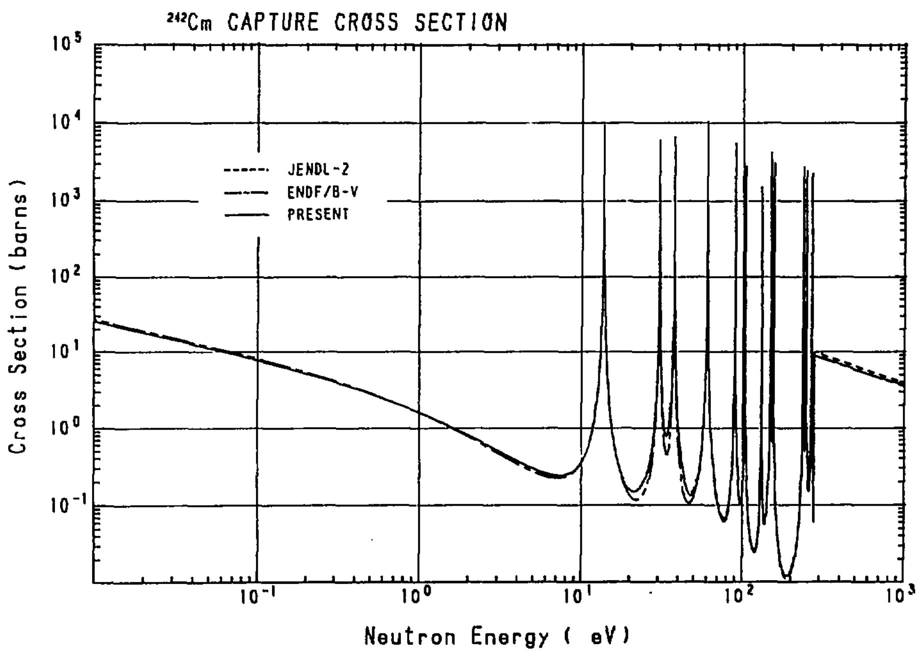

Fig. 10(a) Capture cross section of ^{242}Cm (0.01 eV ~ 1 keV).

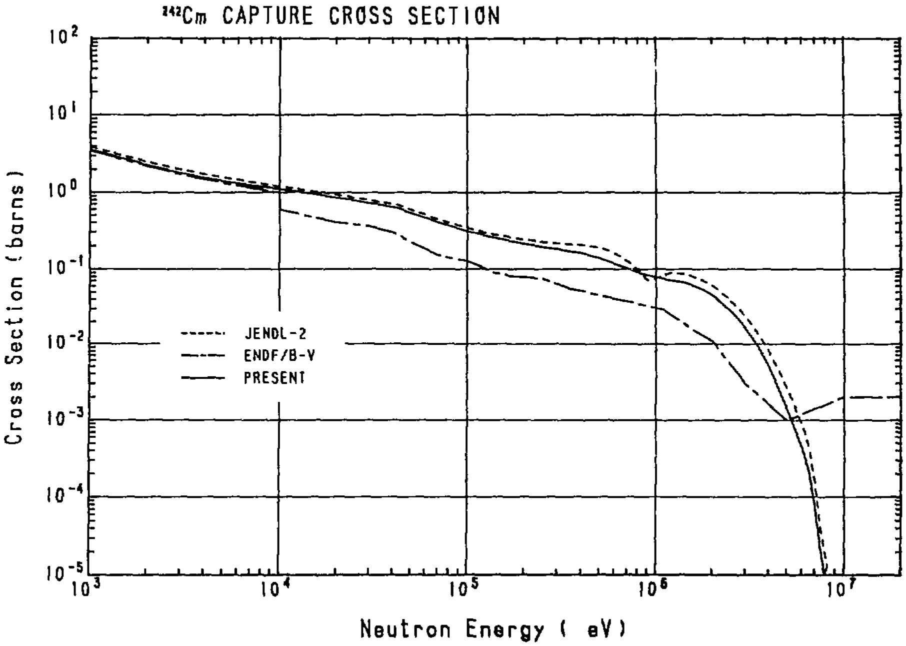

Fig. 10(b) Capture cross section of ^{242}Cm (1 keV ~ 20 MeV).

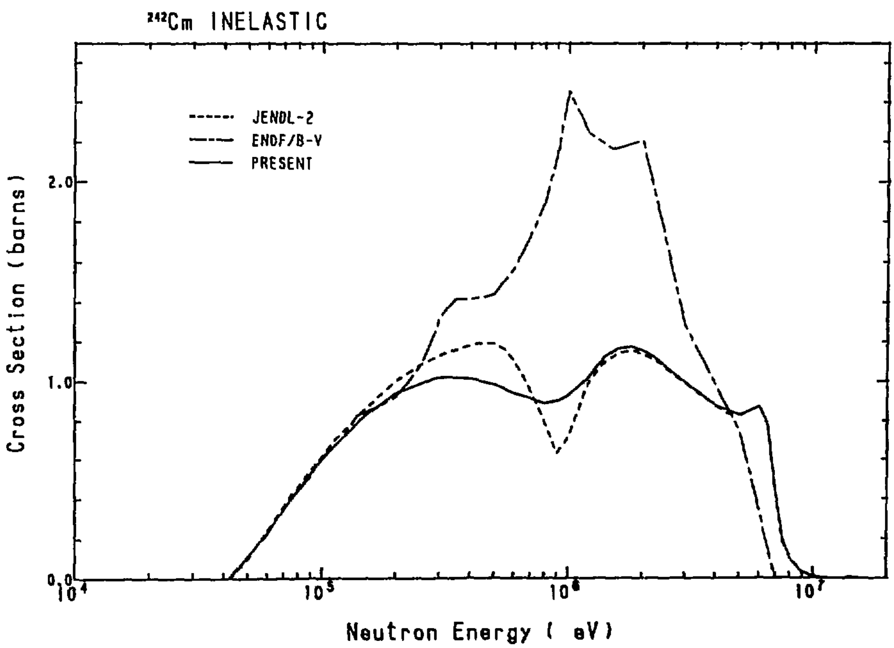

Fig. 11 Inelastic scattering cross section of ^{242}Cm.

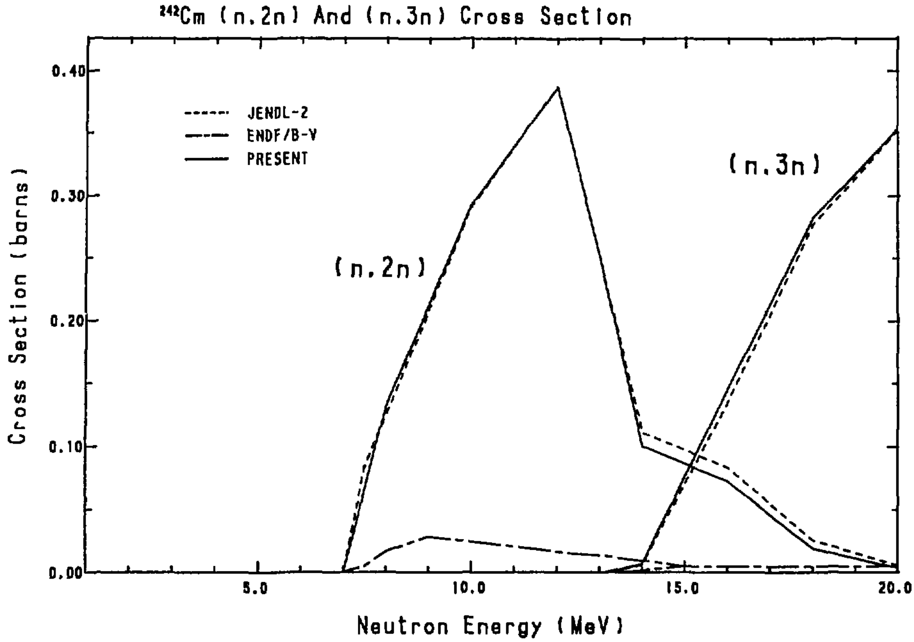

Fig. 12 (n,2n) and (n,3n) reaction cross sections of ^{242}Cm.

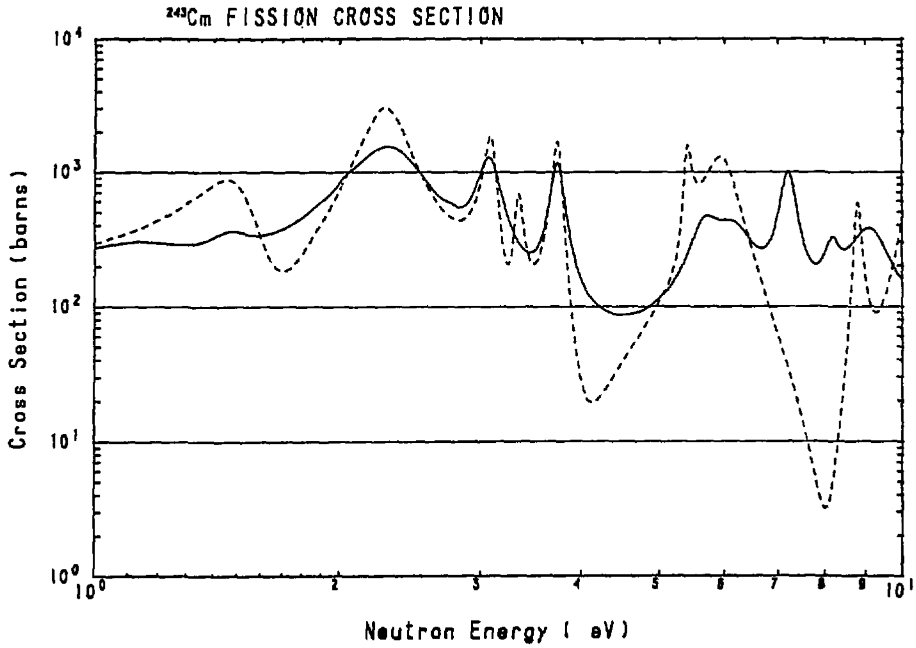

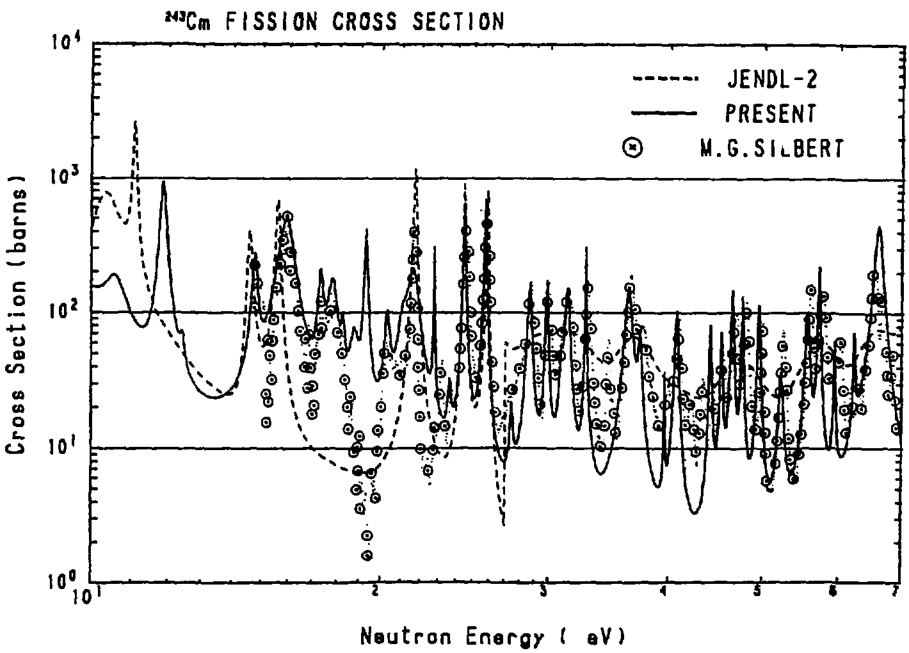

Fig. 13 Fission cross section of ^{243}Cm in the resolved resonance region.

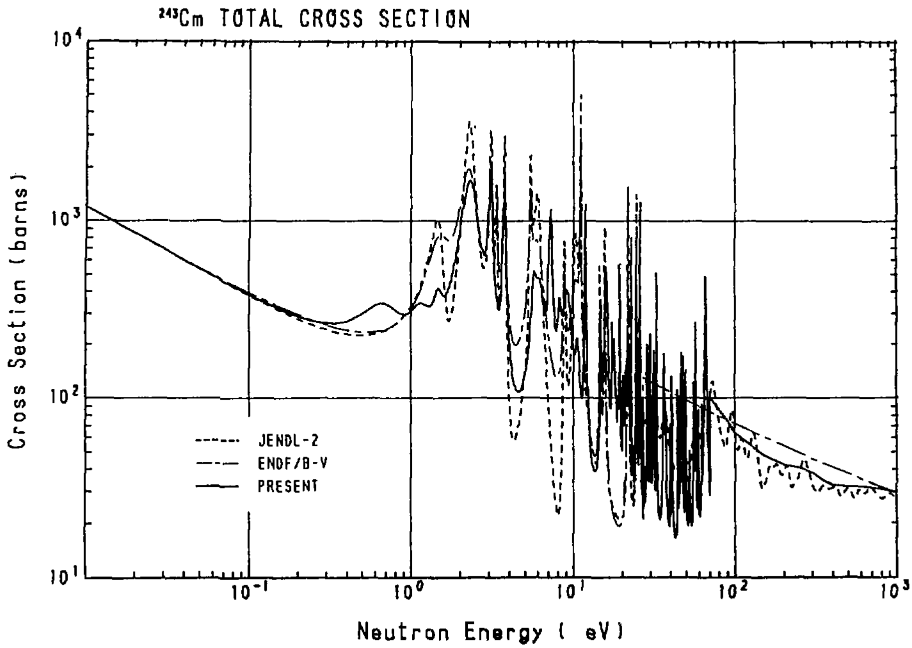

Fig. 14(a) Total cross section of ^{243}Cm (0.01 eV ~ 1 keV).

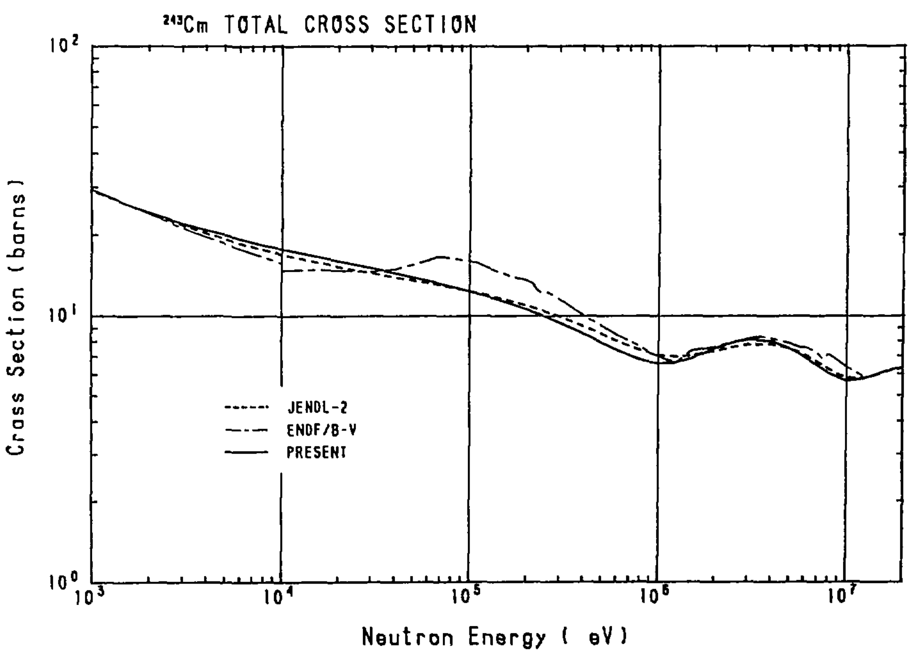

Fig. 14(b) Total cross section of ^{243}Cm (1 keV ~ 20 MeV).

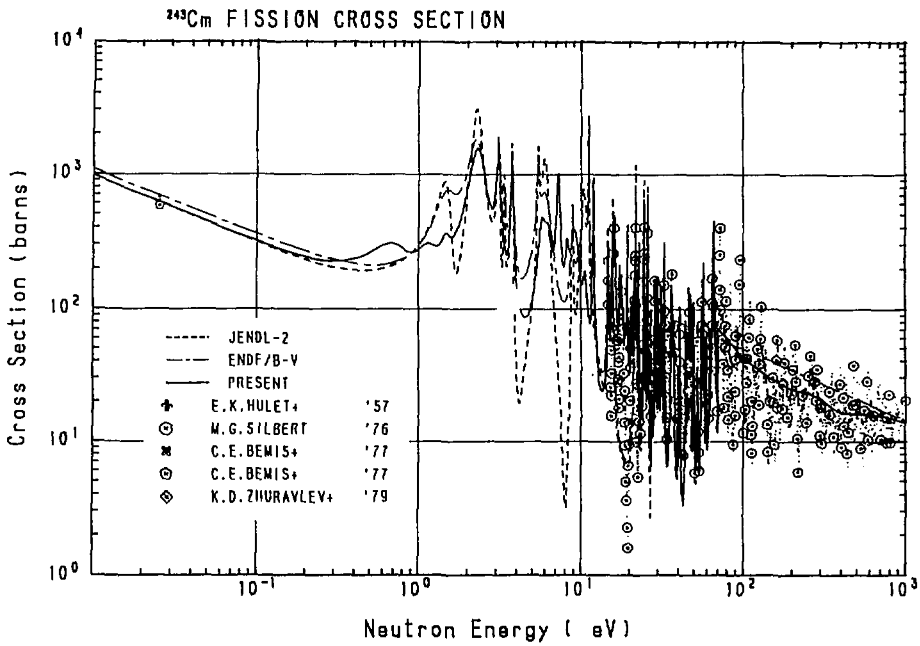

Fig. 15(a) Fission cross section of ^{243}Cm (0.01 eV ~ 1 keV).

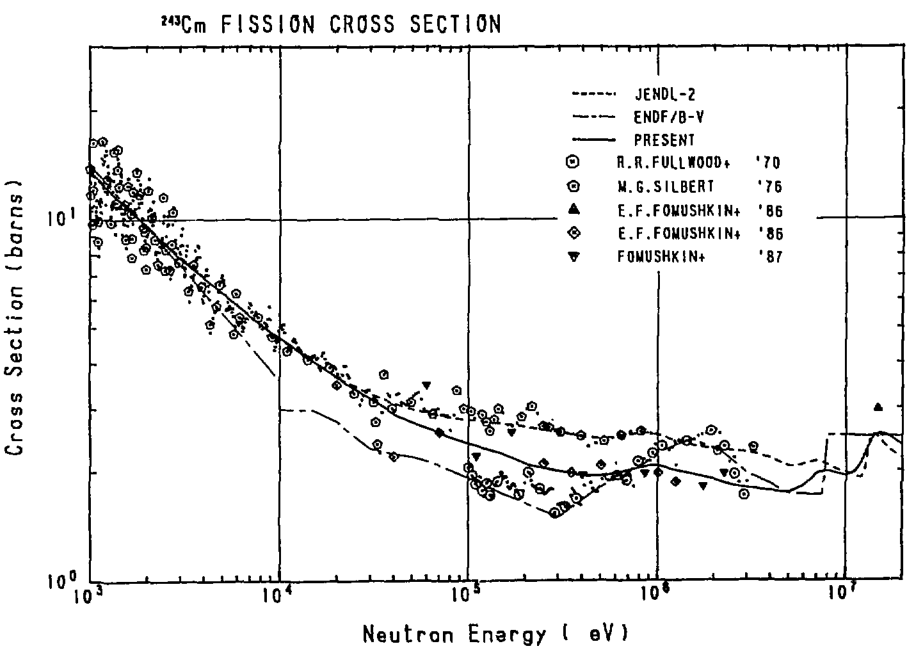

Fig. 15(b) Fission cross section of ^{243}Cm (1 keV ~ 20 MeV).

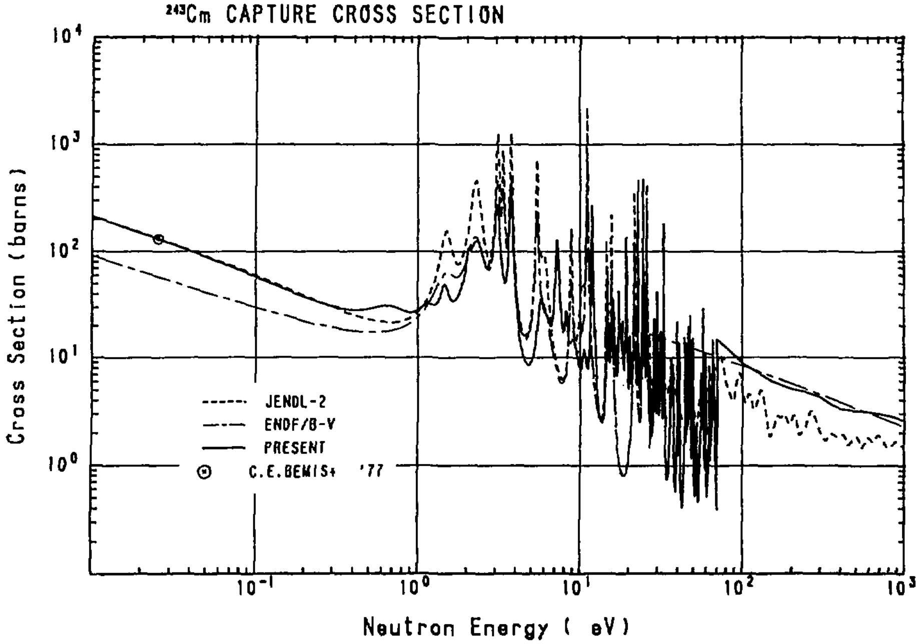

Fig. 16(a) Capture cross section of ^{243}Cm (0.01 eV ~ 1 keV).

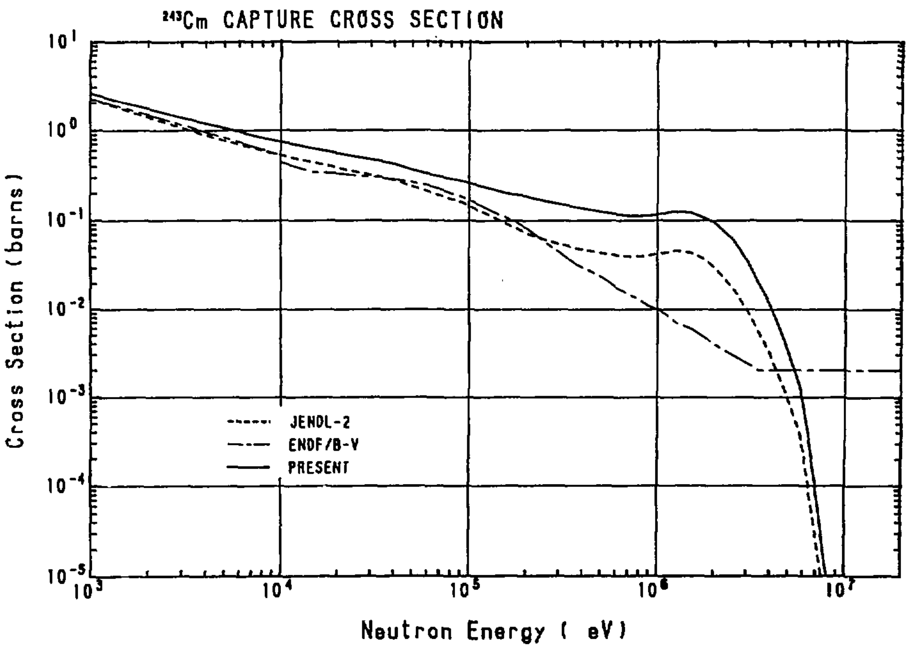

Fig. 16(b) Capture cross section of ^{243}Cm (1 keV ~ 20 MeV).

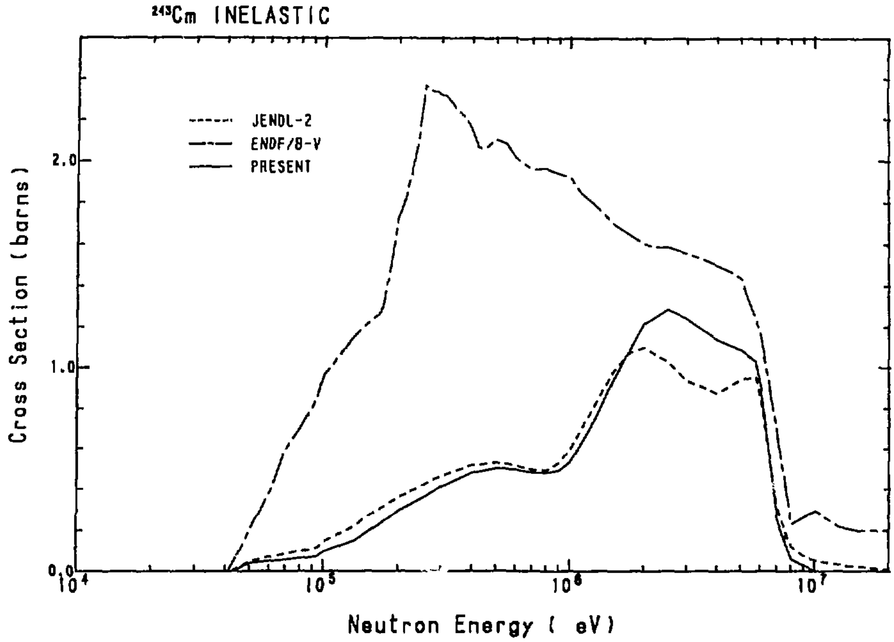

Fig. 17 Inelastic scattering cross section of ^{243}Cm.

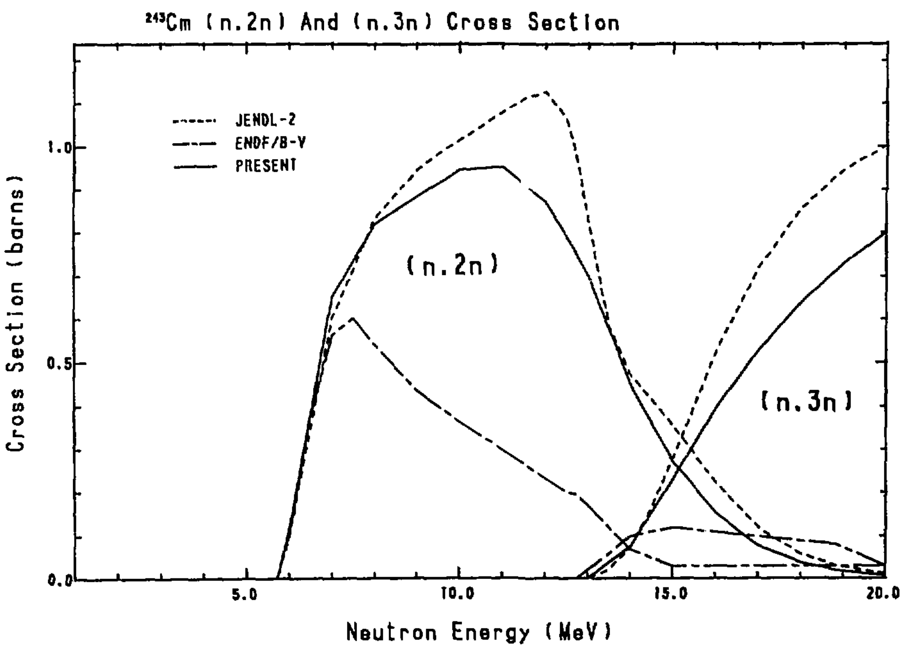

Fig. 18 (n,2n) and (n,3n) reaction cross sections of ^{243}Cm.

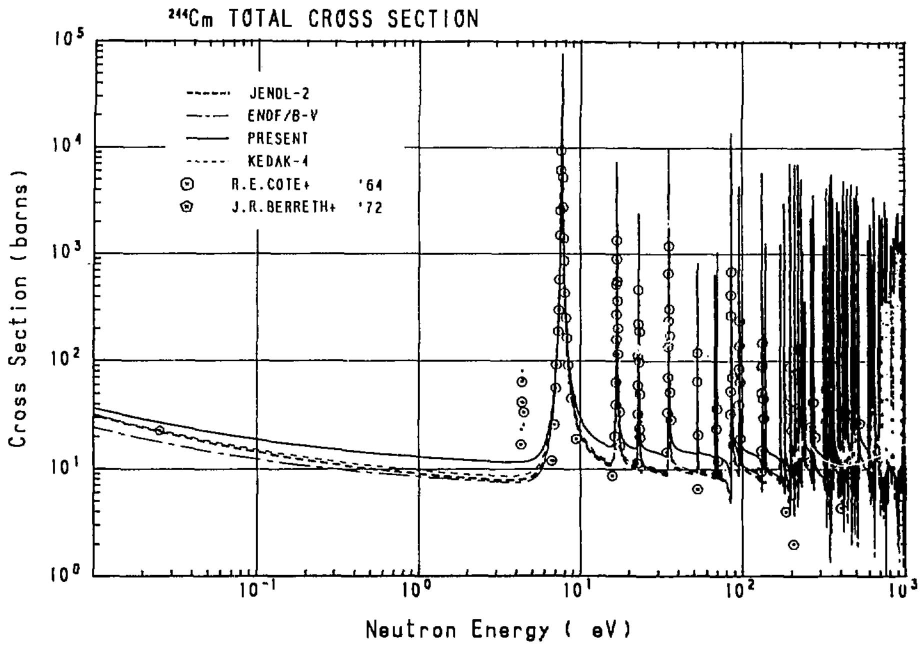

Fig. 19(a) Total cross section of ^{244}Cm (0.01 eV ~ 1 keV).

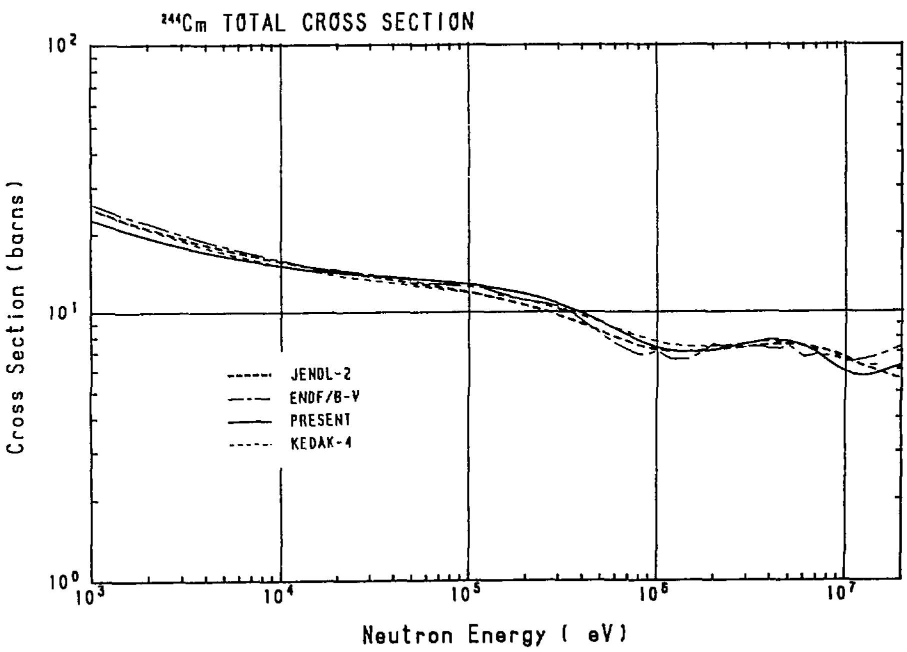

Fig. 19(b) Total cross section of ^{244}Cm (1 keV ~ 20 MeV).

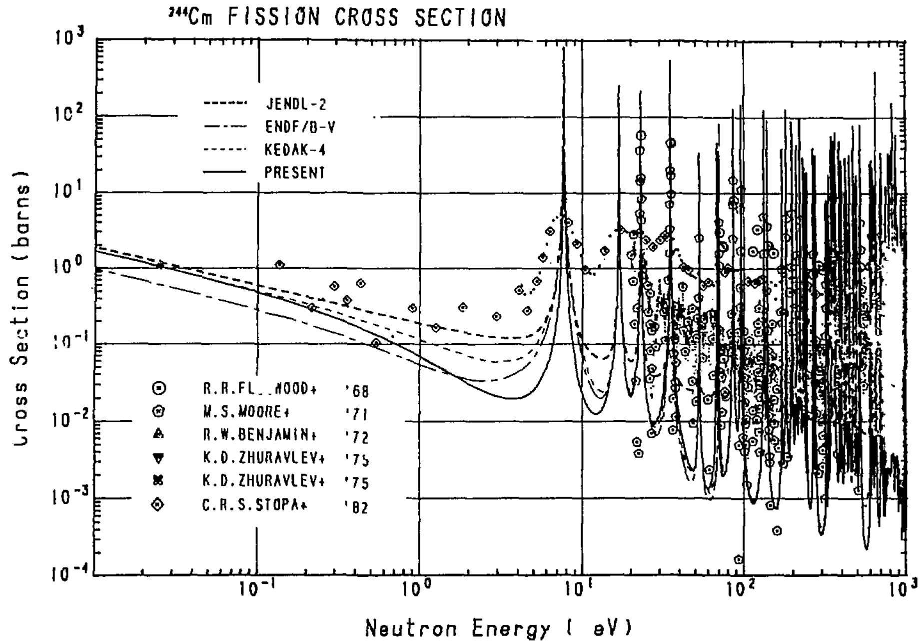

Fig. 20(a) Fission cross section of ^{244}Cm (0.01 eV ~ 1 keV).

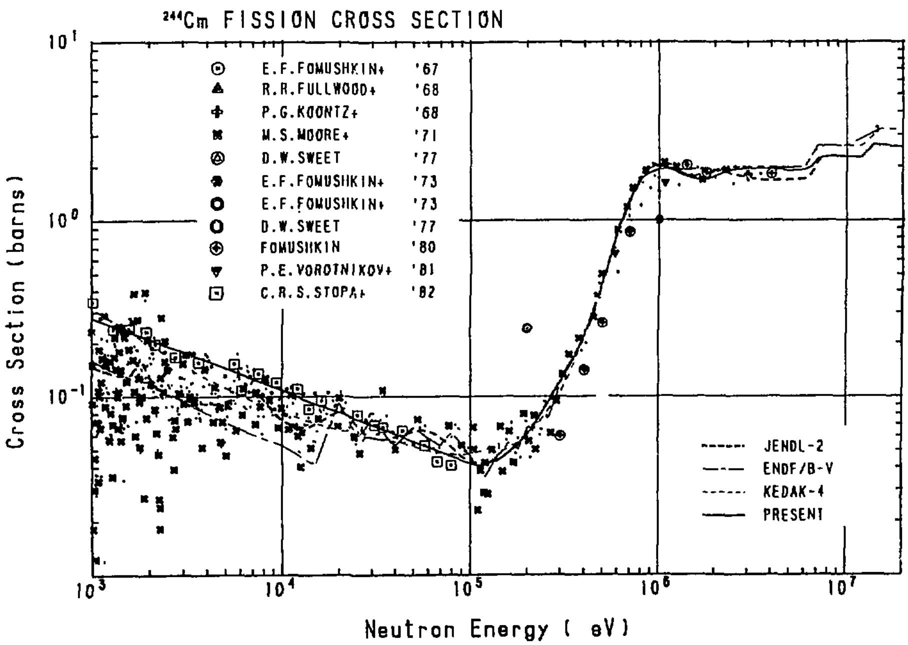

Fig. 20(b) Fission cross section of ^{244}Cm (1 keV ~ 20 MeV).

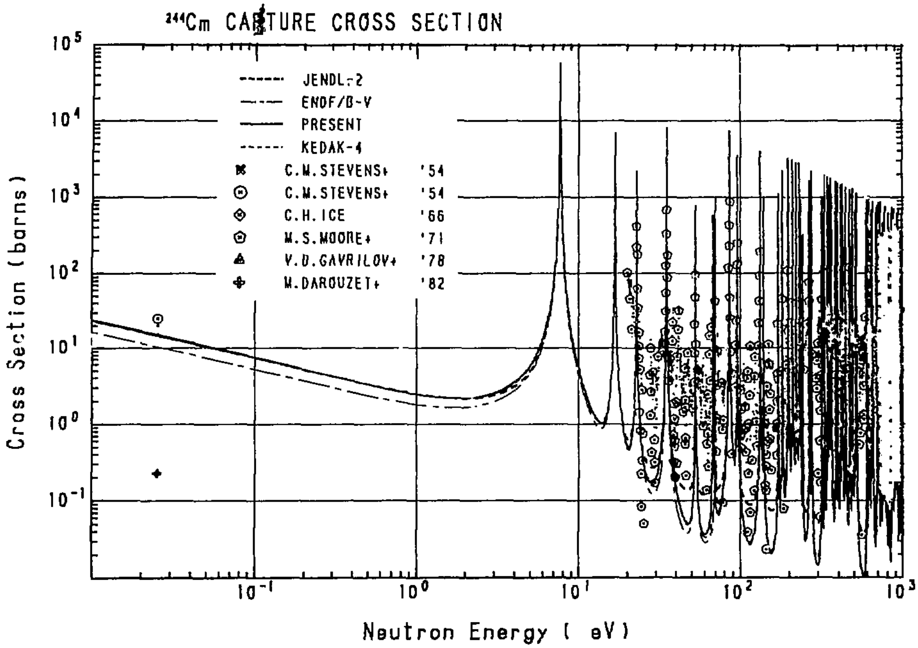

Fig. 21(a) Capture cross section of ^{244}Cm (0.01 eV ~ 1 keV).

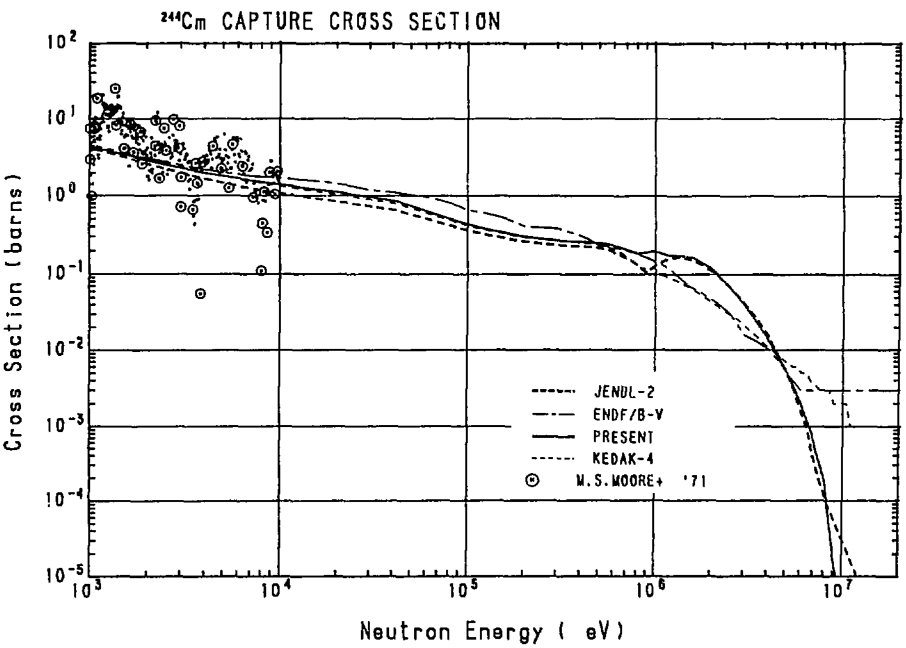

Fig. 21(b) Capture cross section of ^{244}Cm (1 keV ~ 20 MeV).

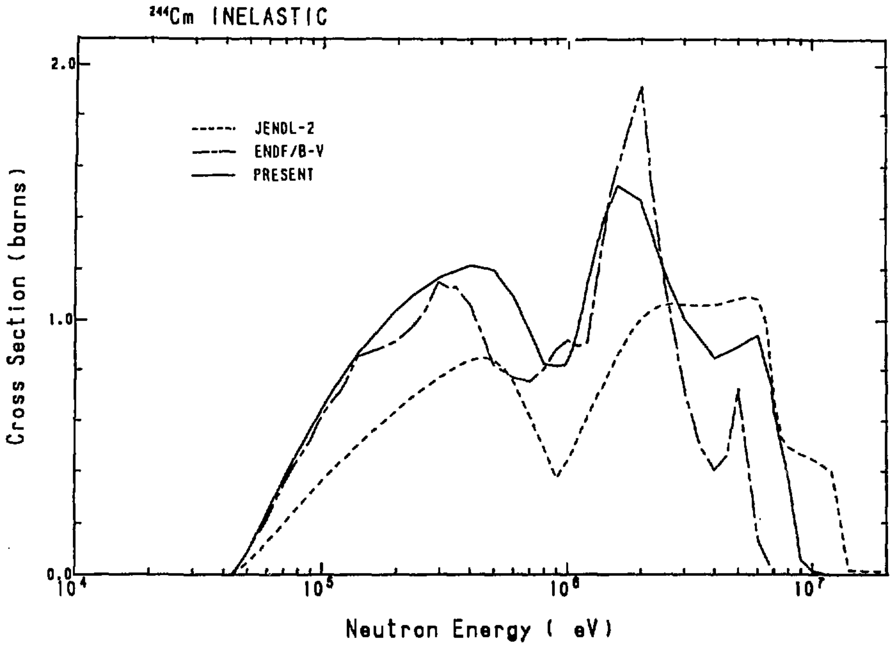

Fig. 22 Inelastic scattering cross section of ^{244}Cm.

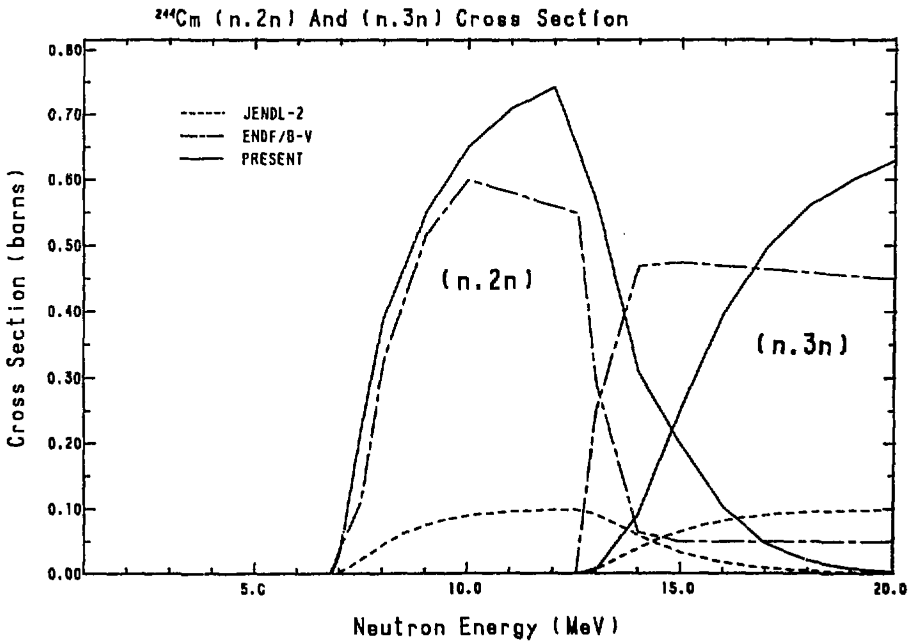

Fig. 23 (n,2n) and (n,3n) reaction cross sections of ^{244}Cm.

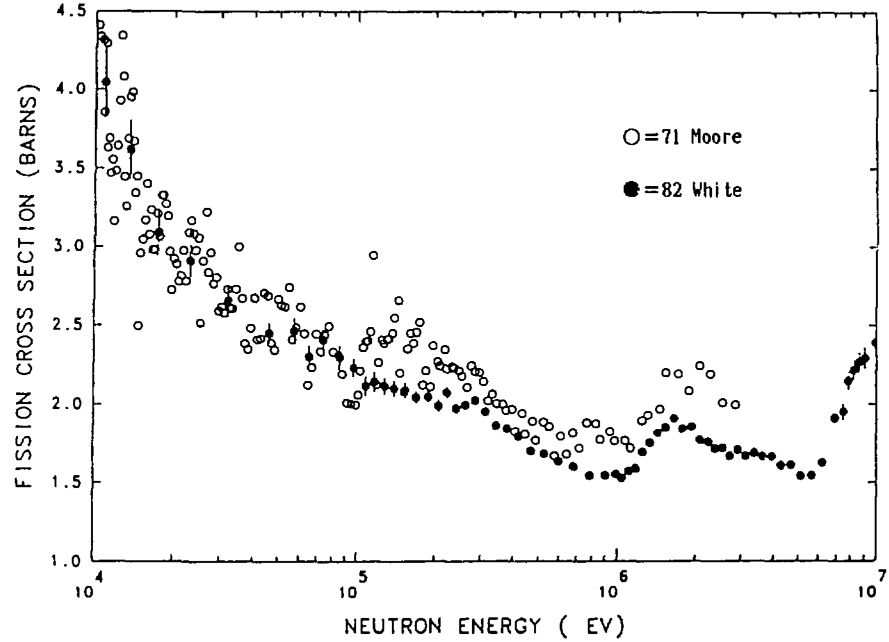

Fig. 24 Fission cross section of ^{245}Cm (taken from Ref. 43).

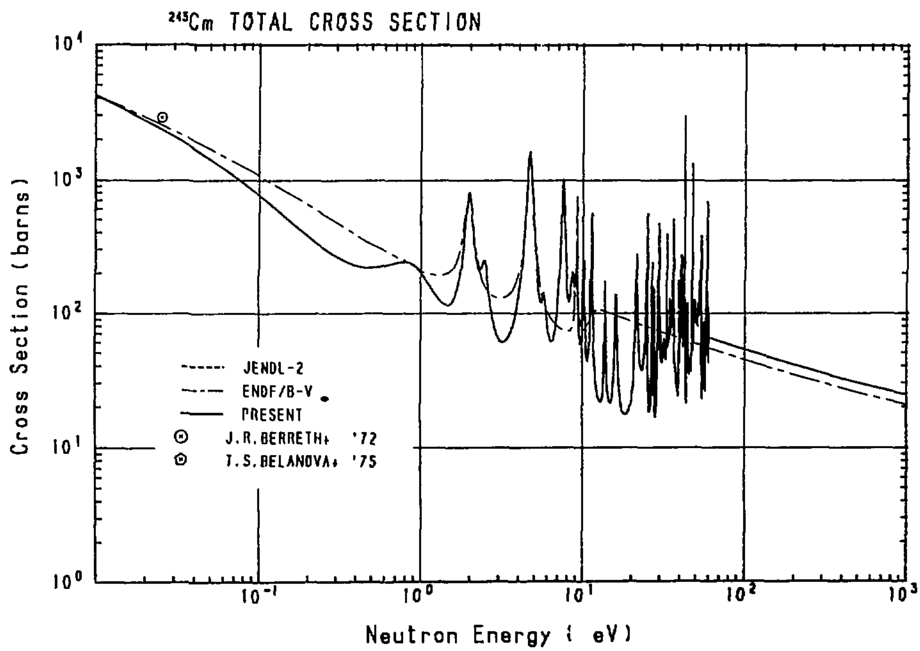

Fig. 25(a) Total cross section of ^{245}Cm (0.01 eV ~ 1 keV).

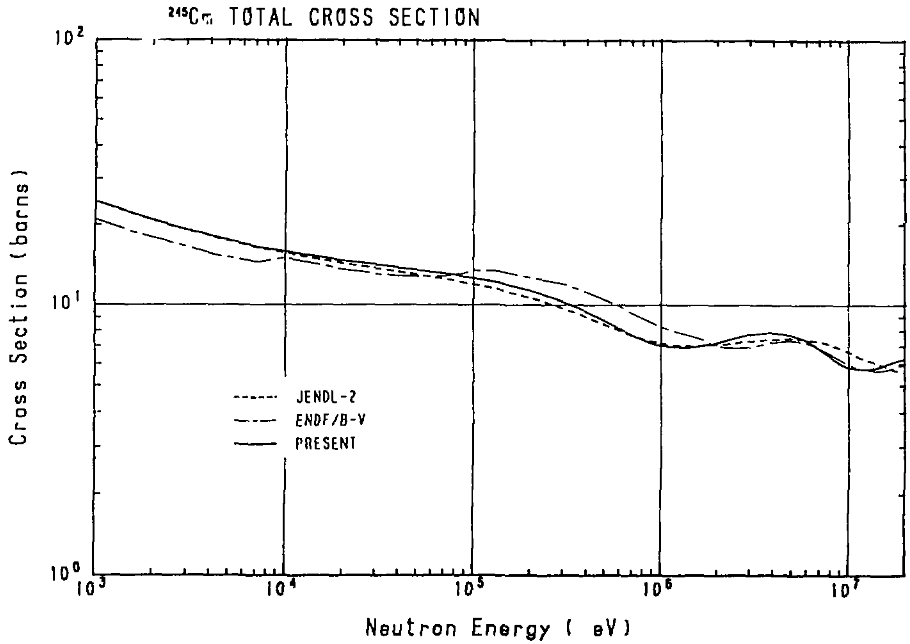

Fig. 25(b) Total cross section of ^{245}Cm (1 keV ~ 20 MeV).

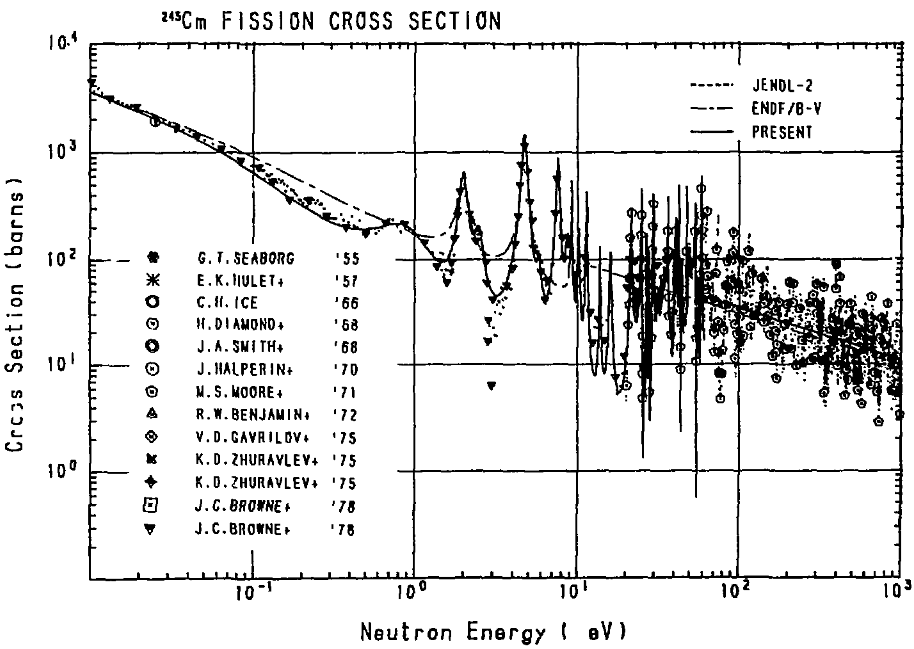

Fig. 26(a) Fission cross section of ^{245}Cm (0.01 eV ~ 1 keV).

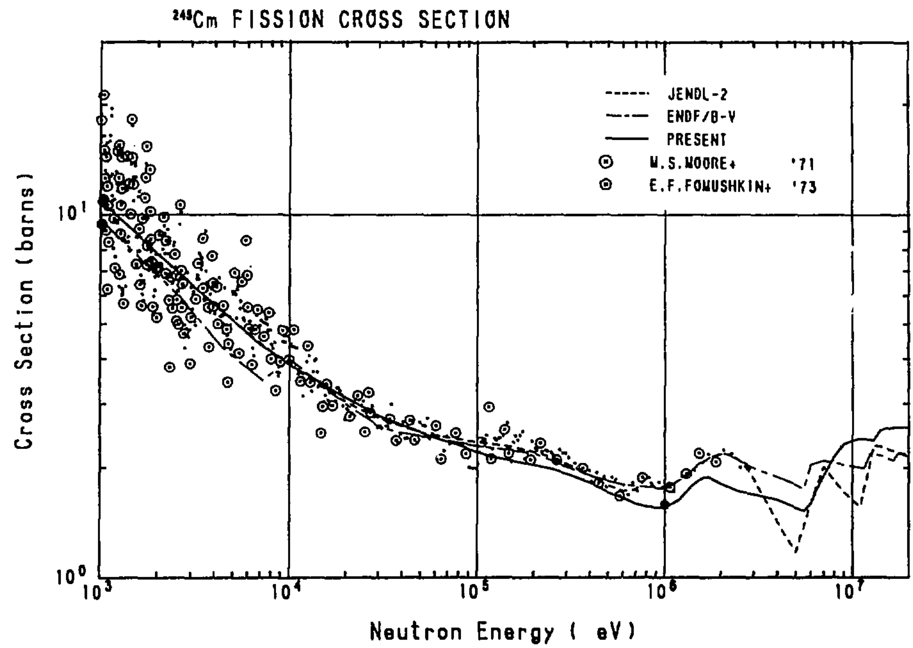

Fig. 26(b) Fission cross section of ^{245}Cm (1 keV ~ 20 MeV).

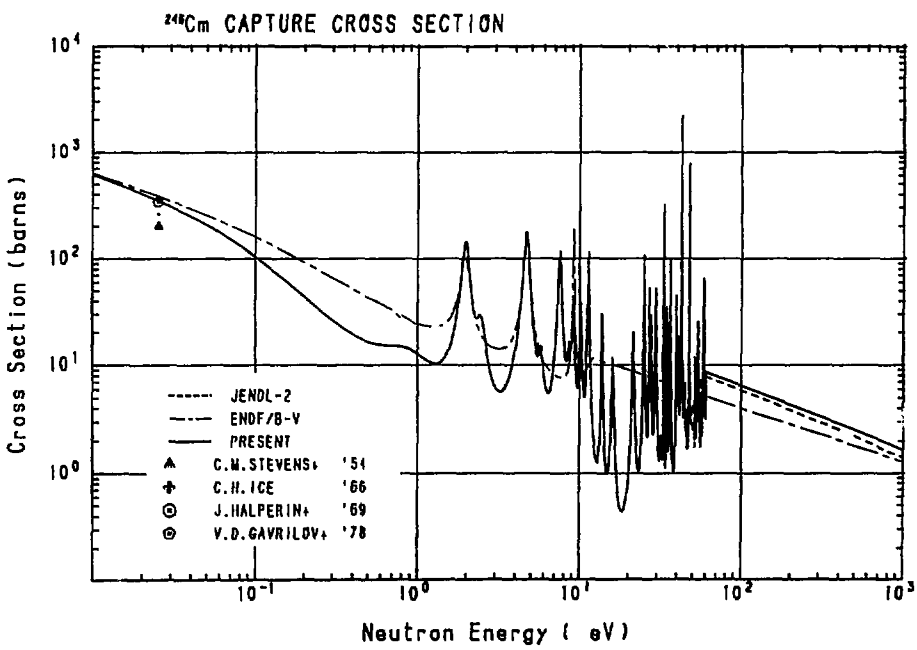

Fig. 27(a) Capture cross section of ^{245}Cm (0.01 eV ~ 1 keV).

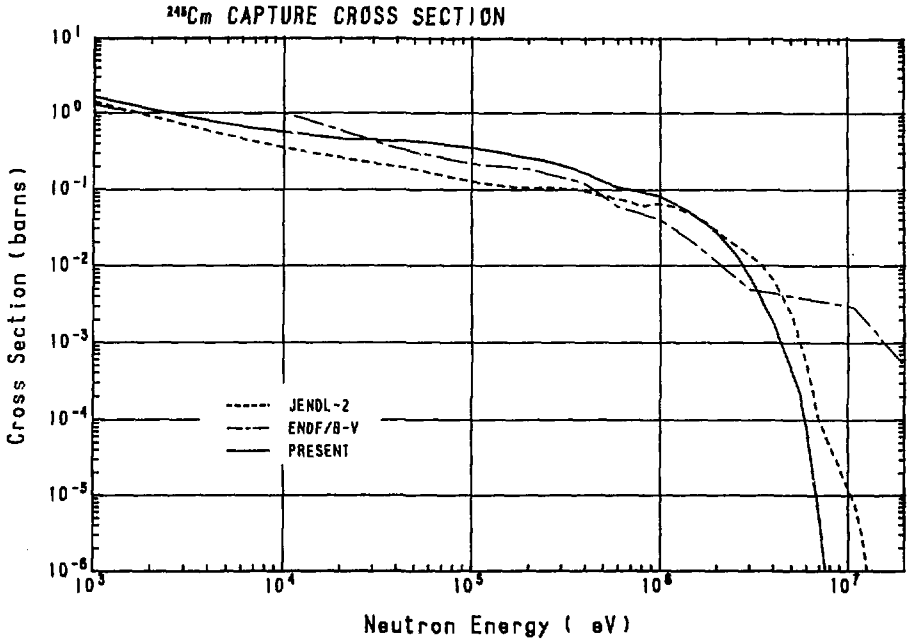

Fig. 27(b) Capture cross section of ^{245}Cm (1 keV ~ 20 MeV).

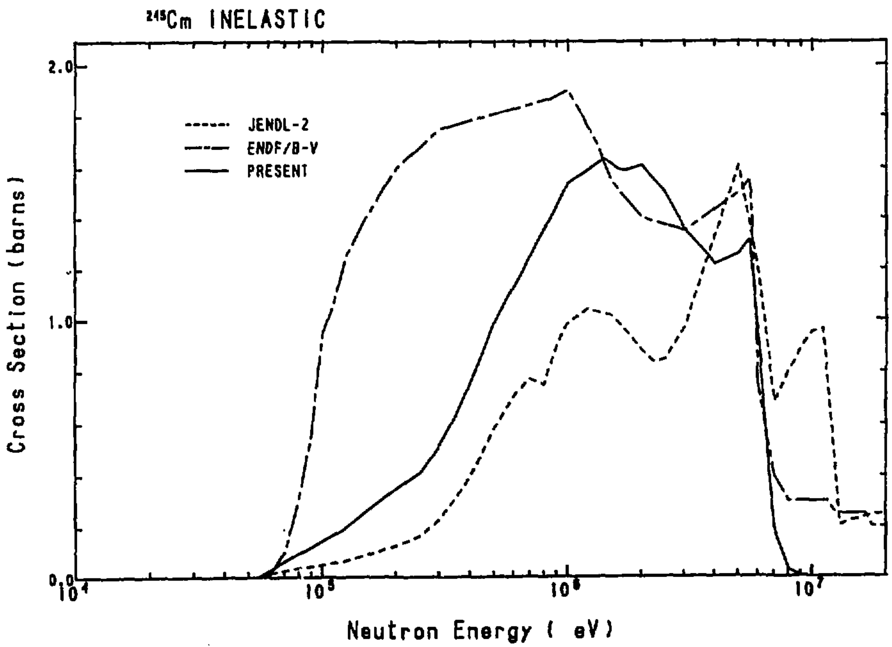

Fig. 28 Inelastic scattering cross section of ^{245}Cm.

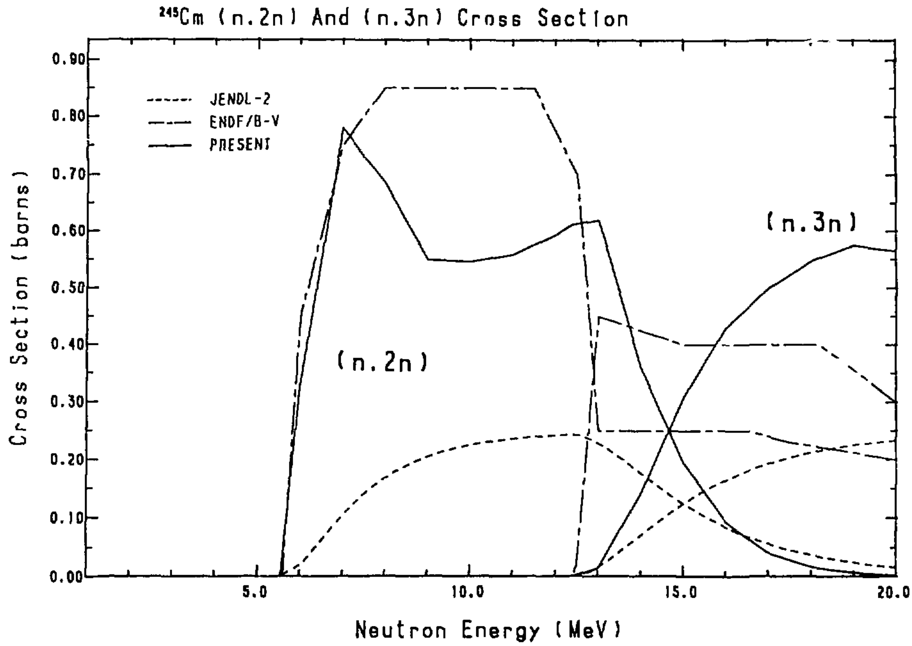

Fig. 29 (n,2n) and (n,3n) reaction cross sections of ^{245}Cm.

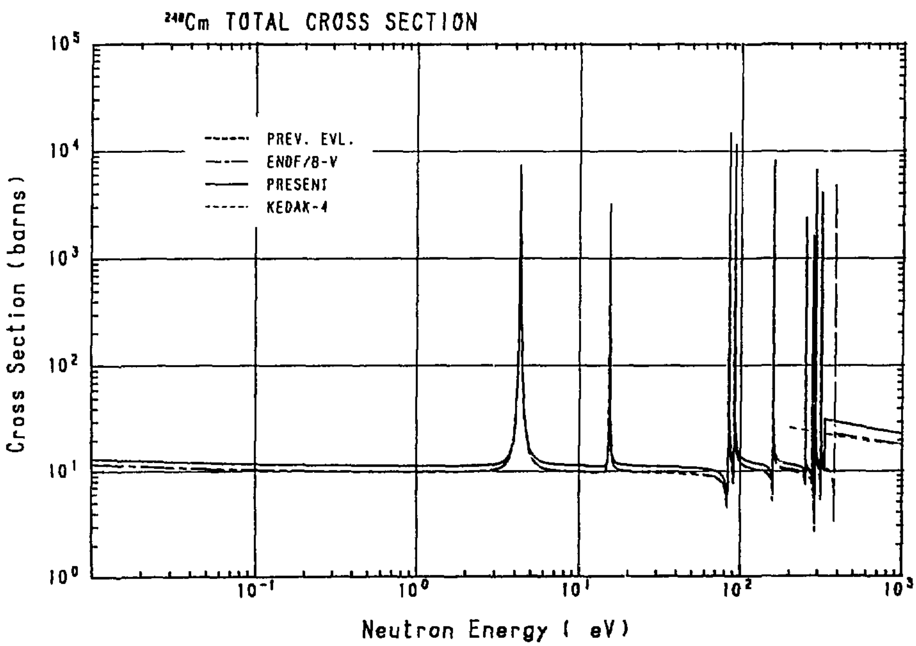

Fig. 30(a) Total cross section of ^{246}Cm (0.01 eV ~ 1 keV).

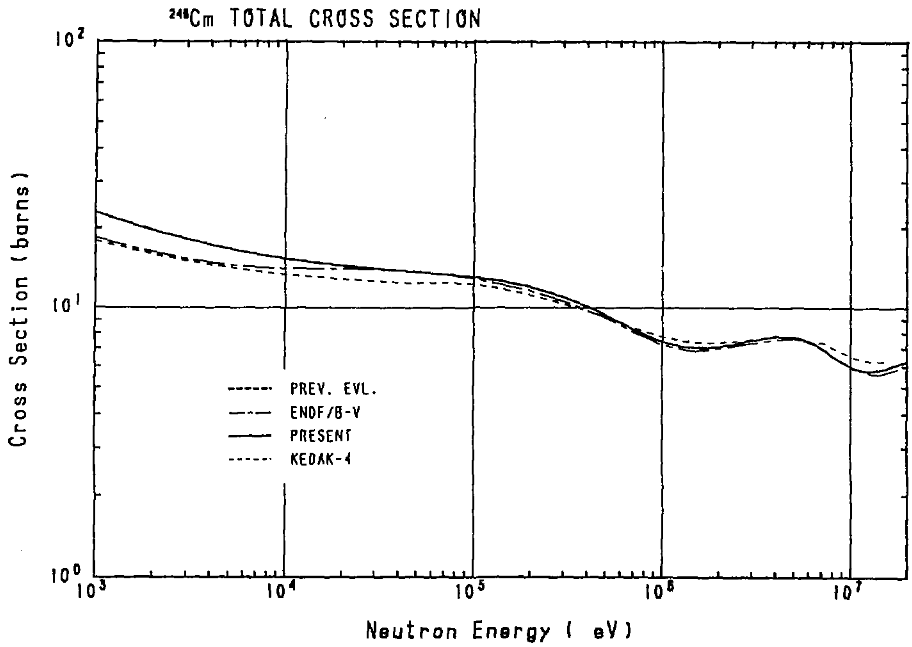

Fig. 30(b) Total cross section of ^{246}Cm (1 keV ~ 20 MeV). The present evaluation is the same as the previous one.

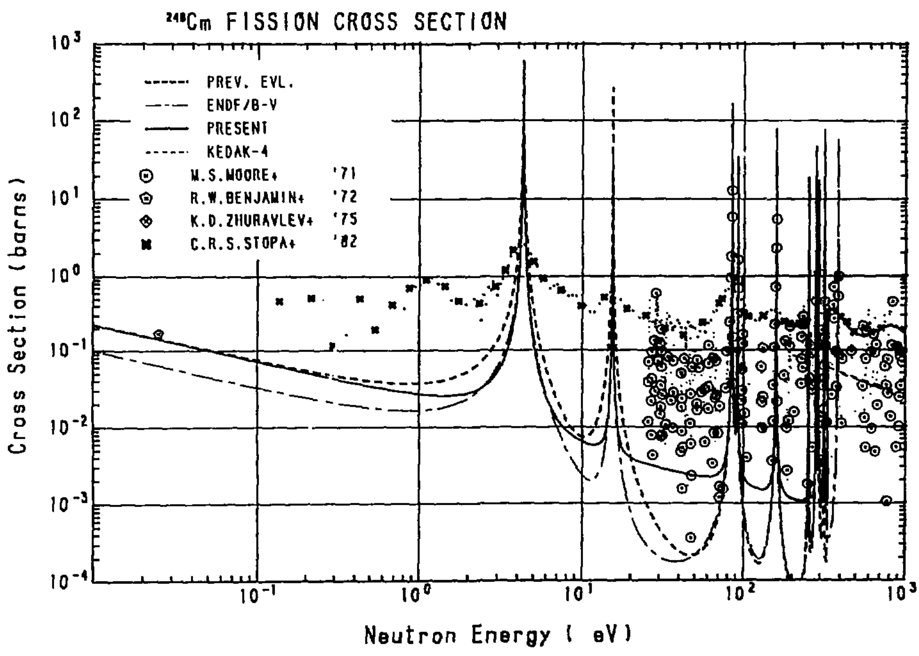

Fig. 31(a) Fission cross section of ^{246}Cm (0.01 eV ~ 1 keV).

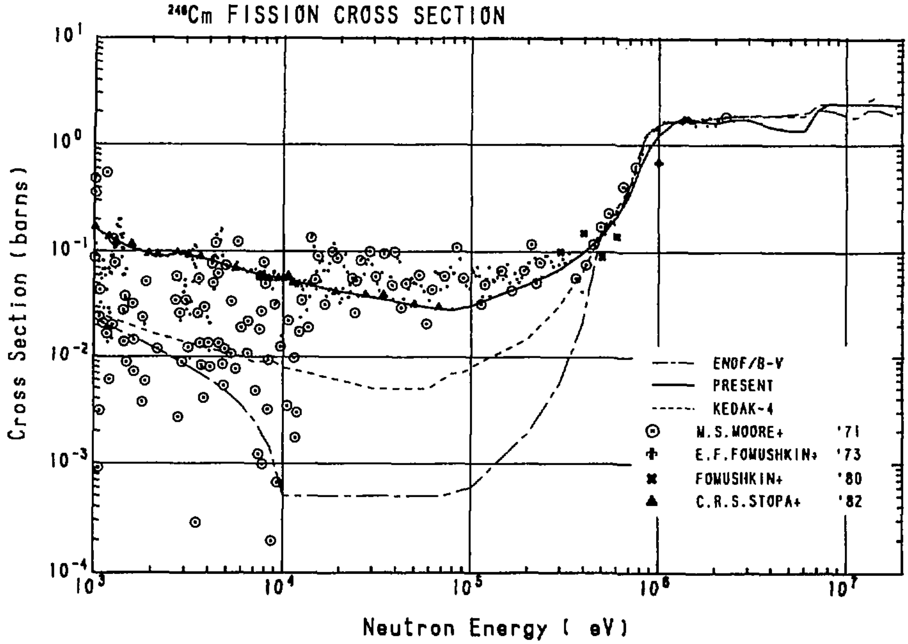

Fig. 31(b) Fission cross section of ^{246}Cm (1 keV ~ 20 MeV). The present evaluation is the same as the previous one.

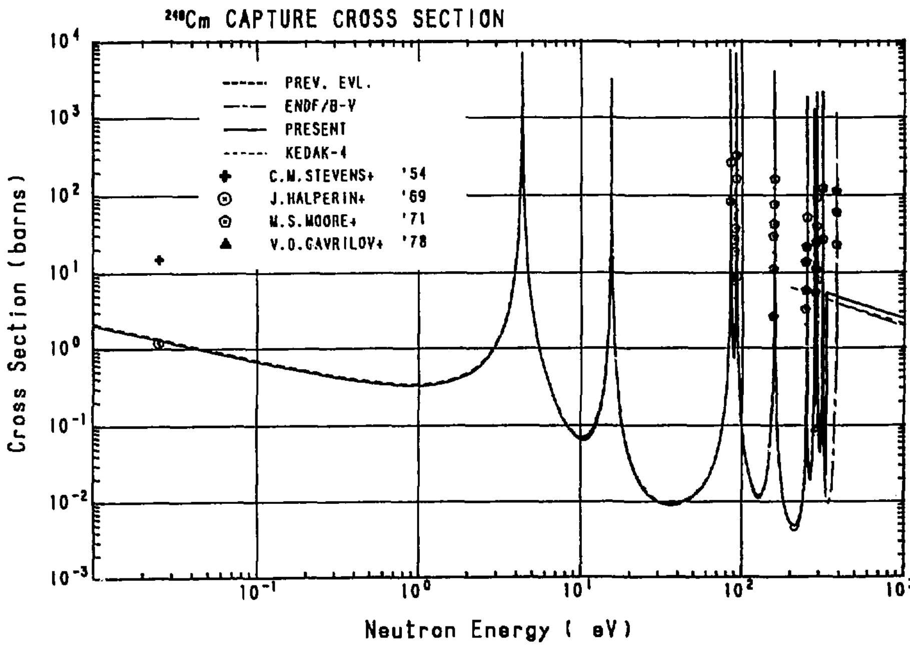

Fig. 32(a) Capture cross section of ^{246}Cm (0.01 eV ~ 1 keV).

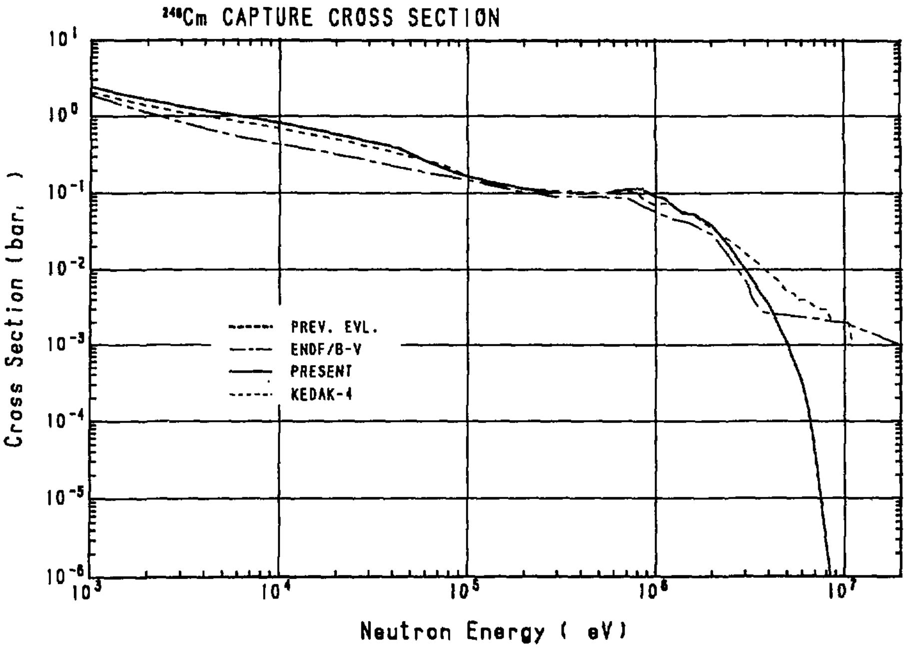

Fig. 32(b) Capture cross section of ^{246}Cm (1 keV ~ 20 MeV). The present evaluation is the same as the previous one.

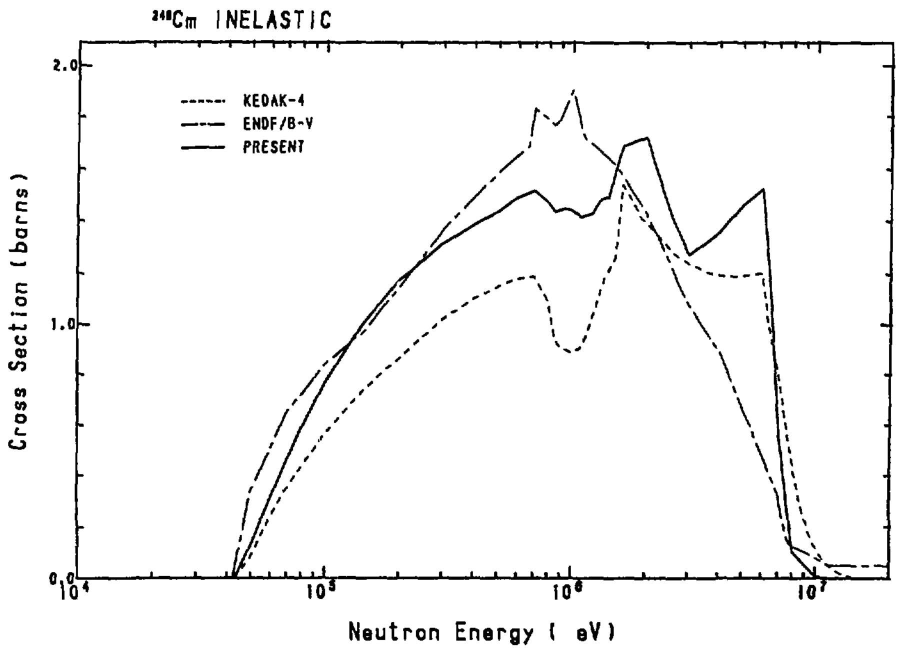

Fig. 33 Inelastic scattering cross section of ^{246}Cm. The present evaluation is the same as the previous one.

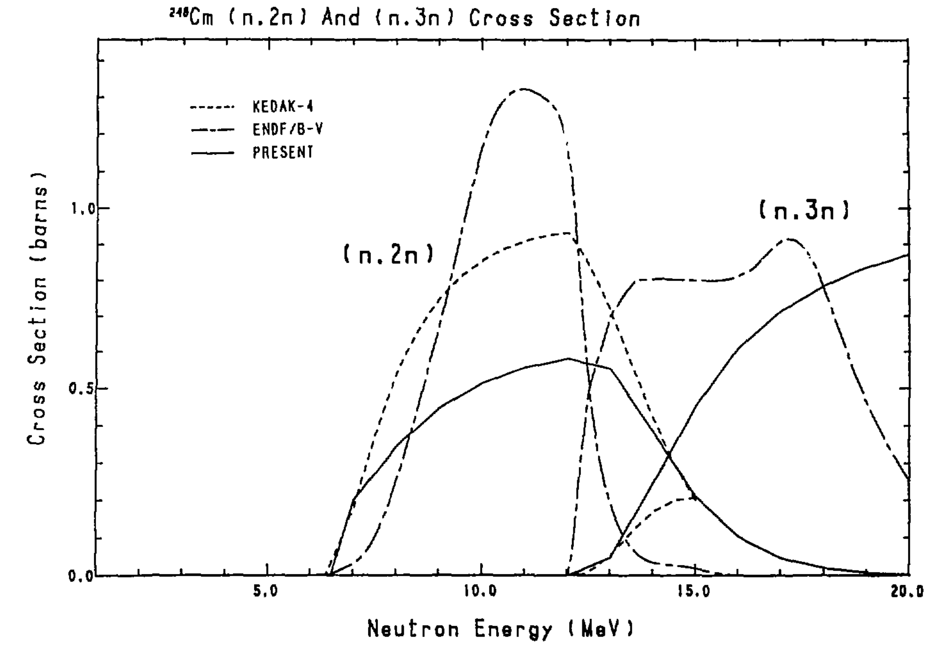

Fig. 34 (n,2n) and (n,3n) reaction cross sections of ^{246}Cm. The present evaluation is the same as the previous one.

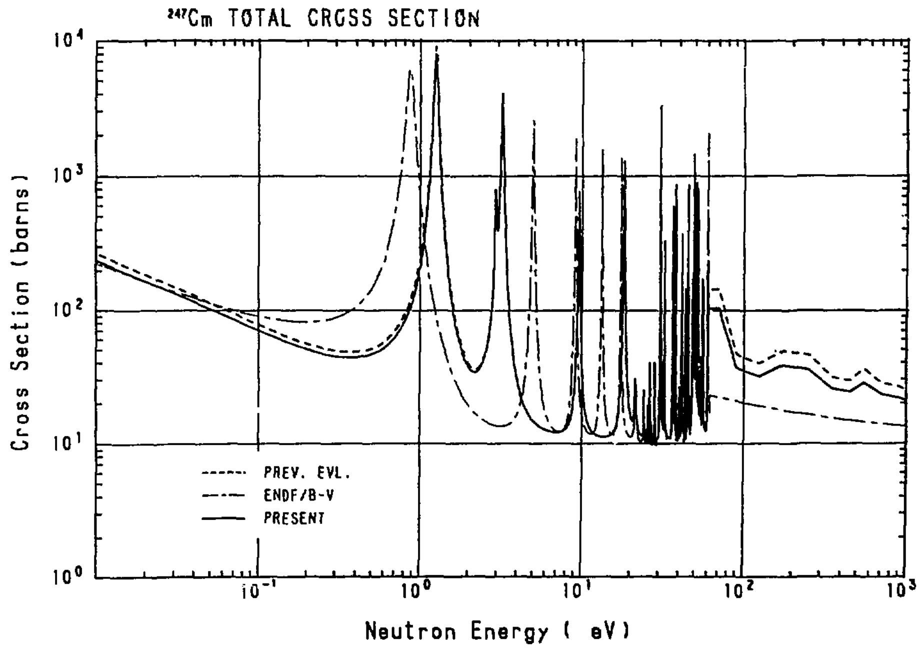

Fig. 35(a) Total cross section of ^{247}Cm (0.01 eV ~ 1 keV).

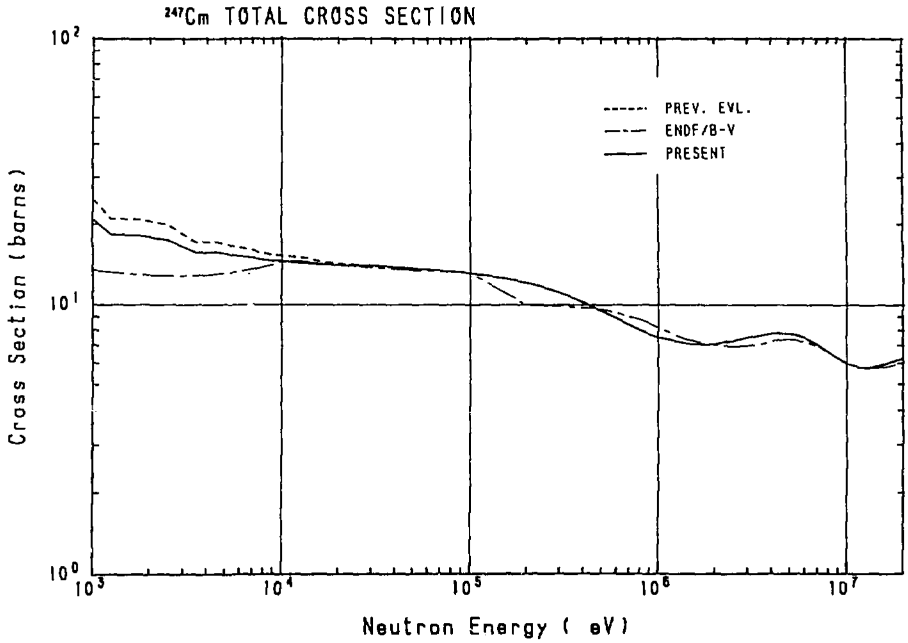

Fig. 35(b) Total cross section of ^{247}Cm (1 keV ~ 20 MeV).

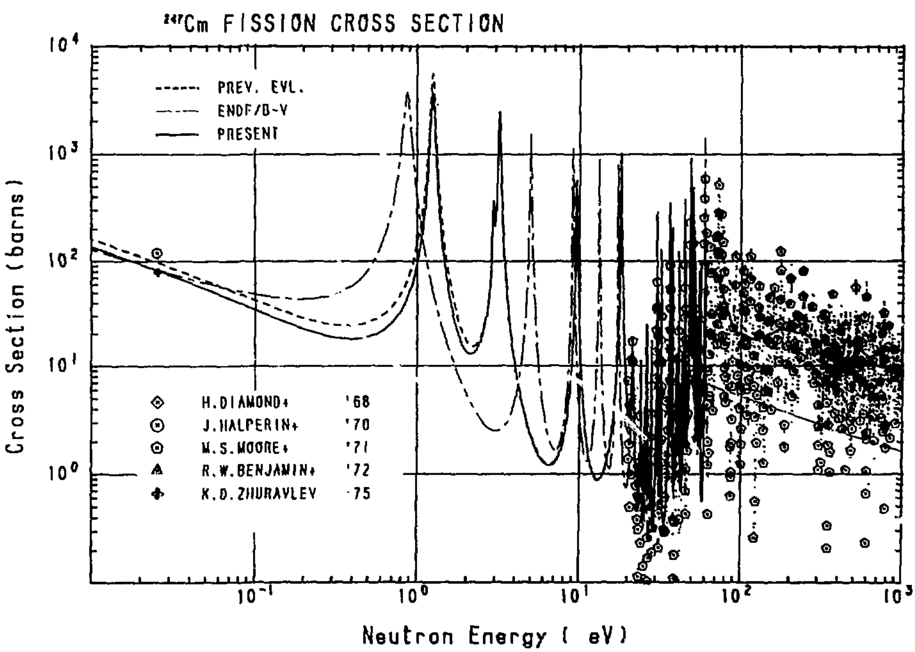

Fig. 36(a) Fission cross section of ^{247}Cm (0.01 eV ~ 1 keV).

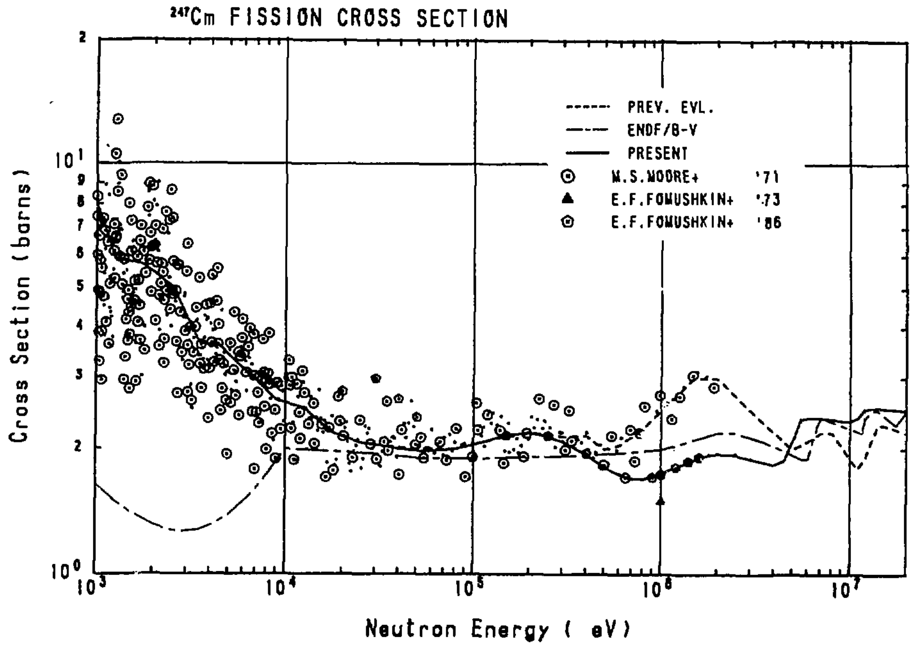

Fig. 36(b) Fission cross section of ^{247}Cm (1 keV ~ 20 MeV).

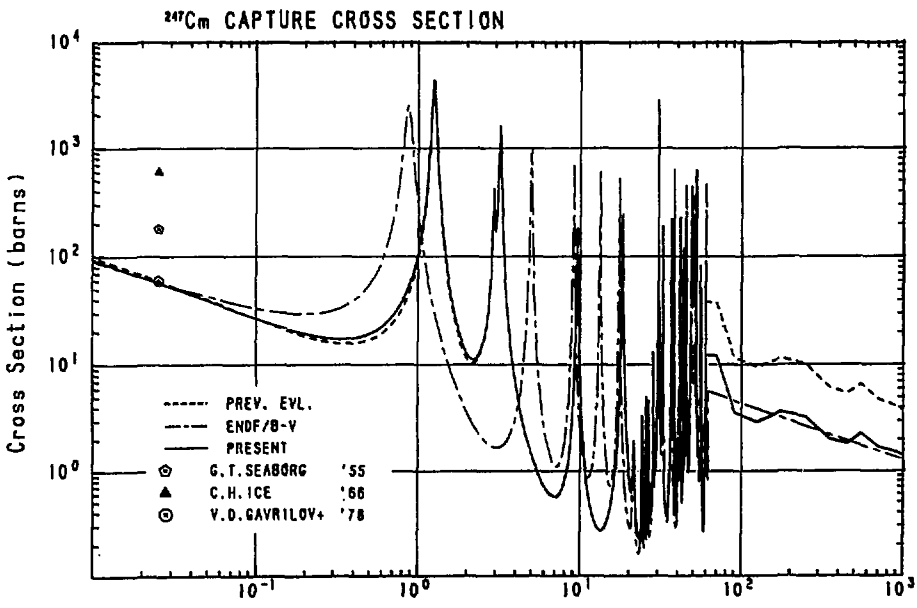

Fig. 37(a) Capture cross section of ^{247}Cm (0.01 eV ~ 1 keV).

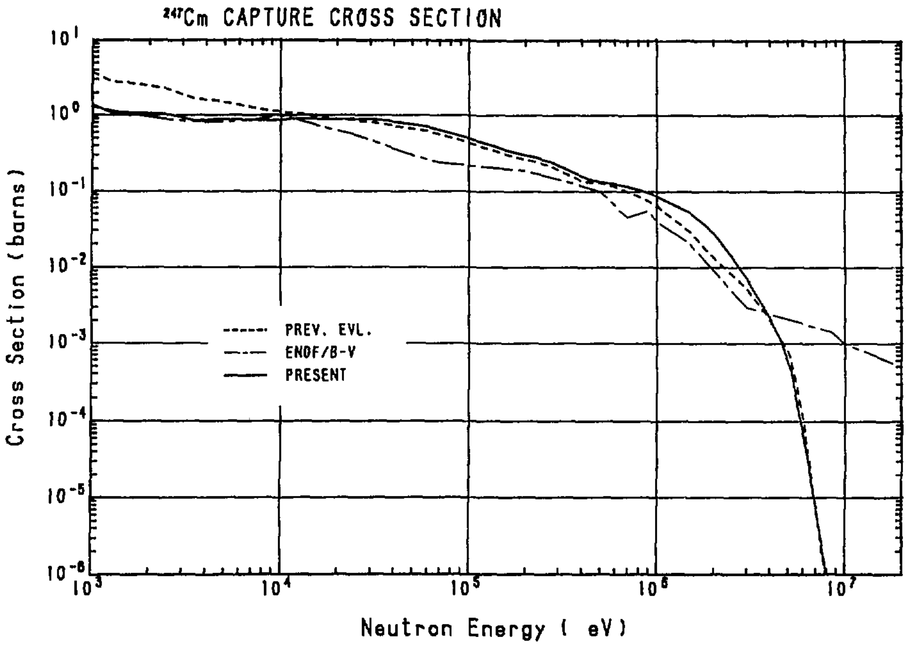

Fig. 37(b) Capture cross section of ^{247}Cm (1 keV ~ 20 MeV).

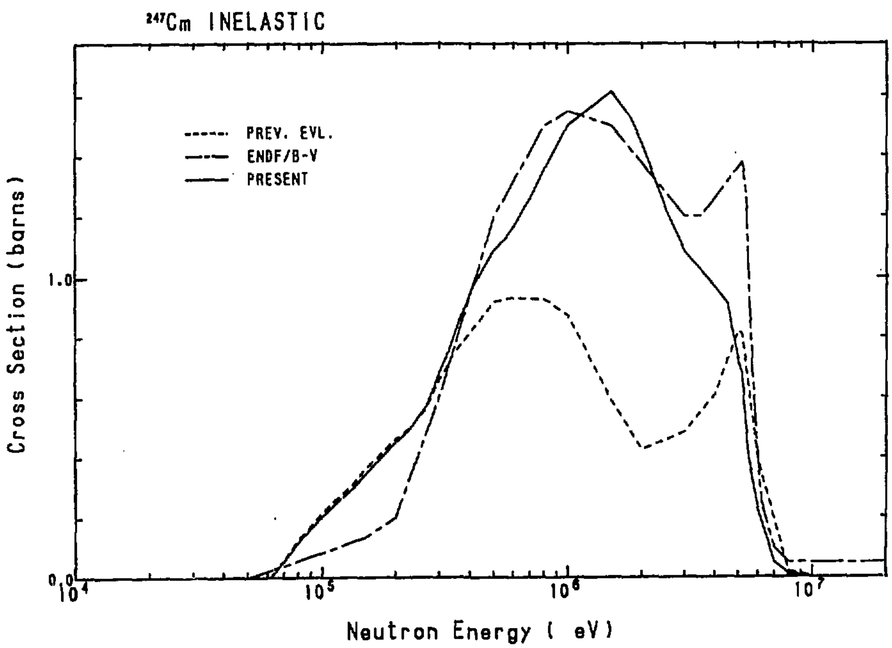

Fig. 38 Inelastic scattering cross section of ^{247}Cm.

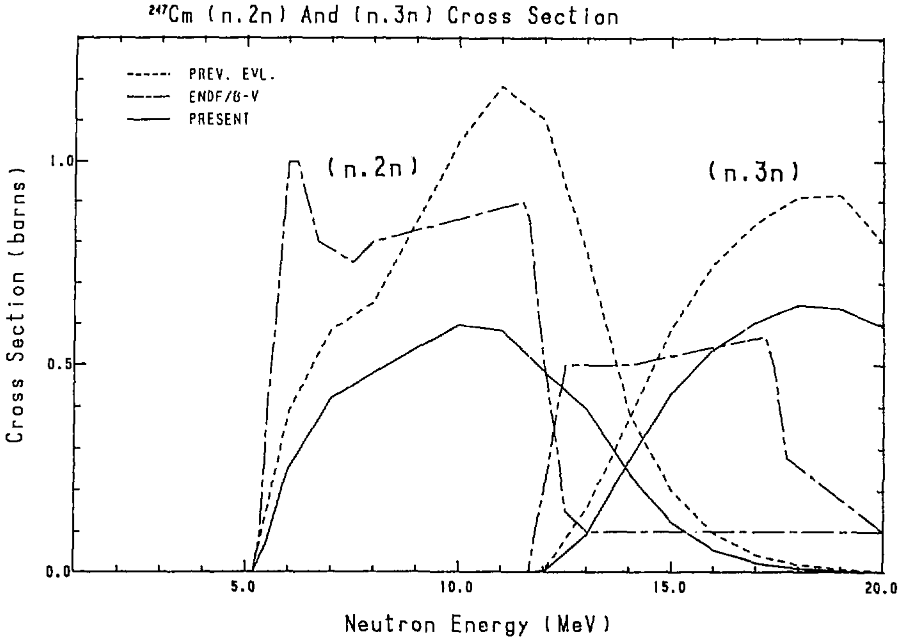

Fig. 39 (n,2n) and (n,3n) reaction cross sections of ^{247}Cm.

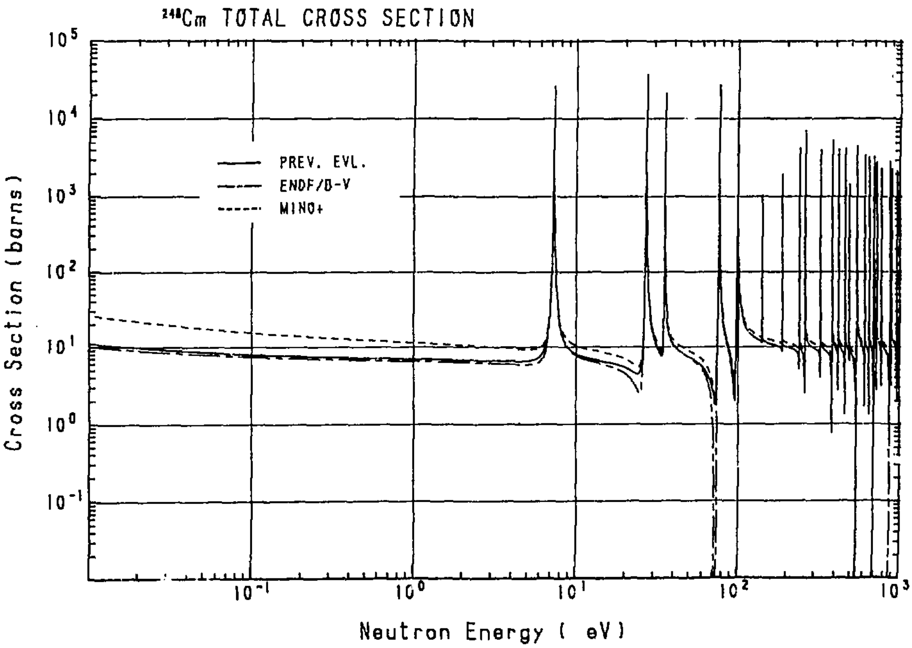

Fig. 40(a) Total cross section of ^{248}Cm (0.01 eV ~ 1 keV). The previous evaluation was adopted in the present work.

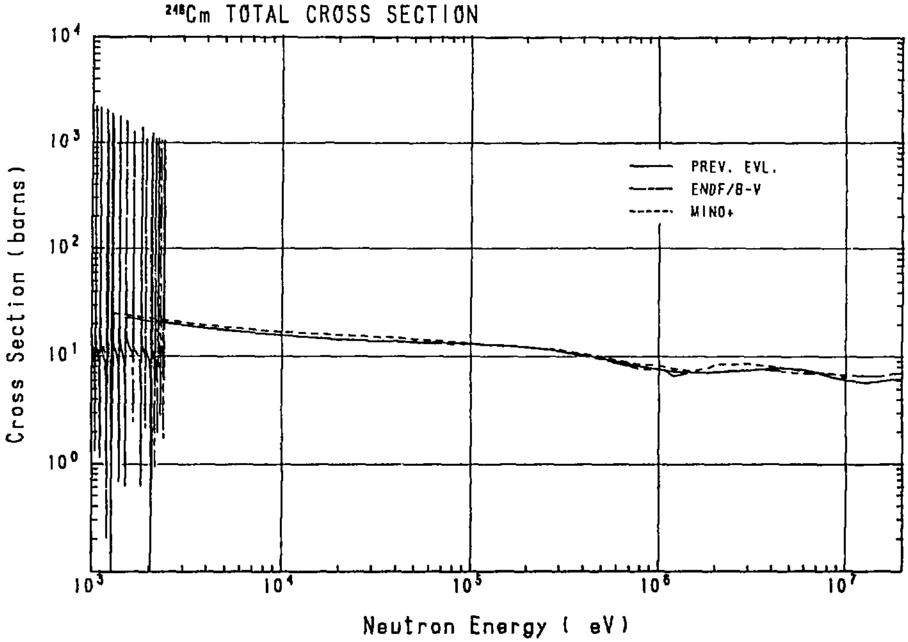

Fig. 40(b) Total cross section of ^{248}Cm (1 keV ~ 20 MeV). The previous evaluation was adopted in the present work.

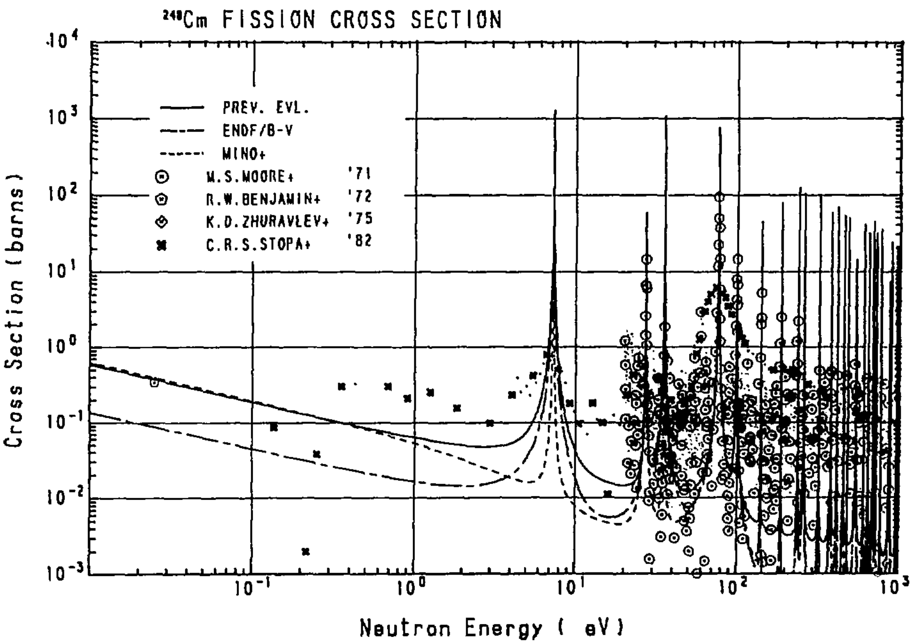

Fig. 41(a) Fission cross section of ^{248}Cm (0.01 eV ~ 1 keV). The previous evaluation was adopted in the present work.

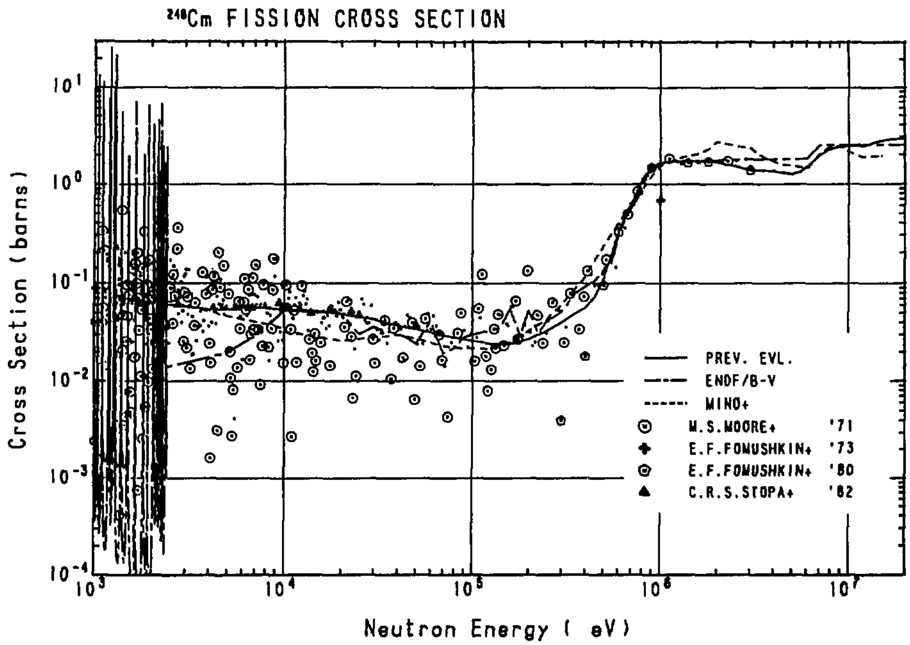

Fig. 41(b) Fission cross section of ^{248}Cm (1 keV ~ 20 MeV). The previous evaluation was adopted in the present work.

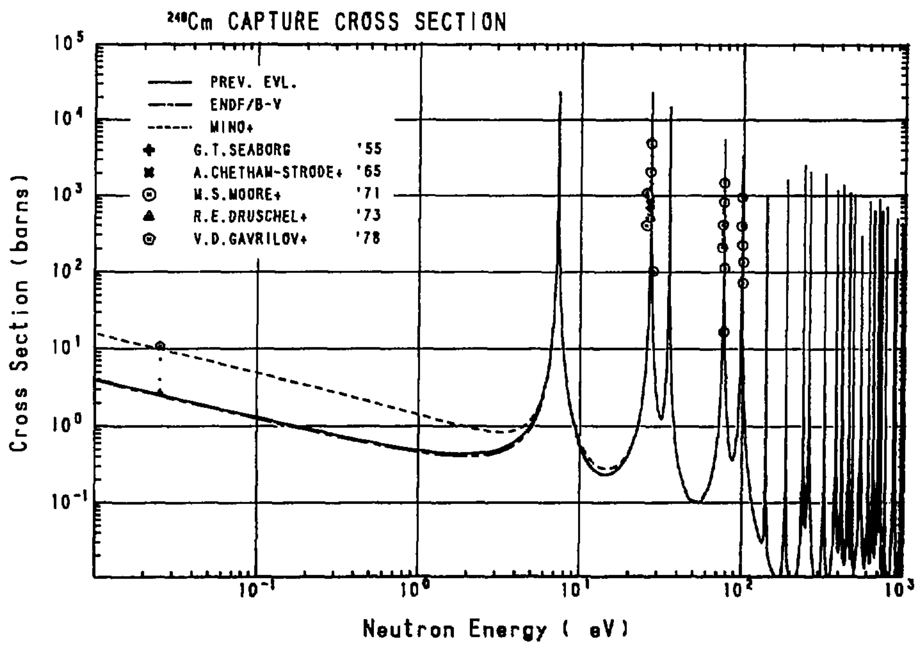

Fig. 42(a) Capture cross section of ^{248}Cm (0.01 eV ~ 1 keV). The previous evaluation was adopted in the present work.

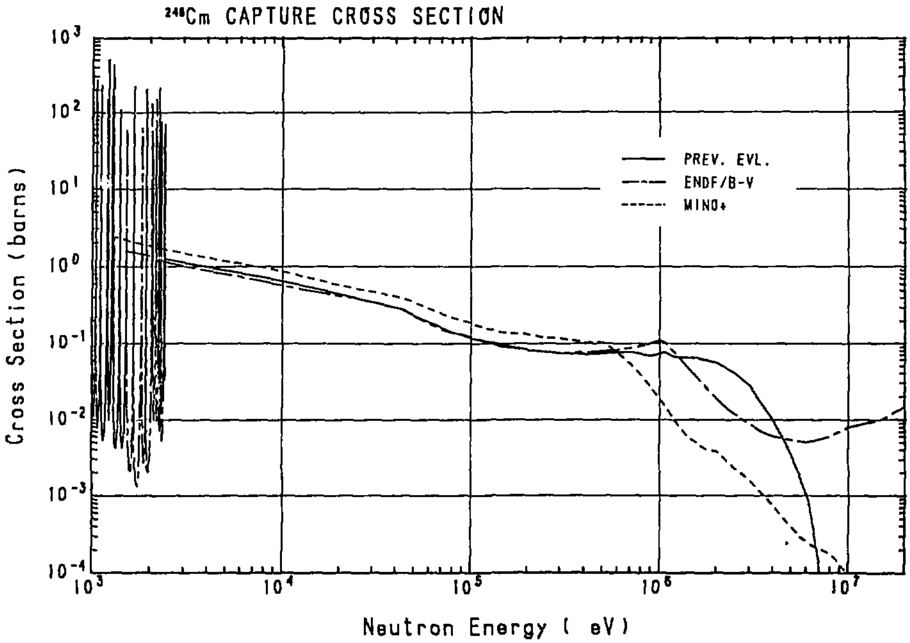

Fig. 42(b) Capture cross section of ^{248}Cm (1 keV ~ 20 MeV). The previous evaluation was adopted in the present work.

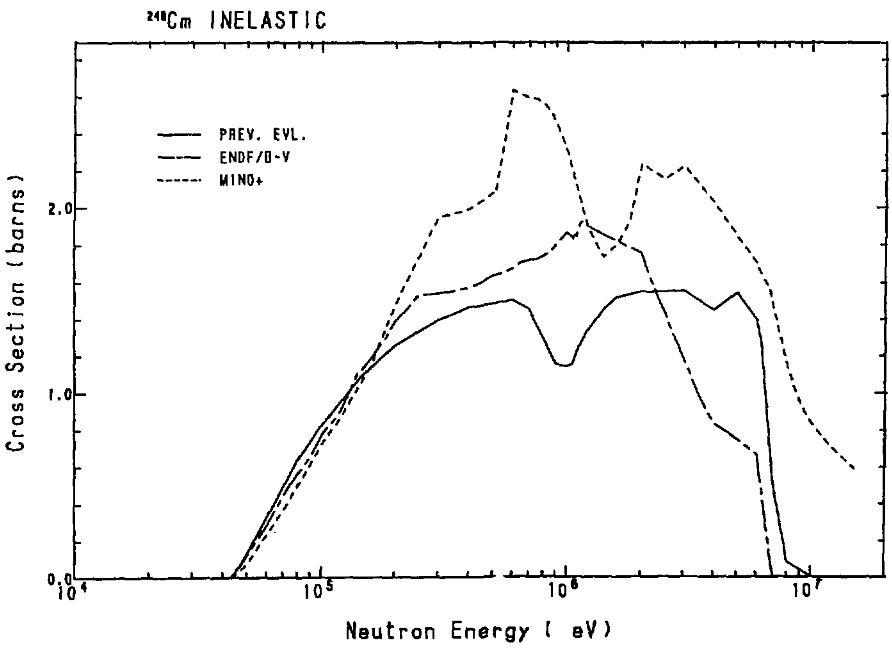

Fig. 43 Inelastic scattering cross section of ^{248}Cm. The previous evaluation was adopted in the present work.

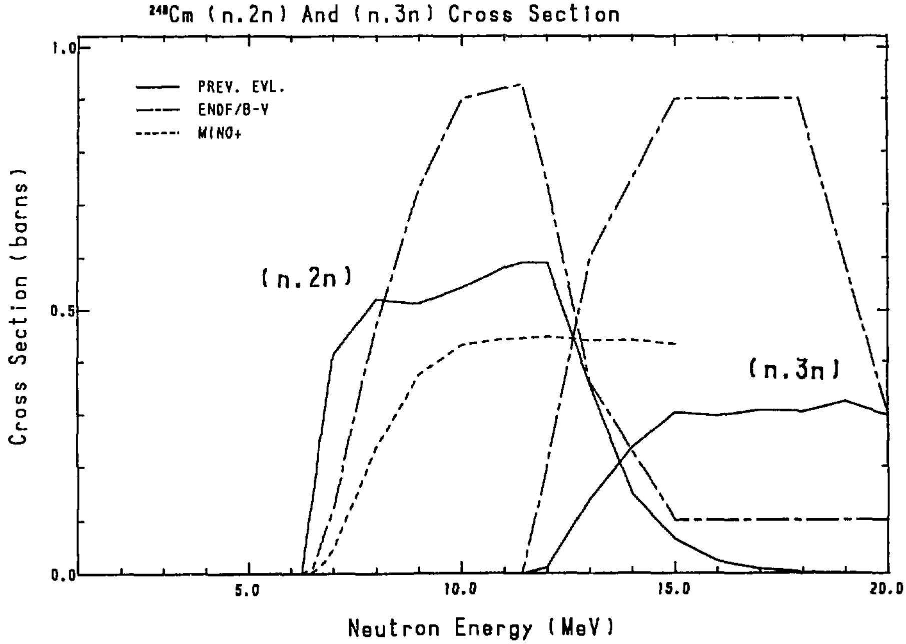

Fig. 44 (n,2n) and (n,3n) reaction cross sections of ^{248}Cm. The previous evaluation was adopted in the present work.

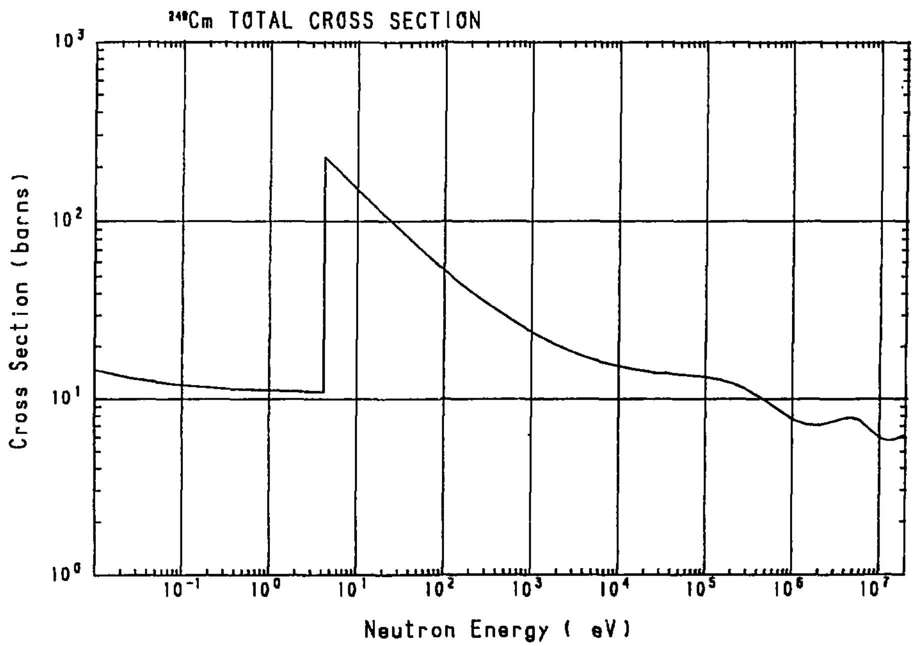

Fig. 45 Total cross section of ^{249}Cm.

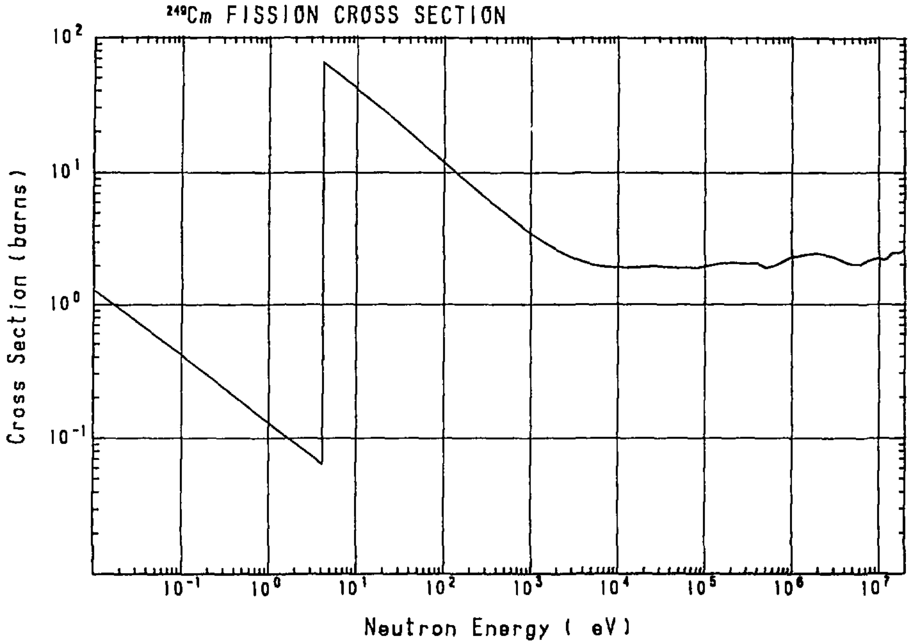

Fig. 46 Fission cross section of ^{249}Cm.

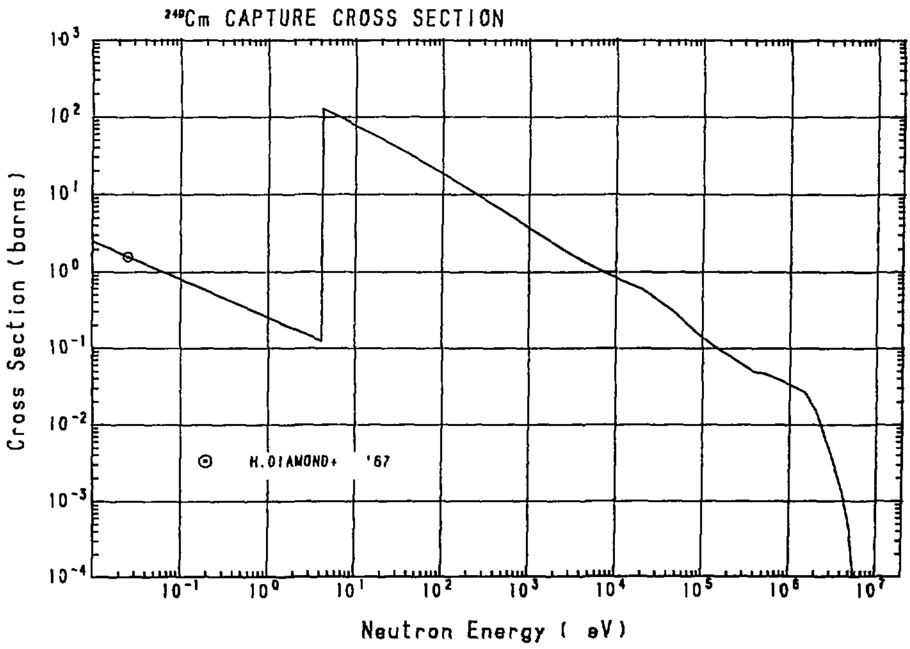

Fig. 47 Capture cross section of ^{249}Cm.

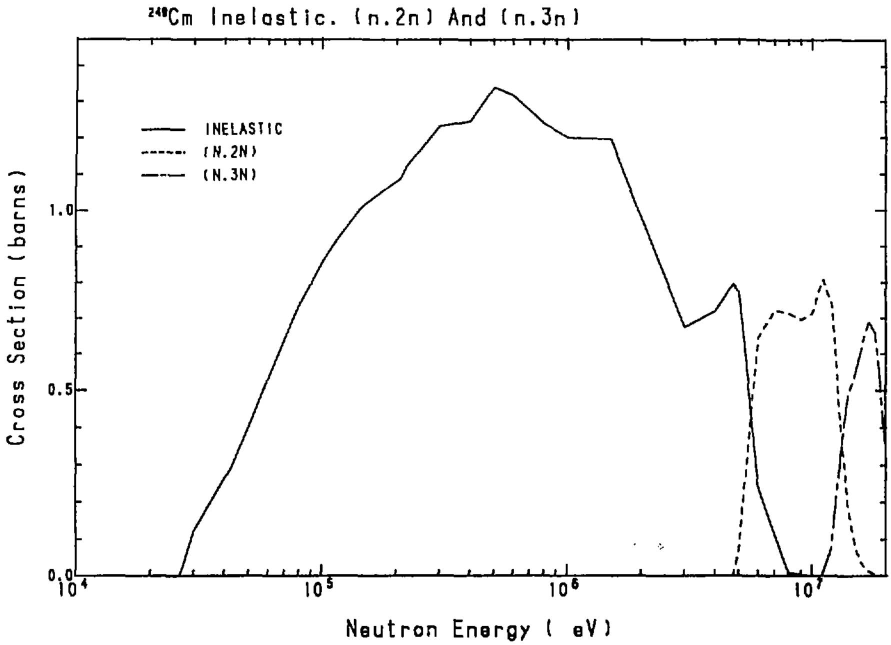

Fig. 48 Inelastic scattering, (n,2n) and (n,3n) reactions cross sections of ^{249}Cm.